TRIBHUVAN UNIVERSITY
INSTITUTE OF ENGINEERING
PULCHOWK CAMPUS

SEISMIC VULNERABILITY ASSESSMENT OF BRIDGES USING FRAGILITY CURVES

BY
PRAMOD TIWARI

A THESIS
SUBMITTED TO THE DEPARTMENT OF CIVIL ENGINEERING
IN PARTIAL FULFILLMENT OF THE REQUIREMENTS FOR THE
DEGREE OF MASTER OF SCIENCE IN STRUCTURAL ENGINEERING

DEPARTMENT OF CIVIL ENGINEERING
LALITPUR, NEPAL

SEPT, 2021

TRIBHUVAN UNIVERSITY
INSTITUTE OF ENGINEERING
PULCHOWK CAMPUS
DEPARTMENT OF CIVIL ENGINEERING

The undersigned certify that the thesis entitled "SEISMIC VULNERABILITY ASSESSMENT OF BRIDGES USING FRAGILITY CURVES" submitted by Pramod Tiwari (075/MSStE/013) has been supervised and recommeded to the Institute of Engineering for the partial fulfillment of requirement for the degree of Master of Science in Structural Engineering.

..……..……

Supervisor, Dr. Gokarna Bahadur Motra
Professor
Department of Civil Engineering
Pulchowk Campus, Institute of Engineering

..……..……

Co-Supervisor, Dr. Kshitij Charana Shrestha
Associate Professor
Department of Civil Engineering
Pulchowk Campus, Institute of Engineering

..……..……

Committee Chairperson, Dr. Kamal Bahadur Thapa
M.Sc Co-ordinator
Department of Civil Engineering
Pulchowk Campus, Institute of Engineering

Date..……

COPYRIGHT

ABSTRACT

This study presents the seismic vulnerability of two spanned RCC bridge in Nepal. The bridges vary in span length from 25m to 35m and has a single circular pier in the middle along with two abutments on the sides. The bridge is modeled on finite element analysis-based program OpenSees. Ten different near fault earthquakes are considered for the non-linear time history analysis of the bridge with the drift ratio taken as the parameter to check the damage states (DS) and the performance limits. The pier of the bridge is taken as the most critical component and the fragility curves are developed considering the non-linear deformation concentrated in the pier only. The pier of two spanned bridges of Nepal are highly susceptible to slight damage for the earthquake with 0.5g PGA while slightly susceptible to moderate and extensive damage and are not susceptible to complete damage. Also, at 1.0g PGA, they are highly susceptible to moderate and extensive damage while low susceptible to complete damage.

ACKNOWLEDGEMENT

I wish to express my sincere gratitude to my supervisors Prof. Dr. Gokarna Bahadur Motra and Assoc. Prof. Dr. Kshitij Charana Shrestha, for their continuous guidance, inspiration, and encouragement during the thesis work and the study period. Their lectures and advice proved to be valuable in the process of this thesis work.

I would like to express my great appreciation Assoc. Prof. Dr. Kamal Thapa, our program coordinator for providing valuable guidance throughout the progress of this thesis work. I would also like to acknowledge all the faculty members of Department of Civil Engineering for the knowledge and concepts they gave me during my study at IOE, Pulchowk Campus.

I am thankful to Roads Board Nepal for providing financial support to conduct this work. Also I am thankful to Centre of Infrastructure Development Studies (CIDS) for providing technical support and knowledge for completion of this study.

I would like to thank Er. Nishan Thapa, Er. Prabin Wagle, Er. Bijay Ban and my classmates for their direct and indirect help over the period of my master's study as well as this thesis.

To my family, thank you for encouraging me in all of my dreams and inspiring me during the thesis work.

I would like to recognize the assistance obtained through the reference books and research papers and would like to thank their authors.

Pramod Tiwari
075/MSStE/013
Sept 2021

TABLE OF CONTENTS

LIST OF FIGURES

LIST OF TABLES

LIST OF SYMBOLS

P( ) = Probability of exceedence

$\emptyset$ = Standard normal cumulative distribution function

λ_{CL}^{i} = ln(median drift for a particular limit state, i)

Σ = summation

g = acceleration due to gravity

LIST OF ACRONYMS AND ABBREVIATIONS

IM = Intensity Measure

DS = Damage State

PGA = Peak Ground Acceleration

PGV = Peak Ground Velocity

GMI = Ground Motion Intensity

3D = Three-dimensional

RCC = Reinforced Cement Concrete

LS = Limit State

SSRN = Statistics of Strategic Road Network

1 CHAPTER ONE: INTRODUCTION

1.1 Introduction

Fragility curves are emerging tools for the seismic vulnerability assessment of highway bridges (Eunsoo, Reginald, & Bryant, 2003). They are conditional probability statements that give the probability of a bridge reaching or exceeding a particular damage level for an earthquake of a given intensity level. The approach is probabilistic rather than a deterministic one. There are various uncertainties in seismic hazards, structural capacity, and function of the structures; thus, a probabilistic approach is preferred to deterministic approach for seismic vulnerability assessment as it incorporates various uncertainties.

Road transportation is the most adopted and economic mode of transportation in Nepal. Being a country with numerous hills and river valleys, bridges are indispensable structural components in the road network of Nepal. There are 2021 bridges in Nepal under Strategic Road Network as per Statistics of Strategic Road Networks SSRN 2017/18 (Department of Roads, 2018). Since Nepal lies in the zone with high seismic activities, these bridges are inevitably vulnerable to the different levels of failures and maybe even collapse due to several large and numerous smaller earthquakes during their service period. Various levels of damages to numerous bridges due to the recent 2015 Gorkha Earthquake also demonstrates and endorse the seismic vulnerability of highway bridges. Out of 339 bridges assessed by the Department of Road jointly with World Bank, 53 bridges suffered major damages and 22 bridges suffered critical damages whereas 284 bridges were recorded as minor damages due to the 2015 Gorkha Earthquake (Gautam, Rupakhety, & Adhikari, 2019). Another study on the 22 bridges of Araniko Highway reported moderate damages on 3 bridges, light damages on 12 bridges, and no comparable damages on 7 bridges due to the 2015 Gorkha Earthquake (Quancai, Gaohu, Hao, Chong, & Baio, 2016).

1.2 Problem Statement

Failure of bridges due to earthquake exacerbate the situation as it can cause the obstruction of important roadways and hinder emergency vehicles from reaching the crisis zone. Further, it results in high economic losses as economic activities are curtailed due to the interrupted road network, and retrofit of the damaged bridge or new construction requires high expenditure. Nepal suffered estimated damages of 2676

million rupees in bridges and 1660 million rupees in highway and feeder roads under Strategic Road Network due to the 2015 earthquake (World Bank). Thus, proper and timely repair and maintenance of bridges is the most effective option for the smooth operation of transportation facilities with limited expenditure on the national budget. But with thousands of bridges in the road network, it has been difficult for the stakeholders to prioritize the bridges for repair and maintenance, retrofit or rebuild. With immense resources and capital at stake, the decision must be based on rational criteria. Fragility curves can become such rational criteria as they help in determining the potential losses resulting from earthquakes and can be used in prioritization for retrofitting of the bridges (Eunsoo, Reginald, & Bryant, 2003). Moreover, they can also be used to optimize bridge retrofit methods and in the development of a post-event action plan (Tavares, Suescun, Paultre, & Padgett, 2013).

After an earthquake, the bridge seeming intact visually may be vulnerable to failure as the cracks in piers, abutments, etc. are not seen from the surface of the bridge. Usage of such a bridge may be a catastrophe as it may fail at any time if used with design loads. The officials are obliged to consider various bridge-level decisions such as lane closures, reduction in traffic volume, or complete bridge closure in such situations. An injudicious decision may cause more harm and a conservative conclusion may lead to social inconveniences and unnecessary costs (Alessandri, Giannini, & Paolacci, 2013). Fragility curves can be used as a tool for rational decisions in this crisis as well. They help in classifying damage levels and assist in prompt and safe decisions regarding the usage of bridges by providing information on the relation between ground motion intensity at bridge sites and the probability of exceeding a certain damage state for a certain class of bridges i.e., bridges having similar structural characteristics, before the occurrence of the earthquake.

1.3 Objectives of the Study

The objectives of the study are:

1. To prepare fragility curves for various two spanned RCC bridges of Nepal.
2. To quantify the seismic vulnerability of the bridges using the developed fragility curves.

1.4 Limitations of the Study

The limitations of the study are presented as follows:

1. The study considers the effects on the bridge pier only. The effects on other components such as abutments, bearing and superstructure are neglected.
2. The foundation is not modeled and the base of the pier is assumed to be fixed.
3. The vertical component of the earthquake time history is not considered in the study.

1.5 Organization of the thesis

The whole research work has presented in eight chapters. Chapter 1 contains the introduction and the need of the study along with the objectives and the limitations of the study. Chapter 2 provides the literature review for the conduction of the study. The methodology followed in this study is presented in Chapter 3. The analytical modeling of the bridge piers is shown in Chapter 4. Chapter 5 contains the analysis part, result and discussion along with the conclusion and further recommendation in Chapter 6.

2 CHAPTER TWO: LITERATURE REVIEW

Over time, different researchers have developed and employed different methods of formulating fragility curves for vulnerability assessment of bridges (Billah & Alam, 2014).

2.1 Different methods of preparing fragility curves

The different methods for preparation of fragility curves are as follows:

2.1.1 Expert based/ judgmental fragility curves

This is the oldest and simplest way of developing fragility curves for the bridges. A survey is conducted about the estimated damage level of different components of bridges to the experts of earthquake engineering as per the ground motion expected in the bridge site. Based on the experts' prediction, fragility curves are developed. This method is quite simple but subjective and provides different curves as per different experts.

2.1.2 Empirical fragility curves

Fragility curves are prepared through the post-earthquake field observations in this method. Different teams of experts visit the field and provide damage levels to different components of the bridge. Based on these damage levels, fragility curves are prepared. The reliability of this method depends upon the expertise of the inspection team, inspection period, damage state definition, etc. As the judgmental method, this method too is subjective and provides different curves as per different inspection teams. (Yamazaki, Motomura, & Hamada, 2000) and (Shinozuka, Feng, Kim, Uzawa, & Ueda, 2001) developed fragility curves for the Hanshin Expressway using the same damage data from the 1995 Kobe earthquake; but their curves differ notably (Billah & Alam, 2014).

2.1.3 Experimental fragility curves

In this method, fragility curves are developed from the response data and damage state of a certain scale model of the bridge in shaking table tests. This method is limited and uncommon as it requires large-scale experiments with sophisticated laboratories.

(Banerjee & Chi, 2013) developed fragility curves for bridges using damage data obtained from the shake table test of a near-full scale bridge. However, the experiment was short in application due to the lack of adequate data points and a weak correlation between geometry and structural properties (Billah & Alam, 2014).

2.1.4 Analytical fragility curves

The analytical method is the most used and preferred method for developing fragility curves of bridges. The curves are developed using numerical analysis rather than visual assessment; thus, providing the most reliable result. As every major uncertainty can be incorporated in the numerical analysis, this method is less biased and more reliable. For this reason, this study of seismic vulnerability of bridges is conducted with analytical fragility curves.

The adopted analytical process differs with the available computational power, time and required accuracy. The analysis procedures are elastic spectral analysis, nonlinear static analysis and nonlinear time history analysis in the increasing order of required computational power, time and accuracy. Elastic spectral analysis is the simplest method of analysis and is suitable for bridges performing in the linear elastic range. The nonlinear static analysis considers the geometric and material nonlinearity of the structure but does not consider the dynamic nature of earthquake loading. Capacity is calculated using nonlinear static pushover analysis and demand is estimated using a scaled-down response spectrum. Along with geometric and material nonlinearity of the structure, nonlinear time history analysis considers the dynamic nature of earthquake loads resulting in an accurate estimate of damage states. Despite being one of the most computationally expensive methods, nonlinear time history analysis is the most reliable method for generating fragility curves (Shiozuka, Feng, Kim, & Kim, 2000). Thus, this study is done with nonlinear time history analysis of the bridges with suitable patterns of ground motions to attain high order of reliability and accuracy in the obtained fragility curves and seismic vulnerability of bridges.

2.2 Intensity Measure (IM) and Damage States (DS)

IM is the representative of the seismic loading on the structure with which seismic demand is estimated and compared with the estimated capacity of the structure to establish the fragility curves. DS is the level of damage the structure is expected to

undergo under the representative IM as per the conditions of the site of the bridge. As the main purpose of the fragility curves is to evaluate the probability of exceedance of certain damage state in the structure due to the expected intensity of the seismic events, choosing the proper IM and accurate quantification of DS has great importance in the reliability and accuracy of proposed fragility curves.

Different researchers have proposed different IM such as spectral acceleration (Sa) and spectral displacement (Sd) at the first-mode period, peak ground acceleration (PGA), peak ground velocity (PGV), arias intensity (AI), etc. (Luco & Cornell, 2007) suggested the three criteria for the selection of appropriate IM i.e., efficiency, sufficiency and hazard computability. Further (Padgett & DesRoches, 2008) recommended the PGA as the optimum IM to describe the severity of the earthquake ground motion. This study also considers PGA as the IM to develop the fragility curves.

(Park & Ang, 1985) quantified the damage index (DI) of the structure through the following relation:

$DI = (\mu_d + \beta . \mu_h) / \mu_u$

where, β = cyclic loading factor taken as 0.15

displacement ductility (μ_d) = ratio of maximum displacement at the top of the pier obtained by the dynamic analysis to the displacement at the yield obtained from static analysis.

ultimate ductility (μ_u) = ratio of maximum displacement to the yield displacement

cumulative energy ductility (μ_h) = ratio of hysteretic energy dissipated during dynamic excitation to the energy at the yield point.

Using damage index, (Ghobarah, Aly, & El-Attar, 1997) proposed damage levels in the range of No Damage to Complete Damage as shown in Table 1:

Table 1: Damage Index for bridges for different damage levels (Ghobarah, Aly, & El-Attar, 1997).

Damage Index, DI	Damage Level	Definition
$0.00 < DI \leq 0.14$	I	No Damage
$0.14 < DI \leq 0.40$	II	Slight Damage
$0.40 < DI \leq 0.60$	III	Moderate Damage
$0.60 < DI < 1.00$	IV	Extensive Damage
$1.00 \leq DI$	V	Complete Damage

The damage ratio (ratio of the frequency of damage index for a particular PGA level to the total number of earthquake ground motions considered) for each damage level is plotted on a lognormal paper to logarithmic values of ground motion parameter (PGA) for determination of the parameters of fragility curves.

Rather than using energy dissipation as damage criteria, (Hwang, J.B.L, & Y.H.C, 2001) proposed the damage state using the displacement ductility ratio of columns.

$\mu_d = \Delta / \Delta_{cy1}$

where Δ is the maximum displacement at the top of a column obtained from dynamic seismic response analysis and Δ_{cy1} is the displacement of a column when the longitudinal reinforcing bars at the bottom of the column reaches the first yield.

Table 2: Bridge Damage State using the displacement ductility ratio of columns (Hwang, J.B.L, & Y.H.C, 2001).

Damage State	Definition
No Damage	$\mu_{cy1} > \mu_d$
Slight Damage	$\mu_{cy} > \mu_d > \mu_{cy1}$
Moderate Damage	$\mu_{c2} > \mu_d > \mu_{cy}$
Extensive Damage	$\mu_{max} > \mu_d > \mu_{c2}$
Complete Damage	$\mu_d > \mu_{cmax}$

where μ_{cy1} is the displacement ductility ratio at the first longitudinal bar yield.

μ_{cy2} is displacement ductility ratio with $\varepsilon c = 0.002$

$\mu_{cmax} = \mu_{cy2} + 3.0$ is the maximum displacement ductility ratio.

Bridge piers are one of the most vulnerable components of the bridge as they tend to enter the nonlinear deformation range under severe earthquake loads (Billah & Alam, 2012). Thus, in this study, fragility curves for the bridges are developed through the damage state levels of the bridge piers only. (Dutta & Mander, 1999) recommended the drift ratio as the demand parameter for the piers and suggested threshold values for different damage states through experiment on real-size bridge pier as :

Table 3: Proposed Damage States Using Column Drift Limits (Dutta & Mander, 1999).

Damage State	Description	Drift Limits
Almost no damage	First yield	0.005
Slight damage	Cracking and spalling	0.007
Moderate damage	Loss of anchorage	0.015
Extensive damage	Incipient column collapse	0.025
Complete damage	Column collapse	0.050

Highlighting the usage of fragility curves in different decision-making scenarios during the occurrence of seismic events, (Mackie & Stojadinovic, 2004) prepared fragility curves for single-bent reinforced concrete highway overpass bridges and proposed different performance levels for following bridge level decision criteria as in the following Table 4:

Table 4: Proposed Performance Levels Using Bridge Level Decision Variables (Mackie & Stojadinovic, 2004).

Objective Name	Traffic Capacity Remaining (Volume)	Loss of Lateral Load Carrying Capacity	Loss of Vertical Load Carrying Capacity
Immediate Access	100%	< 2%	< 5%
Weight Restriction	75%	< 2%	< 10%
1 Lane Open Only	50%	< 5%	< 25%
Emergency Access Only	25%	< 20%	< 50%
Closed	0%	> 20%	> 50%

2.3 Analytical modelling technique

The demand parameters are estimated due to various intensity of seismic loadings using available computer software. Various commercial and open-source software such as OpenSees, SeismoStruct, SAP2000, CSI Bridge, etc. are available for the analysis of bridge structures. OpenSees is an open-source analysis program developed by the Pacific Earthquake Engineering Research Center at the University of California, Berkeley. OpenSees is considered superior for research programs as the prime purpose

of its development was for analysis and research rather than for design purposes as of other commercial software. (Avşar, 2009) considered OpenSees for his Ph.D. thesis for developing fragility curves after comparing various software such as OpenSees, SAP2000, SeismoStruct and LARSA because element library is much more extensive in OpenSees in comparison to other software. Thus, OpenSees software is used in this study.

3 CHAPTER THREE: METHODOLOGY

This study deals with the seismic vulnerability assessment of the two spanned RCC bridges of Nepal. Vulnerability assessment is done with the formulation of fragility curves for the selected bridges. From the population of the bridges, four bridges are selected varying the span length and pier height (as per the availability of the design drawings of the bridges) as sample for the study. A detailed 3-D non-linear analytical model of the bridge piers is generated in OpenSees analysis software. Non-linear static analysis (pushover analysis) is carried out in the analytical model to calculate the capacity of the structure and non-linear time history analysis of structures with numerous ground motions is done to calculate the seismic demand of the structure. The seismic fragility curves are generated for the bridges and further recommendations and conclusions is presented as per the generated curves.

The methodology of the research can be summarized in the flowchart as follows:

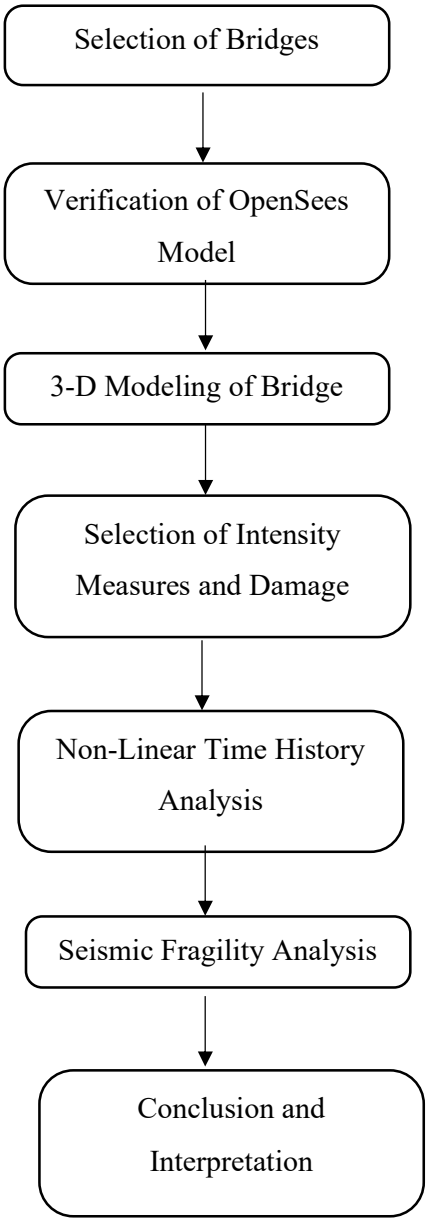

Figure 1: Flowchart of Methodology.

3.1 Selection of Bridges

Table 5 shows the different types of bridges in highways in Nepal (Department of Roads, 2018).

Table 5: Numbers of bridges in Nepal considering superstructure materials. (Department of Roads, 2018).

S.No.	Types of Bridges	Number of bridges	Percentage
1	RCC T-Beam	986	48.8 %
2	RCC Slab	648	32.1 %
3	Steel Truss	85	4.2 %
4	Steel Plate Girder	80	4.0 %
5	Other	222	10.9 %
		Sum = 2021	Sum = 100%

As the maximum number of bridges in Nepal are of RCC superstructure, this study focuses on this type of bridges. As this study only considers the non-linearity and damage state of the column piers only, the study considers the two spanned RCC bridges as the population and selects the four bridges as sample space with varying column height and varying span length and the availability of the bridge structural drawing from the Department of Roads.

3.2 Selection of earthquake time history

Selection of earthquake plays a vital role in the analytical study of seismic vulnerability of structures. It is prominent that the selected earthquake time history represents the proper seismic environment of the site location. The time history can be recorded for real time earthquakes or be synthesized through the usage of computer programs. For this study, various recorded near-fault earthquakes are taken into consideration and the earthquakes are scaled from 0.6 to 2.0 times the original time histories. The earthquakes adopted for this study are listed in Table 6.

Table 6: List of earthquakes used in the study.

EQ ID	Earthquake name	PGA (g)
1	Tabas	0.9
2	Loma Prieta, Los Gatos	0.7
3	Loma Prieta, Lexington Dam	0.67
4	Cape Mendicino	0.62
5	Erzincan	0.42
6	Landers	0.69
7	Northridge, Rinaldi	0.87
8	Northridge, Olive View	0.72
9	Kobe	0.77
10	Gorkha Earthquake	0.177

PGA - Peak ground acceleration; PGV - Peak ground velocity

The response spectrum of the selected earthquakes are shown in the Figure 2.

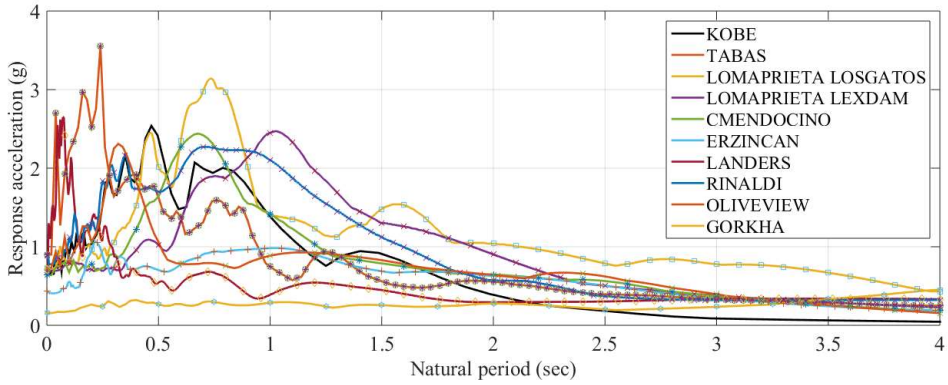

Figure 2: Response spectrum of the time history of the earthquakes.

3.3 Definition of Damage States

This study considers the pier of the bridge as the most prone to failure component. It is assumed that the pier undergoes the initial non-linear deformation and thus the foremost cause of damages to the bridge due to the lateral seismic loads. Due to high moment of inertia in both the horizontal axes, the superstructure of bridge i.e., deck remains elastic and does not undergo failure due to lateral loads. Thus, equivalent loading of superstructure along with live load is transferred to the piers and abutments and the superstructure is not considered as failure components of the bridge in this study.

The damage states have been classified as no damage, slight, moderate, extensive and complete damages. These damage states have been adopted from (Dutta & Mander, 1999) as shown in Table 7.

Table 7: Proposed Damage States Using Columnn Drift Limits (Dutta & Mander, 1999).

Damage State	Description	Drift Limits
Almost no damage	First yield	0.005
Slight damage	Cracking and spalling	0.007
Moderate damage	Loss of anchorage	0.015
Extensive damage	Incipient column collapse	0.025
Complete damage	Column collapse	0.050

3.4 Generation of fragility curves

The fragility curves are obtained by determining the probability of exceeding a specified damage limit state under a given motion intensity.

(Cornell, Asce, Jalayer, Hamburger, & Foutch, 2002) suggested that median demand (S_d) can be represented by following power model:

$S_d = a\ IM^b$

Taking natural logarithmic in the above equation, we get:

$\ln(S_d) = \ln(a) + b \ln(IM)$

Where IM is the seismic intensity measure and a, b are regression coefficients.

Now, the fragility curve can be represented by a lognormal cumulative distribution function as:

$$P_f = F\left(\frac{\ln(S_d/S_c)}{\text{sqrt}(\beta_c^2 + \beta_d^2)}\right)$$

Where

S_c is the median value of structural capacity defined for the damage state

β_c is the lognormal standard deviation of the structural capacity

S_d is the seismic demand in terms of chosen ground motion intensity parameter and

β_d is the lognormal standard deviation for the demand.

4 CHAPTER FOUR: ANALYTICAL MODELING OF BRIDGES

4.1 Material and Section Properties

OpenSees has an extensive library of material properties. This paper uses Steel02 Material – Giuffre-Menegotto-Pinto Model with Isotropic Strain Hardening to represent the reinforcing elements and Concrete02 Material – Linear Tension Softening materials from the OpenSees library. RCC bridge pier is made up of three materials i.e., unconfined concrete, confined concrete and steel reinforcement bars. The unconfined concrete lies on the outer side of transverse reinforcement bars while the confined concrete refers to the concrete inside the transverse reinforcement bars. Concrete02 material is used for both confined and unconfined concrete.

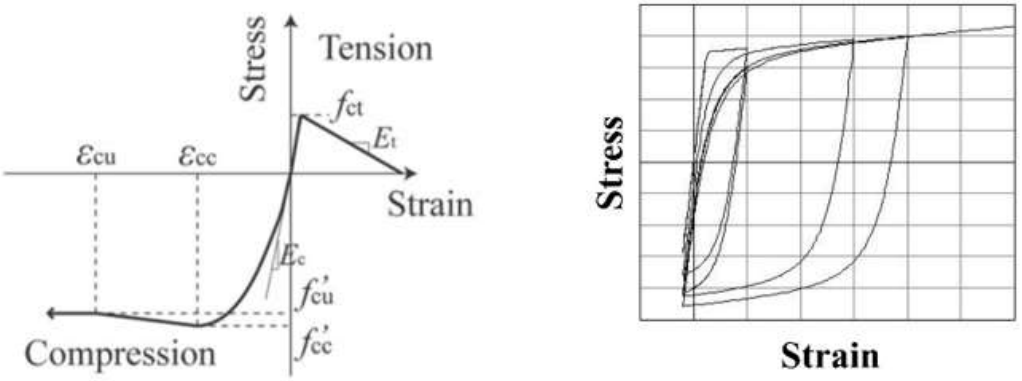

Figure 3: Adopted constitutive material models: (a) Concrete02, (b) Steel02 with isotropic hardening

Fiber section is used to model the bridge pier as the fiber section from the OpenSees library can effectively replicate the non-linear behavior of the pier with required number of fiber sections. The cover concrete and core concrete are divided into four and eight patches respectively. The section is divided into eight wedges in radial direction. The following command is used to create the circular fiber section.

patch circ $matTag $numSubdivCirc $numSubdivRad $xCenter $yCenter $intRad $extRad <$startAng $endAng>

where

$matTag is material integer tag of the previously defined UniaxialMaterial object.

$numSubdivCirc is number of fibers in the circumferential direction.

$numSubdivRad is number of fibers in the radial direction.

$xCenter $yCenter is the x and y coordinates of the center of the circle.

$intRad is internal radius.

$extRad is external radius.

$startAng is starting angle.

$endAng is ending angle.

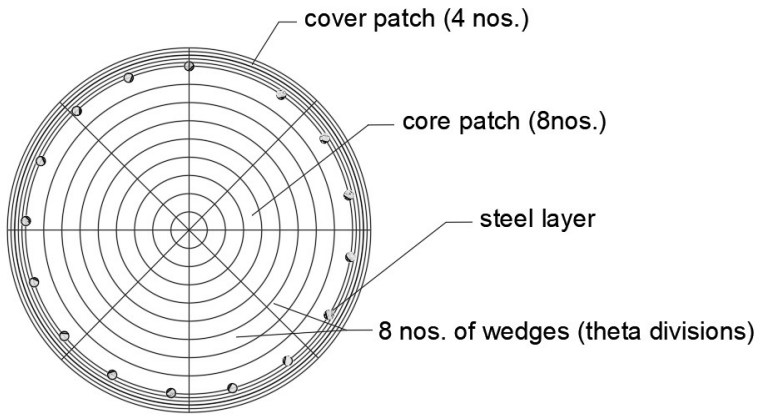

Figure 4: Fiber section of the bridge pier

4.2 Analytical modeling of the bridge

The typical line diagram of the two spanned bridge is shown below with four nodes and three elements.

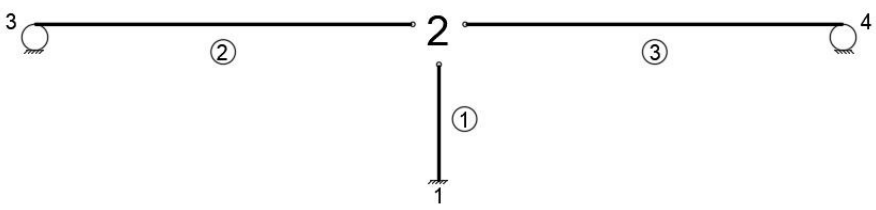

Figure 5: Typical line diagram of two spanned bridge.

The bridge consists of various structural elements: superstructure, abutments, pier and foundation. Bridge piers are the most vulnerable components of the bridge as they tend to enter the nonlinear deformation range under severe earthquake loads (Billah & Alam,

2012). So, the study is done on the effects of earthquake loading on the bridge piers only. Thus, the bridge pier is only modelled including the equivalent superstructure loading to the pier top as shown in the equivalent model.

Figure 6: Equivalent modeling of the bridge pier.

The vulnerability analysis is done for the damage states of the bridge piers only.

4.3 Validation of OpenSees Model

(Moyer & Kowalsky, 2003) conducted an experimental test on cantilever column with four cyclic loading histories. For validation purpose of the bridge model in this study, the cantilever column from the experimental test is modelled in OpenSees validated against the cyclic loading history. The output of the analytical model is then compared with the experimental test result. The material characteristics for Concrete02are:

uniaxialMaterial Concrete02 $matTag $fpc $epsc0 $fpcu $epscu $lambda $ft $Ets

where

$matTag = 1,2 for confined and unconfined concrete.

$fpc = -42.51, -32.7 N/mm2 for confined and unconfined concrete

$epsc0 = -0.00297 , -0.003 for confined and unconfined concrete

$fpcu = -8.502, -6.54 N/ mm2 for confined and unconfined concrete

$epsU = -0.01487, -0.01 for confined and unconfined concrete

$lambda = 0.1

$ft = 4.578 N/ mm2 and

$Ets = 2289 N/ mm2

For Steel02 material model, the material parameters are:

uniaxialMaterial Steel02 $matTag $Fy $E $b $R0 $cR1 $cR2 $a1 $a2 $a3 $a4

where

$matTag = 3

$Fy = 565.4 N/ mm2

$E = 20000 N/ mm2

$b = 0.01

$R0, $cR1, $cR2 = 18, 0.925, 0.15.

$a1, $a2, $a3, $a4 are isotropic hardening parameters (optional).

Material Properties

Concrete Strength: 32.7 MPa

Transverse Steel: Yield Stress: 434.4 MPa

Longitudinal Steel: Yield Stress: 565.4 MPa

Geometry

Diameter: 457.2 mm

Length: 2438.4 mm

Configuration: Cantilever

Loading

Axial Load: 231.3 kN

Longitudinal Reinforcement

Diameter: 19mm

Number of Bars: 12

Reinforcement Ratios: 0.0198

The loading history in the first experimental test is as shown in Figure 3.

The tcl code for the OpenSees model is shown in the Annex A.

The force-displacement curve obtained from the experiment and the analytical model in OpenSees is plotted in Figure 4. The numerical results show good correlation with the test data for the estimated values for base shear, drift, the cyclic hysteresis and the energy dissipation. The same modeling technique is extended to the real scale two-span RCC bridge.

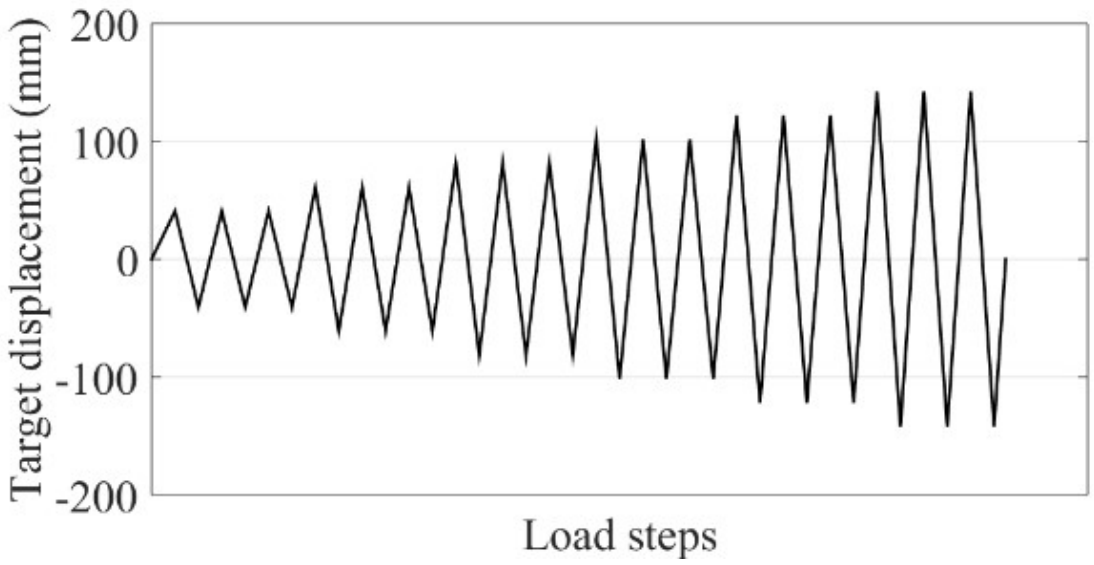

Figure 7: Loading history of experimental test (Moyer & Kowalsky, 2003).

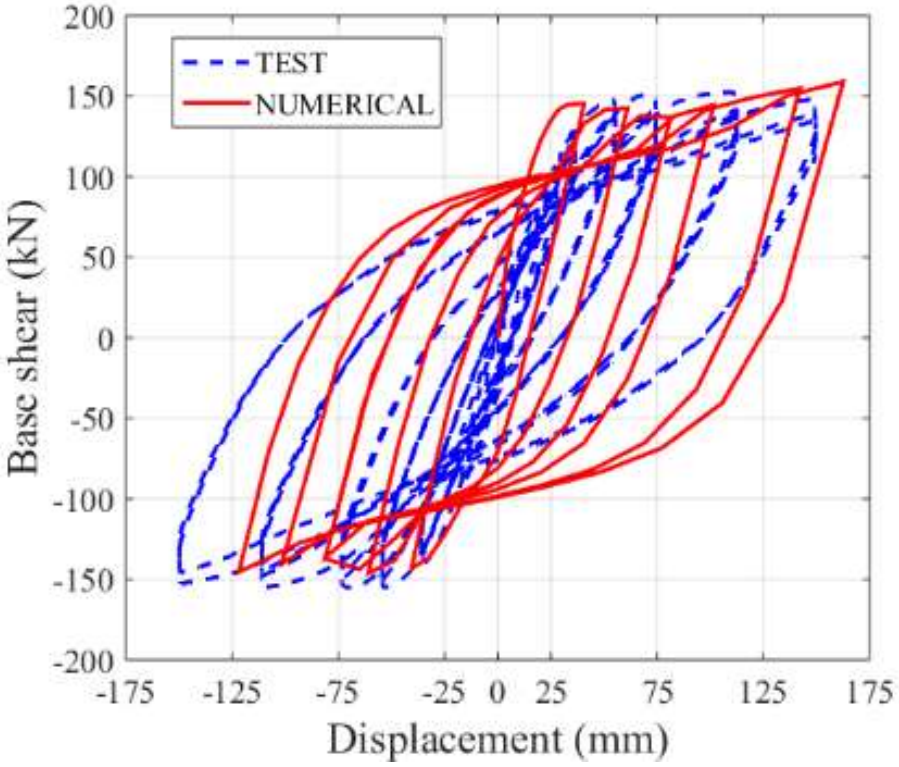

Figure 8: Comparison of experimental result and analytical result.

4.4 Analytical modeling of the Bridge Piers

The details of the pier of the bridges are shown below:

4.4.1 Bijaypur Khola Bridge

Bijaypur Khola Bridge is two spanned RCC bridge of 25m simply supported spans and reinforced concrete deck with precast reinforced concrete beams. The bridge pier is 1950 mm in diameter and 7580 mm in height. The grade of concrete used is M30. Thirty-eight number of longitudinal steel bars with fy=500N/mm^2 are used in the pier. The longitudinal rebar percentage is 1.02%. The tcl code for the analytical model of the bridge pier is given in the Annex B.

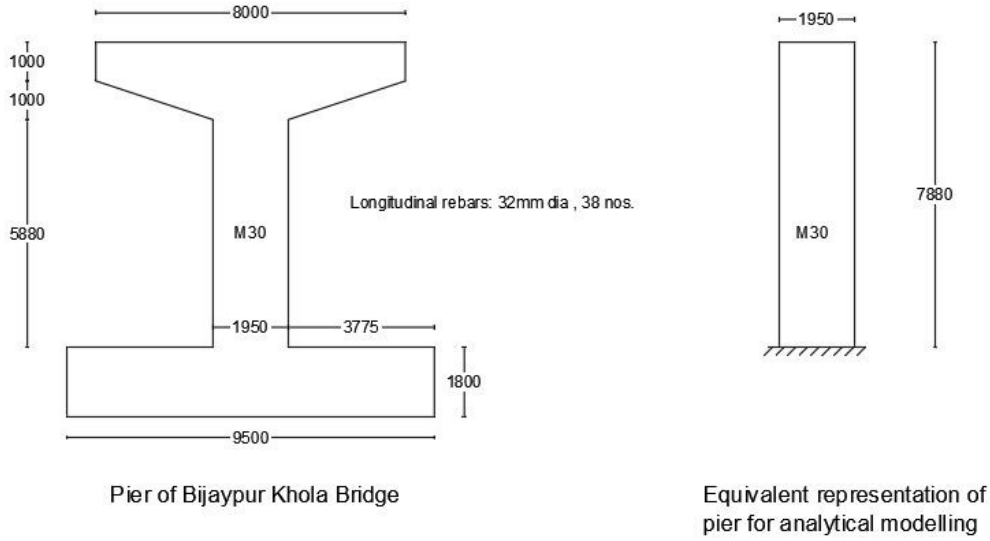

Figure 9: Pier of Bijaypur Khola Bridge with equivalent representation for OpenSees model.

The reinforced concrete pier contains confined and unconfined concrete modeled through Concrete02 material and the reinforcement bars modeled through Steel02 material.

The material characteristics for Concrete02 are:

uniaxialMaterial Concrete02 $matTag $fpc $epsc0 $fpcu $epscu $lambda $ft $Ets

where

$matTag = 1,2 for confined and unconfined concrete.

$fpc = -39.0, -30.0 N/mm2 for confined and unconfined concrete

$epsc0 = -0.00285 , -0.003 for confined and unconfined concrete

$fpcu = -7.8, -6.0 N/ mm2 for confined and unconfined concrete

$epsU = -0.01424, -0.01 for confined and unconfined concrete

$lambda = 0.1

$ft = 4.2 N/ mm2 and

$Ets = 2100 N/ mm2

For Steel02, material model the material parameters are:

uniaxialMaterial Steel02 $matTag $Fy $E $b $R0 $cR1 $cR2 $a1 $a2 $a3 $a4

where

$matTag = 3

$Fy = 500.0 N/ mm2

$E = 20000 N/ mm2

$b = 0.01

$R0, $cR1, $cR2 = 18, 0.925, 0.15.

$a1, $a2, $a3, $a4 are isotropic hardening parameters (optional).

Material Properties

Concrete Strength:	30.0 MPa
Transverse Steel: Yield Stress:	500 MPa
Longitudinal Steel: Yield Stress:	500 MPa

Geometry

Diameter:	1950 mm
Length:	7880 mm
Configuration:	Cantilever

Loading

Axial Load:	4424.31 kN

Longitudinal Reinforcement

Diameter:	32 mm
Number of Bars:	38
Reinforcement Ratios:	0.010233

4.4.2 Lamaha Nadi Bridge

Lamaha Nadi Bridge is two spanned RCC bridge of 35m simply supported spans and two webbed prestressed concrete slab deck. The bridge pier is 2500 mm in diameter and 5797 mm in height. The grade of concrete used is M40. Sixty-five numbers of longitudinal steel bars with fy=500N/mm^2 are used in the pier. The longitudinal rebar percentage is 1.06%.

Material Properties

Concrete Strength:	40.0 MPa
Transverse Steel: Yield Stress:	500 MPa
Longitudinal Steel: Yield Stress:	500 MPa

Geometry

Diameter:	2500 mm
Length:	5797 mm
Configuration:	Cantilever

Loading

Axial Load:	6827.76 kN

Longitudinal Reinforcement

Diameter:	32 mm
Number of Bars:	65
Reinforcement Ratios:	0.0106496

4.4.3 Sewar Khola Bridge

Sewar Khola Bridge is two spanned RCC bridge of 30m simply supported spans and two webbed prestressed concrete slab decks. The bridge pier is 1900 mm in diameter and 8050 mm in height. The grade of concrete used is M25. Fifty numbers of longitudinal steel bars with fy=500N/mm^2 are used in the pier. The longitudinal rebar percentage is 1.41%.

Material Properties

Concrete Strength:	25.0 MPa
Transverse Steel: Yield Stress:	500 MPa

Longitudinal Steel: Yield Stress: 500 MPa

Geometry

Diameter: 1900 mm

Length: 8050 mm

Configuration: Cantilever

Loading

Axial Load: 5532.84 kN

Longitudinal Reinforcement

Diameter: 32 mm

Number of Bars: 50

Reinforcement Ratios: 0.014183

4.4.4 Suikhet Bridge

Suikhet Bridge is two spanned RCC bridge of 30m simply supported spans and two webbed prestressed concrete slab decks. The bridge pier is 2400 mm in diameter and 8850 mm in height. The grade of concrete used is M30. Fifty-seven numbers of longitudinal steel bars with fy=500N/mm^2 are used in the pier. The longitudinal rebar percentage is 1.01%.

Material Properties

Concrete Strength: 30.0 MPa

Transverse Steel: Yield Stress: 500 MPa

Longitudinal Steel: Yield Stress: 500 MPa

Geometry

Diameter: 2400 mm

Length: 8850 mm

Configuration: Cantilever

Loading

Axial Load: 5532.84 kN

Longitudinal Reinforcement

Diameter: 32 mm

Number of Bars: 57

Reinforcement Ratios: 0.01013

5 CHAPTER FIVE: RESULTS AND DISCUSSION

5.1 Non-linear time history analysis

Ten different earthquake time histories are used for the seismic vulnerability assessment of the bridge piers. The fragility curves for the pier of four two spanned bridges of span length from 25m to 35m are prepared. Then, general fragility curve for the pier of two spanned bridge combining the individual fragility curves are prepared. The time history, corresponding drift of the pier and the hysteresis plot for all earthquakes for the bridge pier are shown along with the generated fragility curve for the bridge pier.

5.1.1 BijaypurKhola Bridge

5.1.1.1 Tabas Earthquake

Figure 10 shows the time history of the Tabas earthquake record. Figure 11 shows the hysteretic response of the bridge pier for 100% level of Tabas earthquake. Figure 12 shows the drift time history response of the bridge pier for Tabas earthquake of level 60%, 80%, 100%, 120%, 140%, 160%, 180% and 200%.

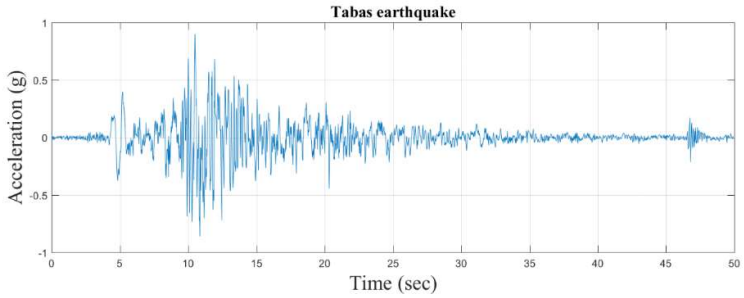

Figure 10: Time history of Tabas Earthquake.

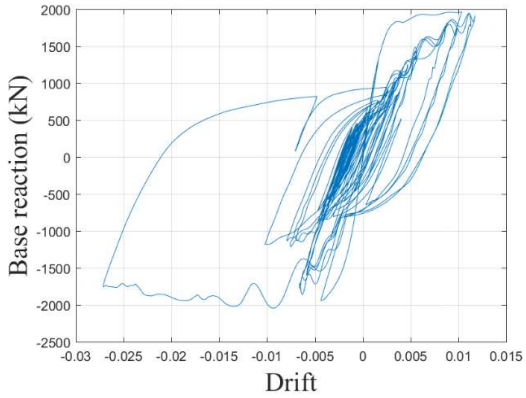

Figure 11: Hysteresis plot for Tabas Earthquake.

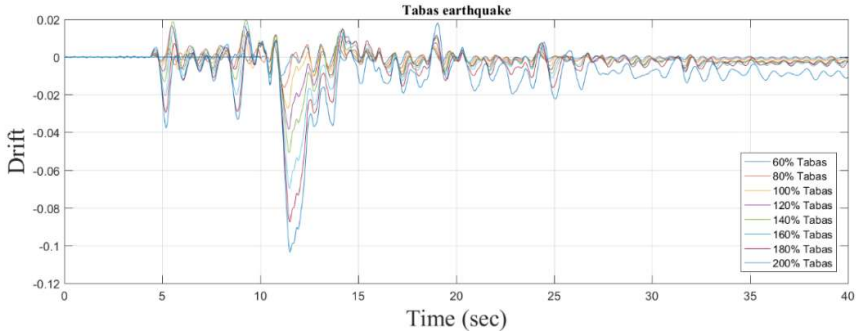

Figure 12: Drift time history for Tabas Earthquake.

5.1.1.2 LomaPrieta Losgatos Earthquake

Figure 13 shows the time history of the LomaPrieta Losgatos earthquake record. Figure 14 shows the hysteretic response of the bridge pier for 100% level of LomaPrieta Losgatos earthquake. Figure 15 shows the drift time history response of the bridge pier for LomaPrieta Losgatos earthquake of level 60%, 80%, 100%, 120%, 140%, 160%, 180% and 200%.

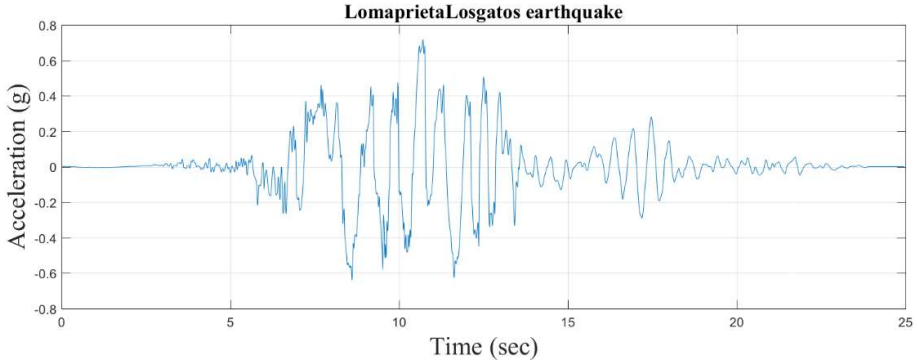

Figure 13: Time history of LomaPrieta Losgatos Earthquake.

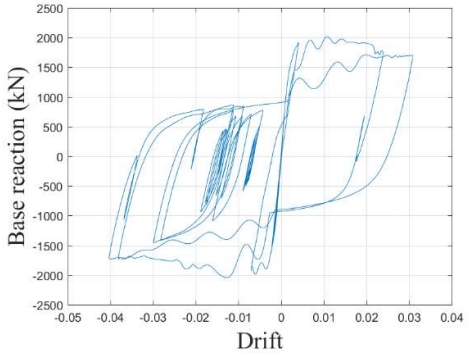

Figure 14: Hysteresis plot for LomaPrieta Losgatos Earthquake.

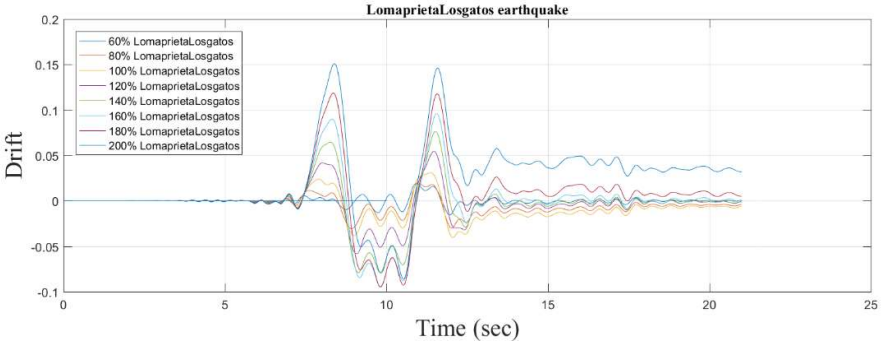

Figure 15: Drift time history for LomaPrieta Losgatos Earthquake.

5.1.1.3 LomaPrieta Lexington Dam Earthquake

Figure 16 shows the time history of the LomaPrieta Lexington Dam earthquake record. Figure 17 shows the hysteretic response of the bridge pier for 100% level of LomaPrieta Lexington Dam earthquake. Figure 18 shows the drift time history response of the bridge pier for LomaPrieta Lexington Dam earthquake of level 60%, 80%, 100%, 120%, 140%, 160%, 180% and 200%.

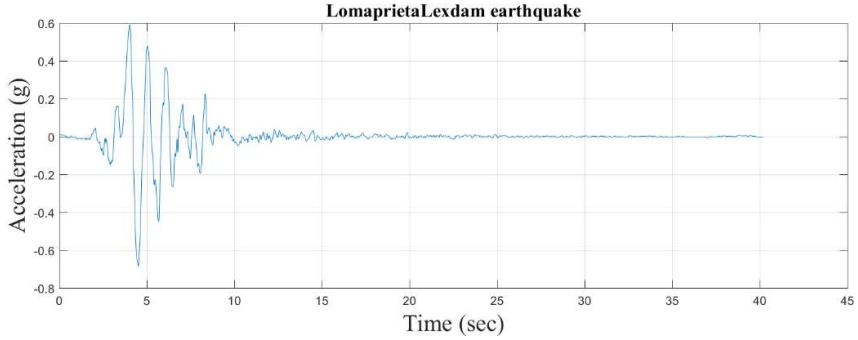

Figure 16: Time history of LomaPrieta Lexington Dam Earthquake.

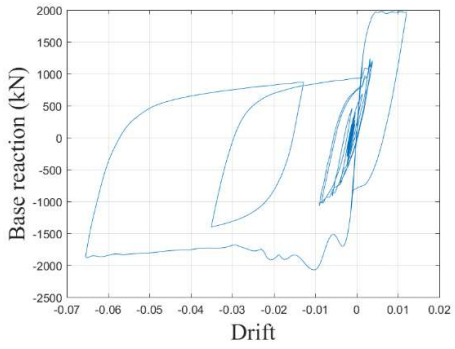

Figure 17: Hysteresis plot for LomaPrieta Lexington Dam Earthquake.

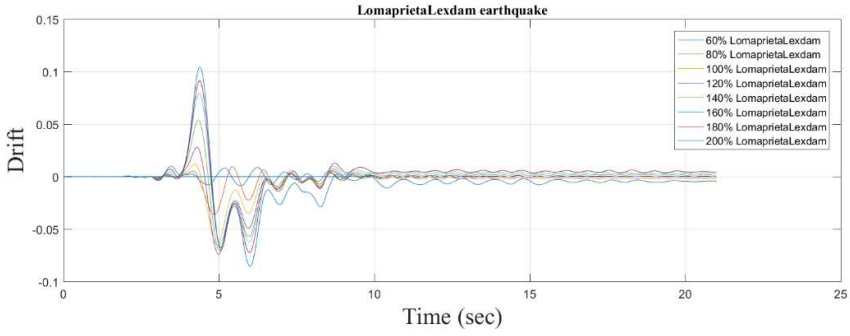

Figure 18: Drift time history for LomaPrieta Lexington Dam Earthquake.

5.1.1.4 Cape Mendecino Earthquake

Figure 19 shows the time history of the Cape Mendecino earthquake record. Figure 20 shows the hysteretic response of the bridge pier for 100% level of Cape Mendecino earthquake. Figure 21 shows the drift time history response of the bridge pier for Cape Mendecino earthquake of level 60%, 80%, 100%, 120%, 140%, 160%, 180% and 200%.

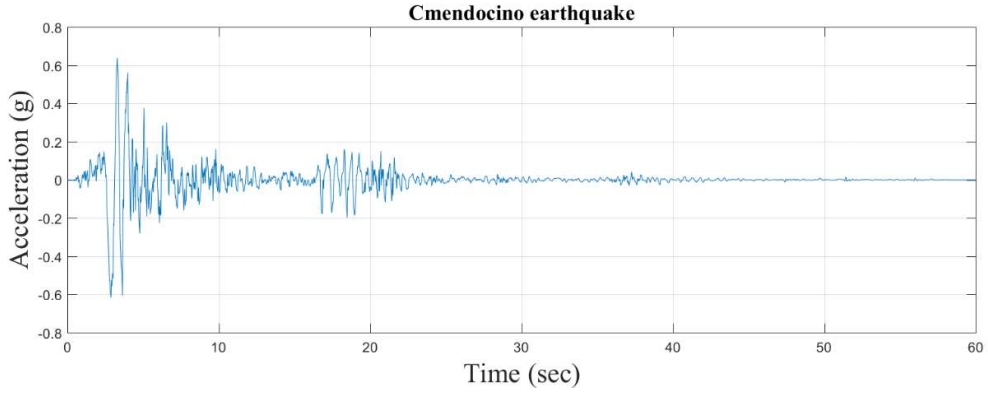

Figure 19: Time history of Cape Mendecino Earthquake.

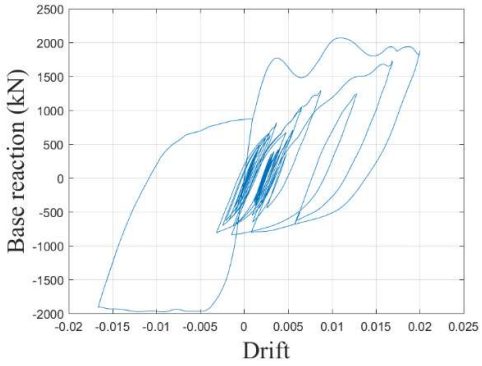

Figure 20: Hysteresis plot for Cape Mendecino Earthquake.

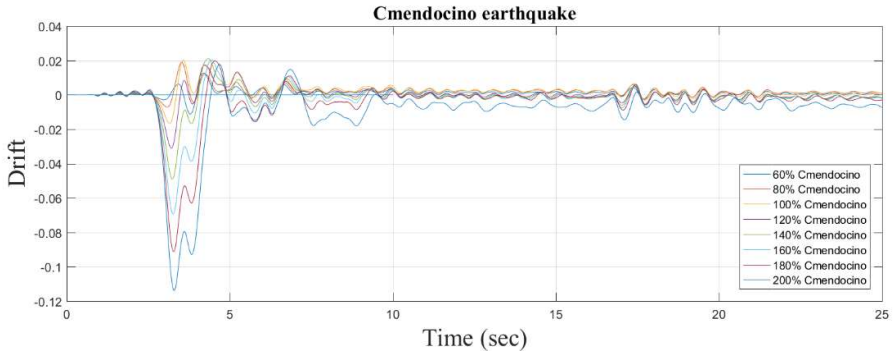

Figure 21: Drift time history for Cape Mendecino Earthquake.

5.1.1.5 *Erzincan Earthquake*

Figure 22 shows the time history of the Erzincan earthquake record. Figure 23 shows the hysteretic response of the bridge pier for 100% level of Erzincan earthquake. Figure 24 shows the drift time history response of the bridge pier for Erzincan earthquake of level 60%, 80%, 100%, 120%, 140%, 160%, 180% and 200%.

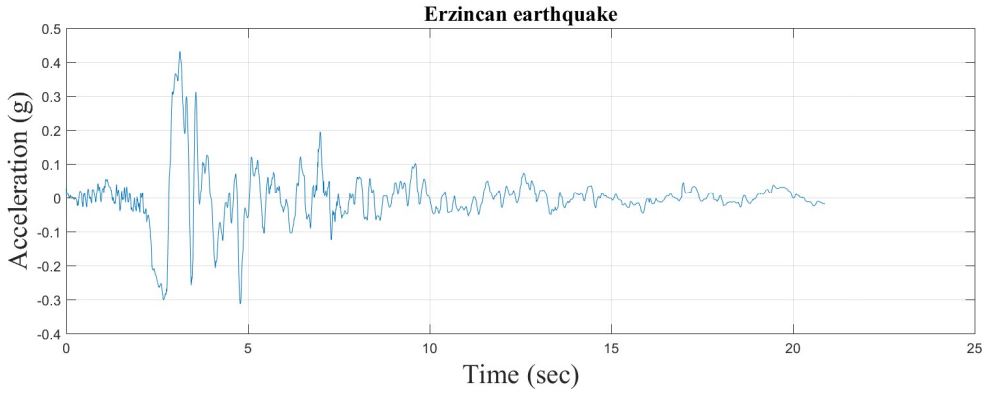

Figure 22: Time history of Erzincan Earthquake.

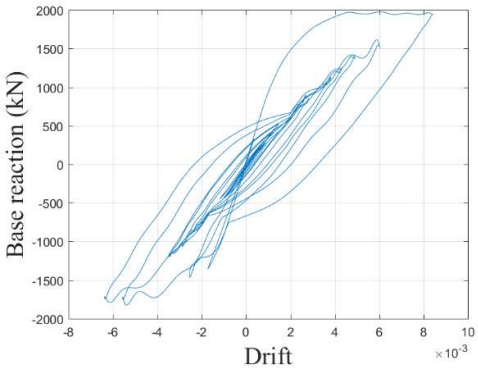

Figure 23: Hysteresis plot for Erzincan Earthquake.

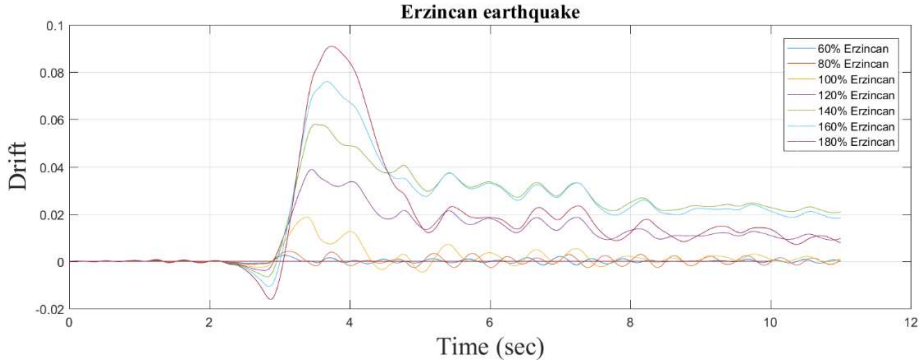

Figure 24: Drift time history for Erzincan Earthquake.

5.1.1.6 *Landers Earthquake*

Figure 25 shows the time history of the Landers earthquake record. Figure 26 shows the hysteretic response of the bridge pier for 100% level of Landers earthquake. Figure 27 shows the drift time history response of the bridge pier for Landers earthquake of level 60%, 80%, 100%, 120%, 140%, 160%, 180% and 200%.

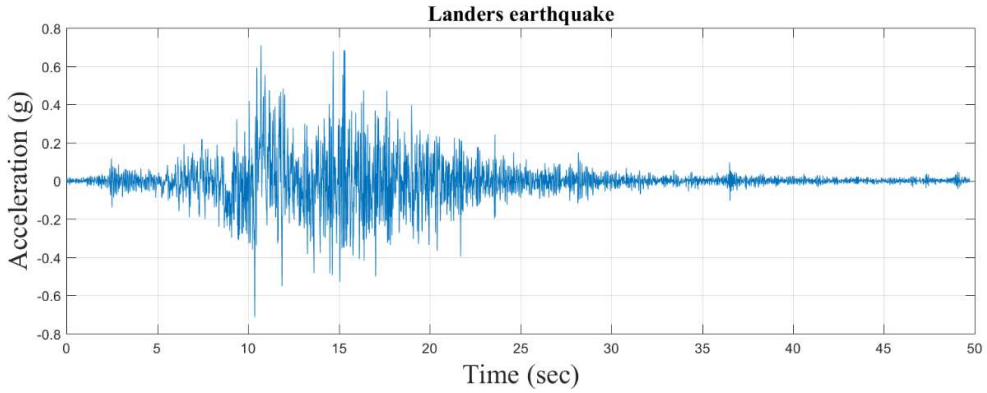

Figure 25: Time history of Landers Earthquake.

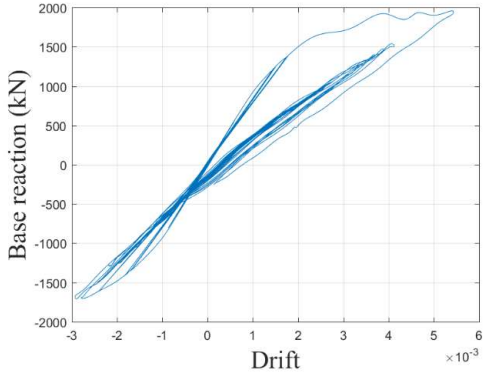

Figure 26: Hysteresis plot for Landers Earthquake.

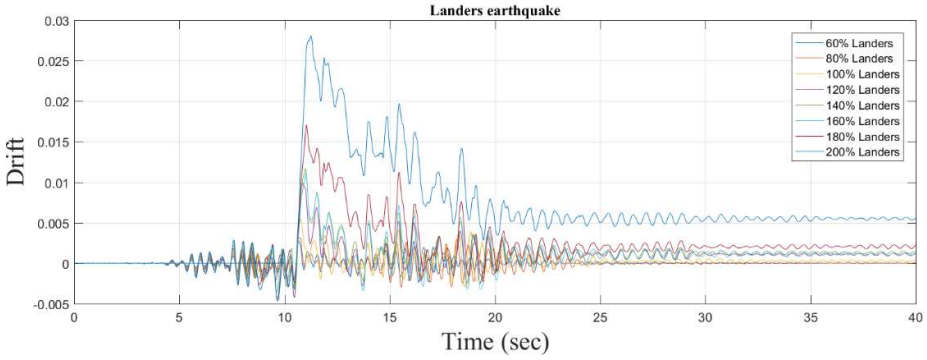

Figure 27: Drift time history for Landers Earthquake.

5.1.1.7 Northridge, Rinaldi Earthquake

Figure 28 shows the time history of the Northridge, Rinaldi earthquake record. Figure 29 shows the hysteretic response of the bridge pier for 100% level of Northridge, Rinaldi earthquake. Figure 30 shows the drift time history response of the bridge pier for Northridge, Rinaldi earthquake of level 60%, 80%, 100%, 120%, 140%, 160%, 180% and 200%.

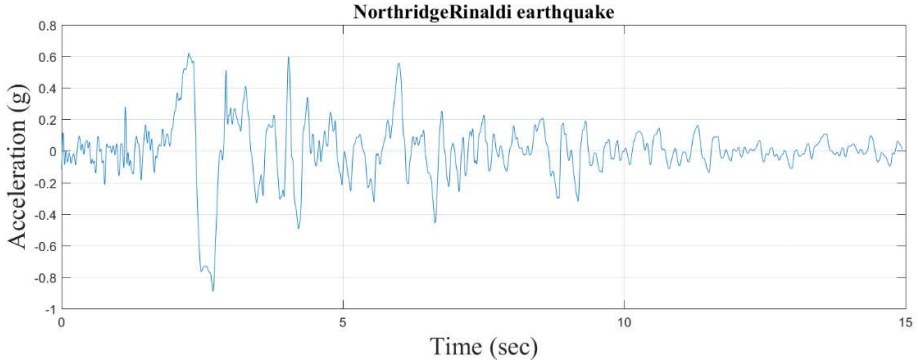

Figure 28: Time history of Northridge, Rinaldi Earthquake.

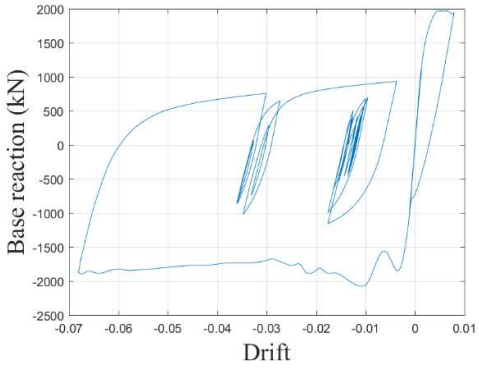

Figure 29: Hysteresis plot for Northridge, Rinaldi Earthquake.

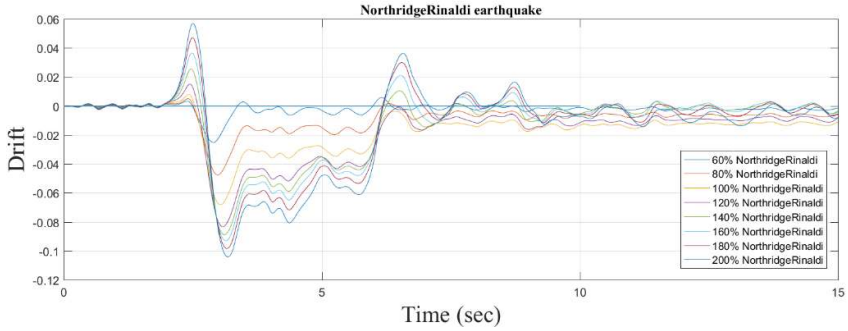

Figure 30: Drift time history for Northridge, Rinaldi Earthquake.

5.1.1.8 Northridge, Oliveview Earthquake

Figure 31 shows the time history of the Northridge, Oliveview earthquake record. Figure 32 shows the hysteretic response of the bridge pier for 100% level of Northridge, Oliveview earthquake. Figure 33 shows the drift time history response of the bridge pier for Northridge, Oliveview earthquake of level 60%, 80%, 100%, 120%, 140%, 160%, 180% and 200%.

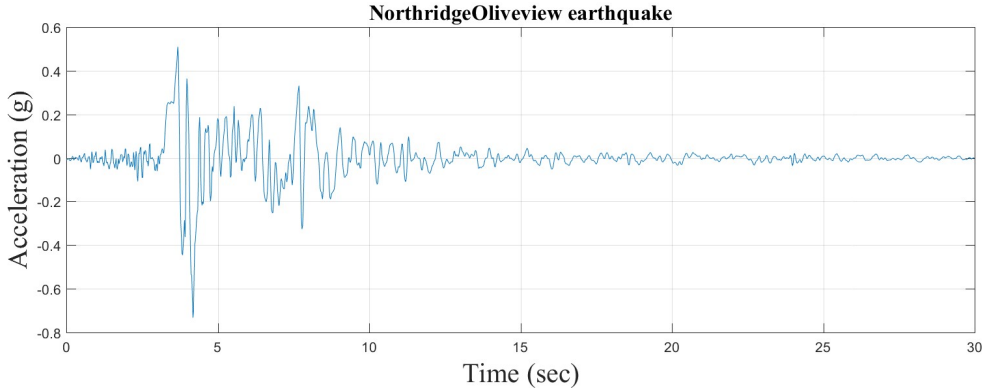

Figure 31: Time history of Northridge, Oliveview Earthquake.

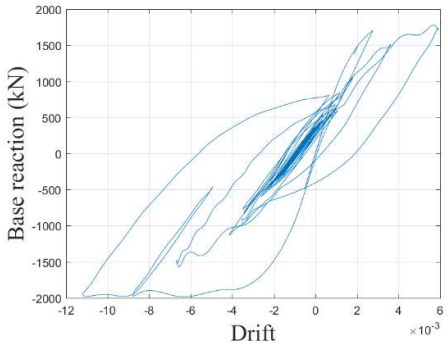

Figure 32: Hysteresis plot for Northridge, Oliveview Earthquake.

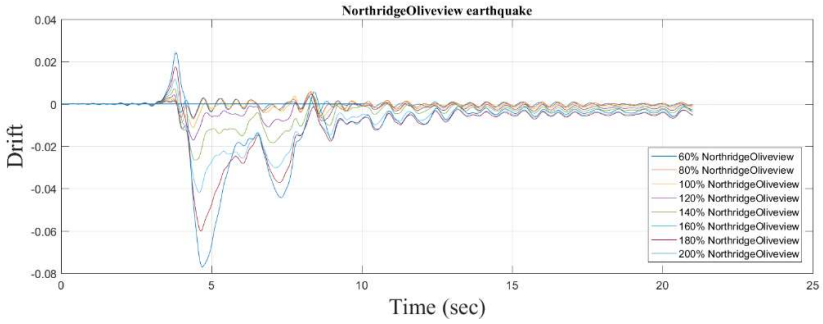

Figure 33: Drift time history for Northridge, Oliveview Earthquake.

5.1.1.9 Kobe Earthquake

Figure 34 shows the time history of the Kobe earthquake record. Figure 35 shows the hysteretic response of the bridge pier for 100% level of Kobe earthquake. Figure 36 shows the drift time history response of the bridge pier for Kobe earthquake of level 60%, 80%, 100%, 120%, 140%, 160%, 180% and 200%.

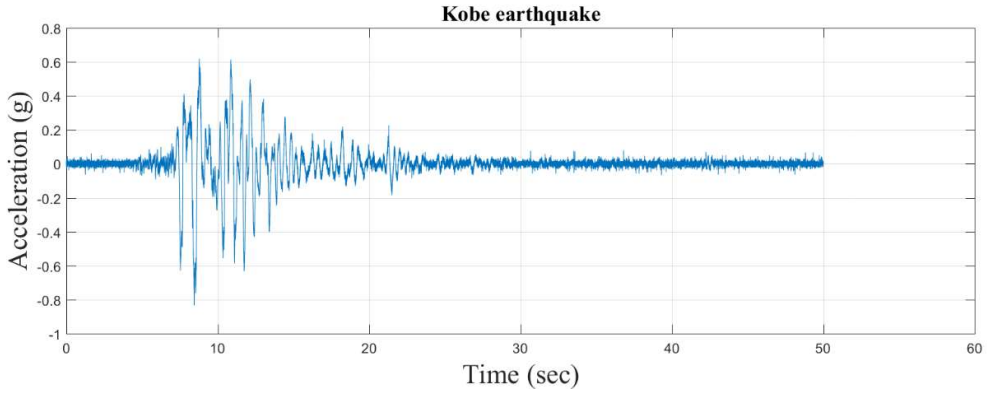

Figure 34: Time history of Kobe Earthquake.

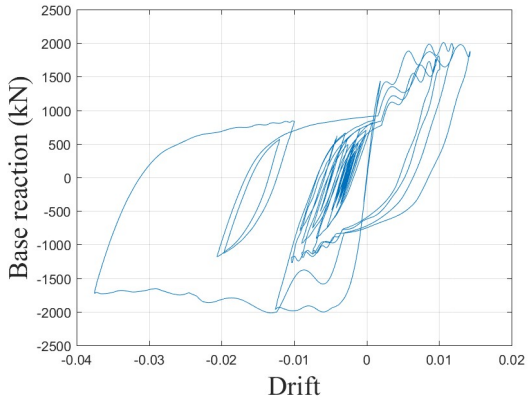

Figure 35: Hysteresis plot for Kobe Earthquake.

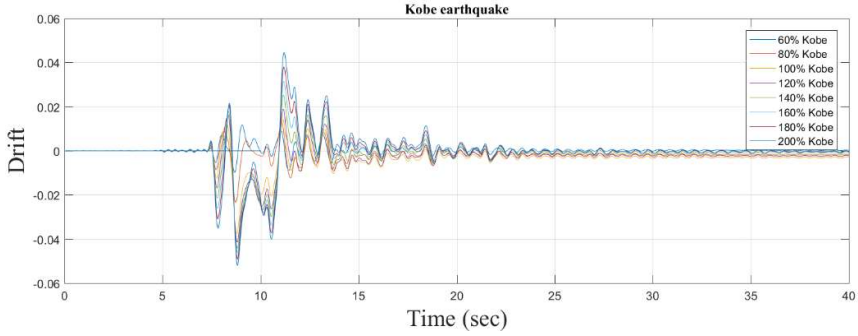

Figure 36: Drift time history for Kobe Earthquake.

5.1.1.10 Gorkha Earthquake

Figure 37 shows the time history of the Gorkha earthquake record. Figure 38 shows the hysteretic response of the bridge pier for 100% level of Gorkha earthquake. Figure 39 shows the drift time history response of the bridge pier for Gorkha earthquake of level 60%, 80%, 100%, 120%, 140%, 160%, 180% and 200%.

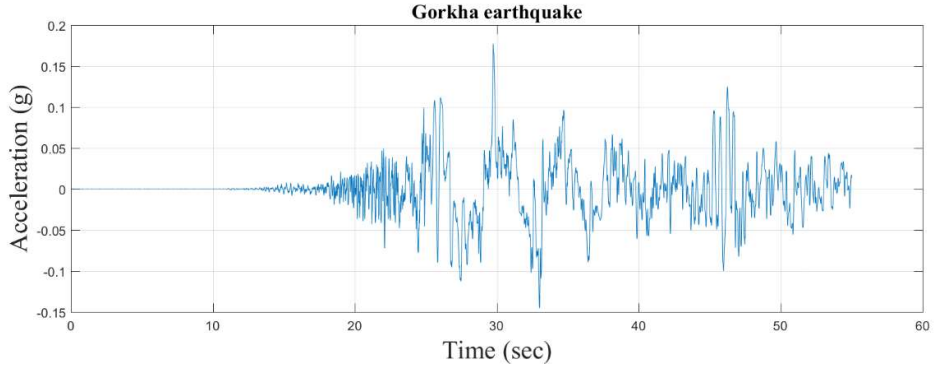

Figure 37: Time history of Gorkha Earthquake.

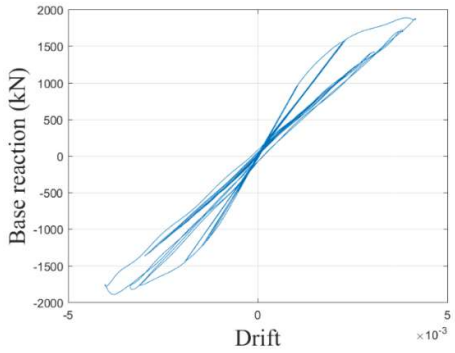

Figure 38: Hysteresis plot for Gorkha Earthquake.

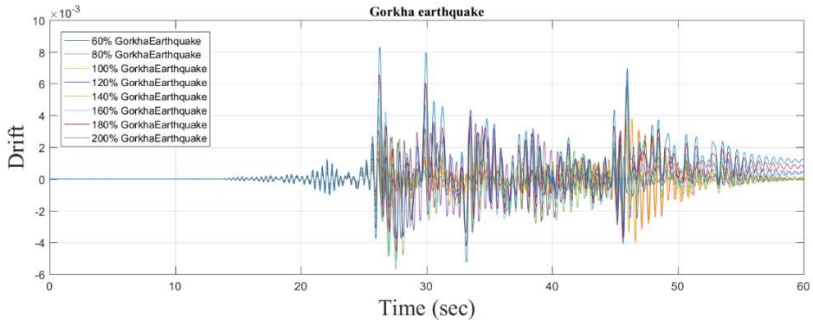

Figure 39: Drift time history for Gorkha Earthquake.

The PGA and the maximum drift from the above scaled time histories are plotted on the ln(PGA) and the ln(drift) axes and the fragility curve is developed.

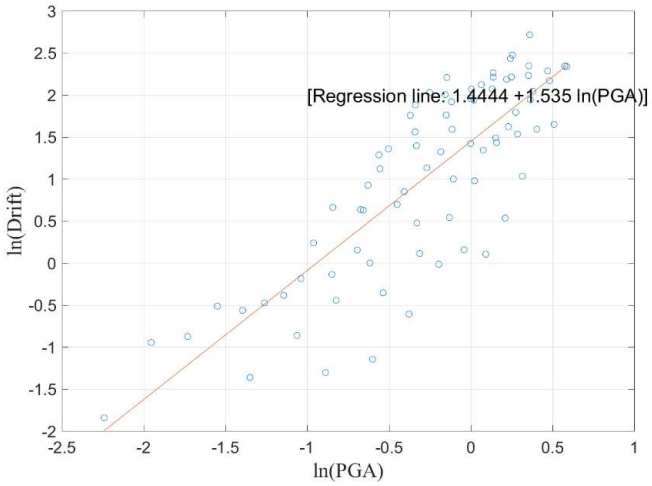

Figure 40: ln(PGA) vs ln(Drift) plot.

The curve shows that at 0.5g PGA, the probability that the bridge suffers slight, moderate, extensive and complete damage is 0.70, 0.50, 0.33 and 0.28 respectively whereas at 1g PGA, the probability that the bridge suffers slight, moderate, extensive and complete damage is 0.91, 0.78, 0.64 and 0.44 respectively.

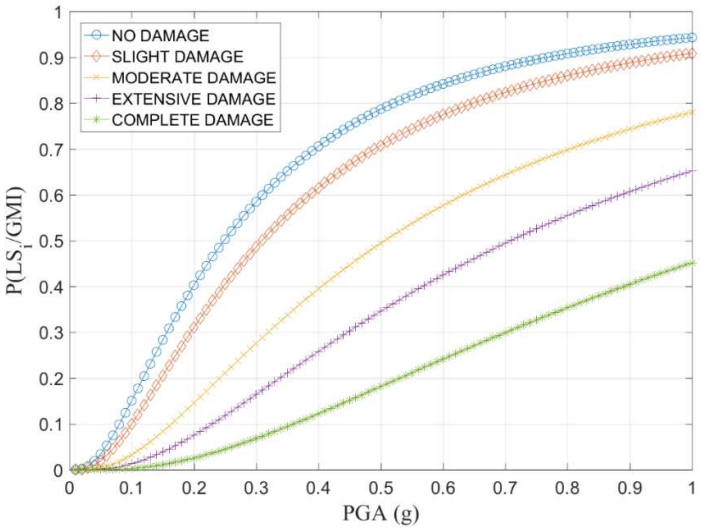

Figure 41: Fragility curve of Bijaypur Bridge.

5.1.2 Lamaha Nadi Bridge

5.1.2.1 Tabas Earthquake

Figure 42 shows the time history of the Tabas earthquake record. Figure 43 shows the hysteretic response of the bridge pier for 100% level of Tabas earthquake. Figure 44 shows the drift time history response of the bridge pier for Tabas earthquake of level 60%, 80%, 100%, 120%, 140%, 160%, 180% and 200%.

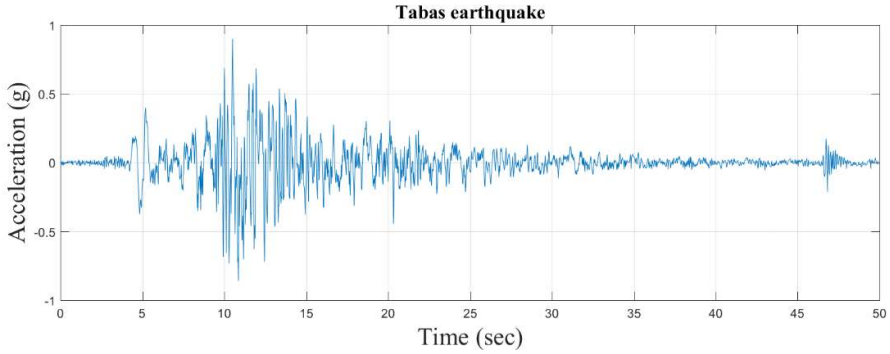

Figure 42: Time history of Tabas Earthquake.

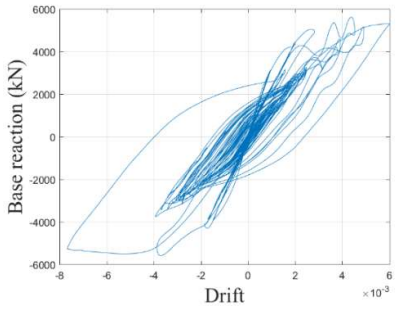

Figure 43: Hysteresis plot for Tabas Earthquake.

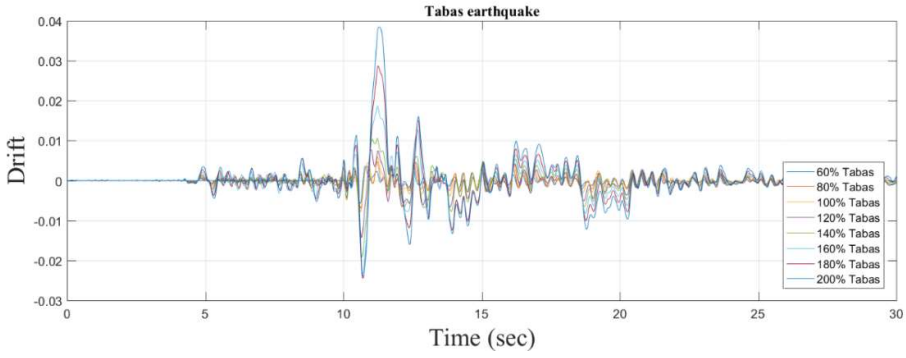

Figure 44: Drift time history for Tabas Earthquake.

Similarly, the figures for the other earthquakes are shown in the Annex C.

The plot of ln(PGA) and the ln(drift) axes along with the fragility curve is shown.

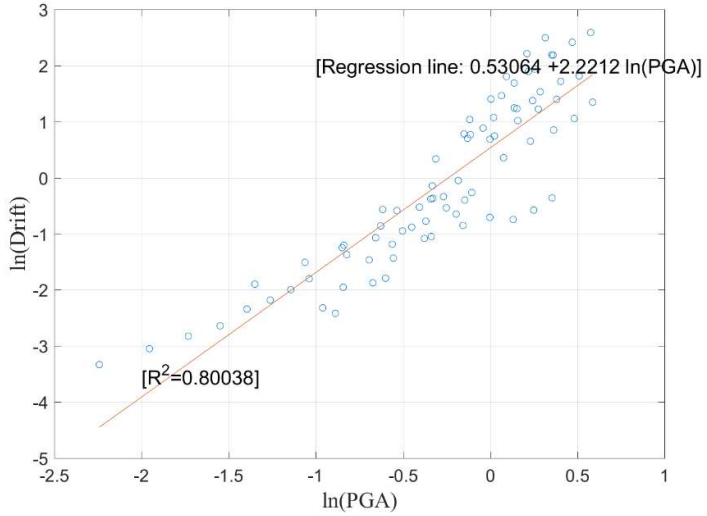

Figure 45: ln(PGA) vs ln(Drift) plot.

The curve shows that at 0.5g PGA, the probability that the bridge suffers slight, moderate damage is 0.20, 0.04 respectively and no possibility of extensive and complete damage whereas at 1g PGA, the probability that the bridge suffers slight, moderate, extensive and complete damage is 0.88, 0.58, 0.30 and 0.09 respectively.

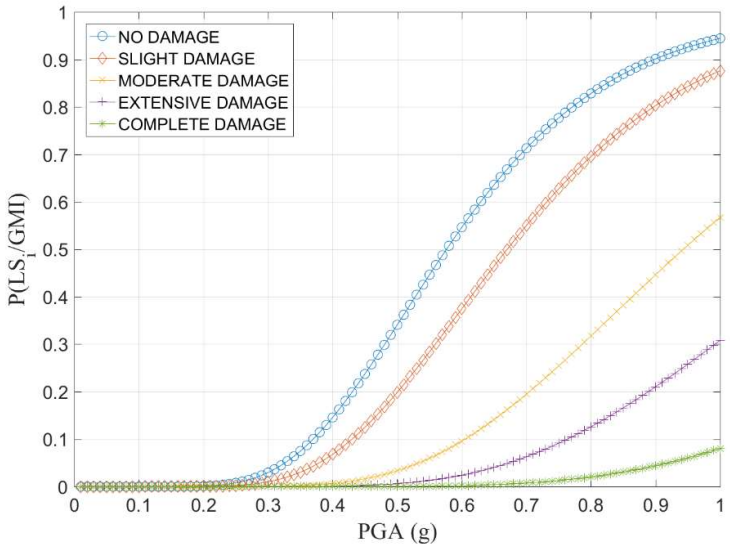

Figure 46: Fragility curve of Lamaha Nadi Bridge.

5.1.3 Sewar Khola Bridge

5.1.3.1 Tabas Earthquake

Figure 47 shows the time history of the Tabas earthquake record. Figure 48 shows the hysteretic response of the bridge pier for 100% level of Tabas earthquake. Figure 49

shows the drift time history response of the bridge pier for Tabas earthquake of level 60%, 80%, 100%, 120%, 140%, 160%, 180% and 200%.

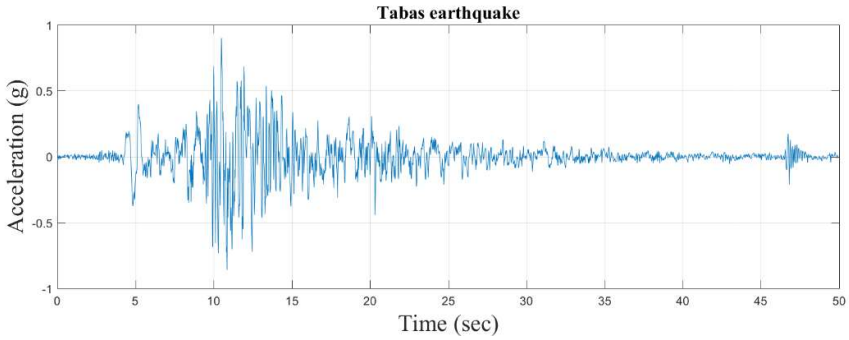

Figure 47: Time history of Tabas Earthquake.

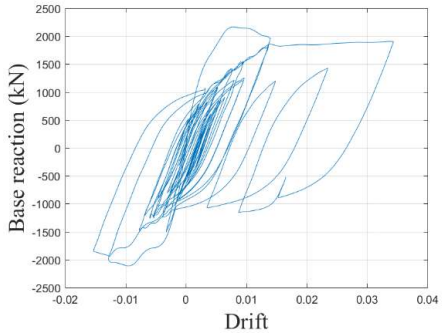

Figure 48: Hysteresis plot for Tabas Earthquake.

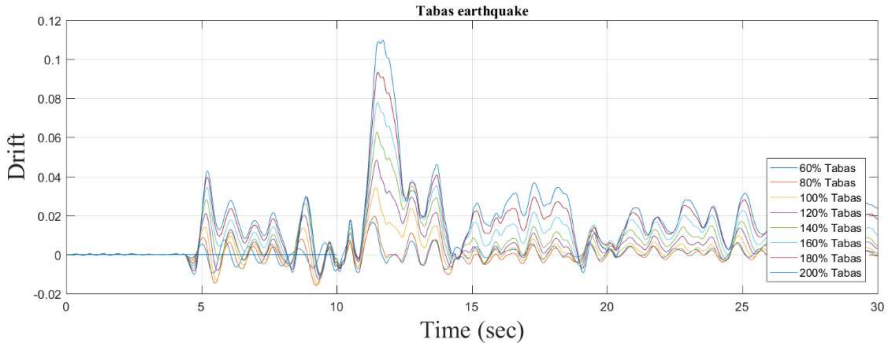

Figure 49: Drift time history for Tabas Earthquake.

Similarly, the figures for the other earthquakes are shown in the Annex D.

The plot of ln(PGA) and the ln(drift) axes along with the fragility curve is shown.

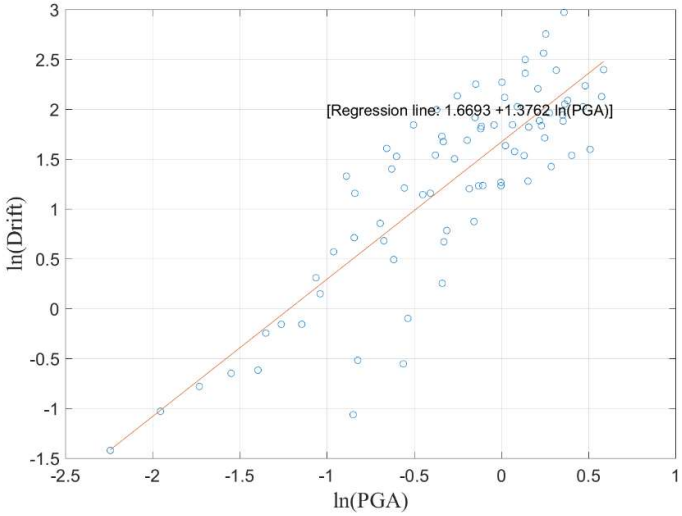

Figure 50: ln(PGA) vs ln(Drift) plot.

The curve shows that at 0.5g PGA, the probability that the bridge suffers slight, moderate, extensive and complete damage is 0.74, 0.58, 0.44 and 0.29 respectively whereas at 1g PGA, the probability that the bridge suffers slight, moderate, extensive and complete damage is 0.90, 0.78, 0.68 and 0.51 respectively.

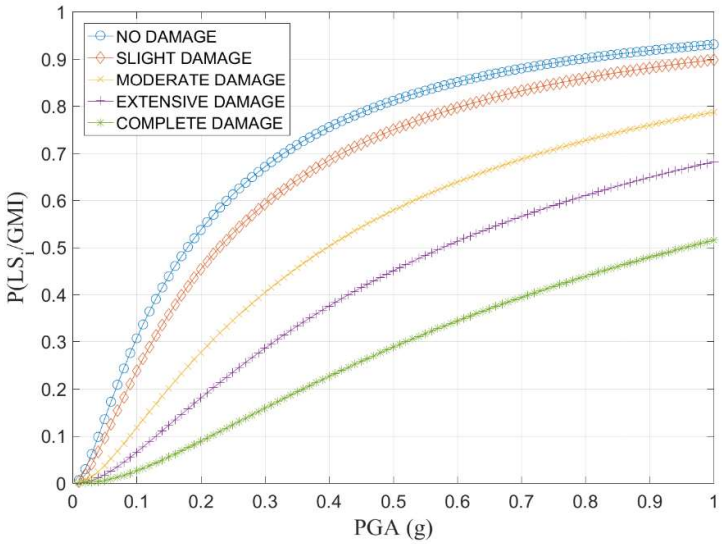

Figure 51: Fragility curve of Sewar Khola Bridge.

5.1.4 Suikhet Bridge

5.1.4.1 Tabas Earthquake

Figure 52 shows the time history of the Tabas earthquake record. Figure 53 shows the hysteretic response of the bridge pier for 100% level of Tabas earthquake. Figure 54

shows the drift time history response of the bridge pier for Tabas earthquake of level 60%, 80%, 100%, 120%, 140%, 160%, 180% and 200%.

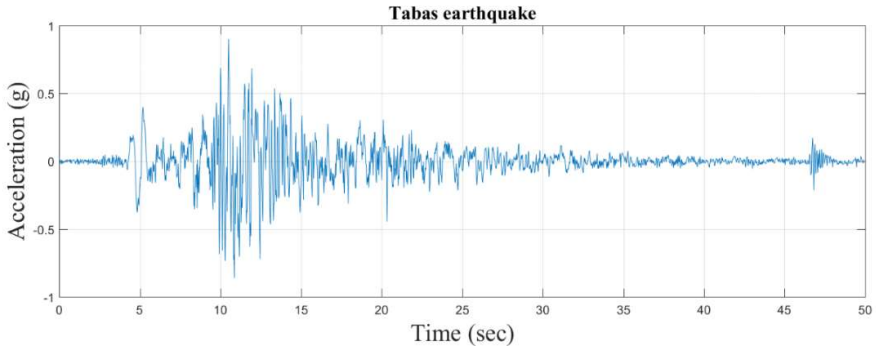

Figure 52: Time history of Tabas Earthquake.

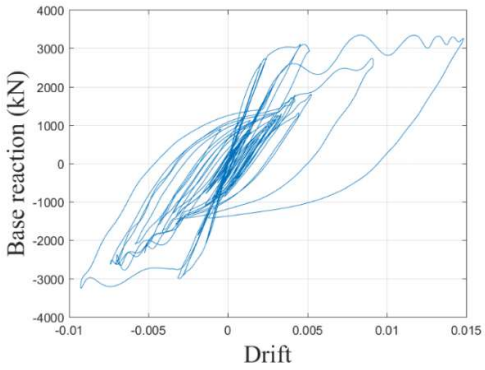

Figure 53: Hysteresis plot for Tabas Earthquake.

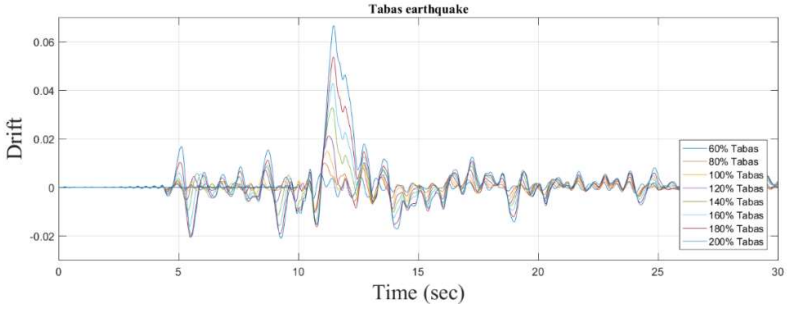

Figure 54: Drift time history for Tabas Earthquake.

Similarly, the figures for the other earthquakes are shown in the Annex E.

The plot of ln(PGA) and the ln(drift) axes along with the fragility curve is shown.

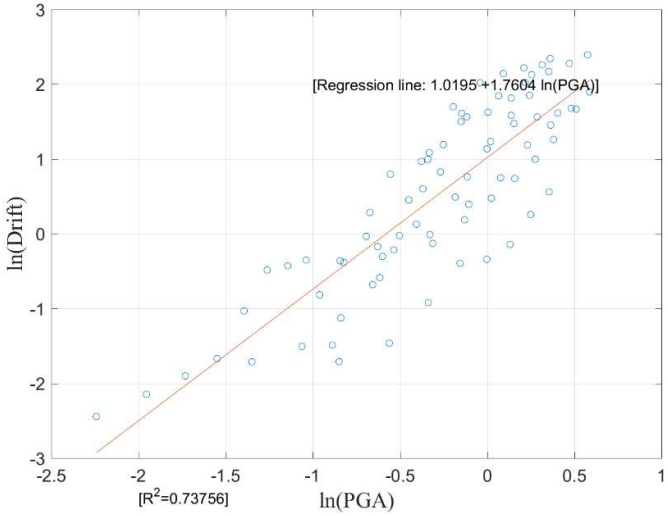

Figure 55: ln(PGA) vs ln(Drift) plot.

The curve shows that at 0.5g PGA, the probability that the bridge suffers slight, moderate, extensive and complete damage is 0.58, 0.26, 0.12 and 0.04 respectively whereas at 1g PGA, the probability that the bridge suffers slight, moderate, extensive and complete damage is 0.92, 0.74, 0.54 and 0.26 respectively.

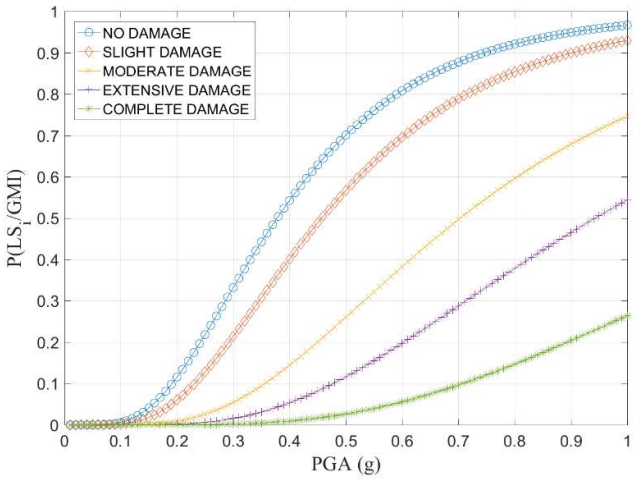

Figure 56: Fragility curve of Suikhet Bridge.

The ln(PGA) and ln(drift) from the individual bridges are combined and single fragility curves for the two spanned reinforced concrete bridges with several damage states are prepared.

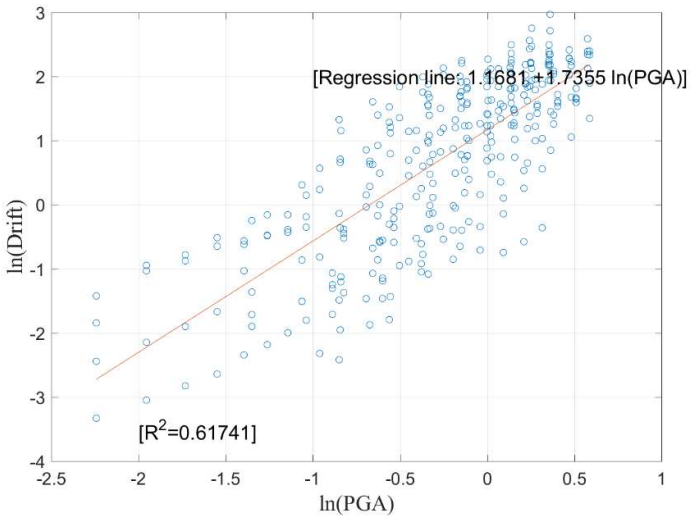

Figure 57: ln(PGA) vs ln(Drift) plot.

The curve shows that at 0.5g PGA, the probability that the bridge suffers slight, moderate, extensive and complete damage is 0.61, 0.34, 0.28 and 0.06 respectively whereas at 1g PGA, the probability that the bridge suffers slight, moderate, extensive and complete damage is 0.92, 0.76, 0.59 and 0.34 respectively

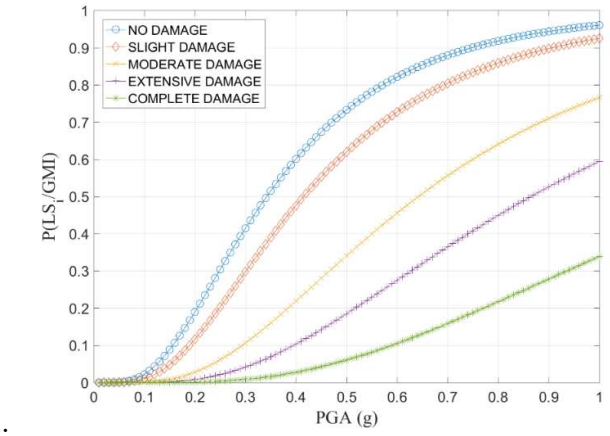

Figure 58: Fragility curve of two spanned bridge.

6 CHAPTER SIX: CONCLUSION

In this thesis, non-linear time history analysis is done for the selected four bridges with two spans and single circular pier in the middle. The drift calculated is utilized to generate fragility curves for the bridge pier using the drift limit as the damage state and peak ground acceleration as the intensity measure. These curves prove to be effective for the rational decision-making criteria as they provide the damage expectations beforehand for the earthquakes of different peak ground accelerations.

6.1 Conclusions

The major conclusions of this research work are listed below:

1. The two spanned RCC bridges of Nepal are susceptible to slight damage with thirty percent probability of exceedance for the earthquake with 0.25g PGA while negligible susceptible to moderate, extensive and complete damage.
2. The two spanned RCC bridges of Nepal are highly susceptible to slight damage for the earthquake with 0.5g PGA while slightly susceptible to moderate and extensive damage and are not susceptible to complete damage.
3. The two spanned RCC bridges of Nepal are highly susceptible to moderate and extensive damage for the earthquake with 1.0g PGA while slightly susceptible to complete damage.

6.2 Recommendations

The following points can be incorporated in the further continuations of this research work:

1. The foundation can be modeled using spring mass system.
2. The study can be done for bridges with several spans and the bridges with other construction materials other than reinforced cement concrete.

7 References

AASHTO. (2010). *LRFD Bridge Design Specifications.* Washington, D.C.: American Association of State Highway and Transportation Officials.

Alessandri, S., Giannini, R., & Paolacci, F. (2013). Aftershock risk assessment and the decision to open traffic on bridges.

Avşar, Ö. (2009). Fragility based seismic vulnerability assessment of ordinary highway bridges in turkey. Middle East Technical University, Turkey.

Banerjee, S., & Chi, C. (2013). State-dependent fragility curves of bridges based on vibration measurements. *Probabilistic Engineering Mechanics*(33), 116-125.

Billah, A. M., & Alam, M. S. (2014). Seismic fragility assessment of highway bridges: a state-of-the-art review. *Structure and Infrastructure Engineering*.

Billah, M. A., & Alam, S. M. (2012). Development of fragility curves for retrofitted multi-column bridge bent subjected to near fault ground motion. *15 WCEE.* Lisboa.

Cornell, C., Asce, M., Jalayer, F., Hamburger, R., & Foutch, D. (2002). Management agency steel moment frame guidelines.

Department of Roads. (2018). Statistics of Strategic Road Networks.

Dutta, A., & Mander, J. (1999). Seismic fragility analysis of highway bridges. *Center-to-Center Project Workshop on Earthquake Engineering in Transportation Systems.* Tokyo.

Eunsoo, C., Reginald, D., & Bryant, N. (2003). Seismic fragility of typical bridges in moderate seismic zones. *Engineering Structures*.

Ferreira, F., Moutinho, C., Cunha, A., & Caetano, E. (2019). *An artificial accelerogram generator code written in matlab.* WILEY.

Gautam, D., Rupakhety, R., & Adhikari, R. (2019). Empirical fragility functions for Nepali highway bridges affected by the 2015 Gorkha Earthquake.

Ghobarah, A., Aly, N. M., & El-Attar, M. (1997). Performance level criteria and evaluation. *Proceedings of the International Workshop on Sesmic Design Methodologies for the next generation of codes*, (pp. 207-215). Balkema: Rotterdam.

Hwang, H., J.B.L, & Y.H.C. (2001). *Seismic fragility analysis of highway bridges.* Center for Earthquake Research and Information, The University of Memphis.

Jin-Hak Yi, S.-H. K. (2007). PDF interpolation technique for seismic fragility analysis of bridges. *Engineering Structures, 29*(7), 1312-1322. doi:https://doi.org/10.1016/j.engstruct.2006.08.019.

Luco, N., & Cornell, A. (2007). Structure-specific scalar intensity measures for near source and ordinary earthquake ground motions. *Earthquake Spectra*(23), 357-392.

Mackie, K., & Stojadinovic, B. (2004). Fragility curves for reinforced concrete highway overpass bridges. *13th World Conference on Earthquake Engineering.* Vancouver, Canada.

Moyer, M. J., & Kowalsky, M. J. (2003). Influence of Tension Strain on Buckling of Reinforcement in Concrete Columns. *ACI Structural Journal*.

Nielson, B. G. (2005). Analytical fragility curves for highway bridges in moderate seismic zones.

Nielson, B. G., & DesRoches, R. (2006). Seismic fragility methodology for highway bridges using a component level approach. *Earthquake Engineering and Structural Dynamics*, 823-839.

Nielson, B., & DesRoches, R. (2007). Seismic fragility curves for typical highway bridge classes in the central and southeastern United States. *Earthquake Spectra*, 615-633.

Padgett, J., & DesRoches, R. (2008). Methodology for the development of analytical fragility curves for retrofitted bridges. *Earthquake Engineering and Structural Dynamics*.

Park, Y. J., & Ang, A.-S. (1985). Sesmic damage analysis of reinforced concrete buildings. *Journal of Structural Engineering, 111*(4), 740-757.

Quancai, X., Gaohu, L., Hao, C., Chong, X., & Baio, F. (2016). Seismic damage to road networks subjected to earthquakes in Nepal, 2015.

Shinozuka, M., Feng, M., Kim, H., Uzawa, T., & Ueda, T. (2001). *Statistical analysis of fragility curves.* Buffalo: MCEER, University at Buffalo.

Shiozuka, M., Feng, M., Kim, H., & Kim, S. (2000). Nonlinear static procedure for fragility curve development. *ASCE Journal of Engineering Mechanics*(126), 1287-1296.

Silvia Mazzoni, F. M. (n.d.). OpenSees Command Language Manual.

Tavares, D., Padgett, J., & Paultre, P. (2012). Fragility curves of typical as-built highway bridges in eastern canada. *Engineering Structures*.

Tavares, D., Suescun, J., Paultre, P., & Padgett, J. (2013). Seismic fragility of a highway bridge in Quebec.

World Bank. (n.d.). Nepal earthquake post disaster needs assessment. *http://documents.worldbank.org/curated/en/546211467998818313/pdf/97501-WP-PUBLIC-Box391481B-nepal-post-disaster-needs-assement-report-PUBLIC.pdf*.

Yamazaki, F., Motomura, H., & Hamada, T. (2000). Damage assessment of expressway networks in japan based on seismic monitoring. *12th World Conference on Earthquake Engineering.* Auckland, New Zealand.

Yi, J.-H., Kim, S.-H., & Kushiyama, S. (2007). PDF interpolation technique for seismic fragility analysis of bridges. *Engineering Structures*, 1312-1322.

8 ANNEXES

ANNEX A

Tcl code for the validation of the OpenSees model.

```
# Code for the validation of the model.
#
#   ^Y
#   |
#   2       __
#   |        |
#   |        |
#   |        |
#  (1)      LCol
#   |        |
#   |        |
#   |        |
#  =1=      _|_  -------->X
#
#Setup
# units: kN, mm, sec

wipe;                                   # clear memory of all past model definitions
file mkdir Moyervalidationcyclic;       # create data directory
model BasicBuilder -ndm 2 -ndf 3;       # ndm=#dimension, ndf=#dofs


#define Geometry
set LCol 2438.4                         # column length
set Weight 11.445.;                     # self weight
# define section geometry
set DCol 457.2;                         # column depth
set pi [expr acos(-1)];

# calculated parameters
set PCol [expr $Weight/2];              # nodal dead-load weight per column
set g 9810              ;                       # g.
set Mass [expr $PCol/$g];               # nodal mass
# calculated geometry parameters
set ACol [expr $pi*$DCol*$DCol/4.];  # cross-sectional area
set IzCol [expr 1./64.*pow($DCol,4)];  # Column moment of inertia

# nodal coordinates:
node 1 0 0;                             # node#, X, Y
node 2 0 $LCol

# Single point constraints -- Boundary Conditions
fix 1 1 1 1;                            # node DX DY RZ

# nodal masses:
mass 2 $Mass  1e-9 0.;                  # node#, Mx My Mz, Mass=Weight/g, neglect rotational inertia at nodes

# Define ELEMENTS & SECTIONS -------------------------------------------------------------
set ColSecTag 1;                        # assign a tag number to the column section
# define section geometry
set coverCol 7.95;                      # Column cover to reinforcing steel NA.
set numBarsCol 12;                      # number of longitudinal-reinforcement bars
set barAreaCol [expr $pi*19*19/4] ;     # d=19;area of longitudinal-reinforcement bars
```

```
# MATERIAL parameters ------------------------------------------------------------------
set IDconcCore 1;
set IDconcCover 2;                      # material ID tag -- unconfined cover concrete
set IDreinf 3;                          # material ID tag -- reinforcement

set fc -0.0327;                         # CONCRETE Compressive Strength (+Tension, -Compression)
set Ec [expr 5.000*sqrt(-$fc*1000)];    # Concrete Elastic Modulus
# confined concrete
set Kfc 1.3;
set fc1C [expr $Kfc*$fc];
set eps1C [expr 2.*$fc1C/$Ec];
set fc2C [expr 0.2*$fc1C];
set eps2C [expr 5*$eps1C];

# unconfined concrete
set fc1U   $fc;                         # UNCONFINED concrete (todeschini parabolic model), maximum stress
set eps1U-0.003;                        # strain at maximum strength of unconfined concrete
set fc2U   [expr 0.2*$fc1U];            # ultimate stress
set eps2U-0.01;                         # strain at ultimate stress
set lambda 0.1;                         # ratio between unloading slope at $eps2 and initial slope $Ec
# tensile-strength properties
set ftU [expr -0.14*$fc1U];
set ftC [expr -0.14*$fc1C];             # tensile strength +tension
set Ets [expr $ftU/0.002];              # tension softening stiffness
# ----------
set Fy 0.5654;                          # STEEL yield stress
set Es 200.00;                          # modulus of steel
set Bs 0.01;                            # strain-hardening ratio
set R0 18;                              # control the transition from elastic to plastic branches
set cR1 0.925;                          # control the transition from elastic to plastic branches
set cR2 0.15;                           # control the transition from elastic to plastic branches

uniaxialMaterial Concrete02 $IDconcCore $fc1C $eps1C $fc2C $eps2C $lambda $ftU $Ets;
uniaxialMaterial Concrete02 $IDconcCover $fc1U $eps1U $fc2U $eps2U $lambda $ftU $Ets;
uniaxialMaterial Steel02 $IDreinf $Fy $Es $Bs $R0 $cR1 $cR2;

# FIBER SECTION properties -------------------------------------------------------------
#
#
# RC section:
  set ri 0.0;                   # inner radius of section. only for hollow sections
  set ro [expr $DCol/2.];       # outer radius of the section
  set nfCoreR 8;                # number of radial divisions in the core (number of rings)
  set nfCoreT 8;                #number of theta divisions in the core (number of wedges)
  set nfCoverR 4;               # number of radial divisions in the cover
  set nfCoverT 8;               #number of theta divisions in the cover



  section fiberSec $ColSecTag   {;      # Define the fiber section
        set rc [expr $ro - $coverCol];
        patch circ $IDconcCore $nfCoreT $nfCoreR 0 0 $ri $rc 0 360;         # Define the concrete patch
        patch circ $IDconcCover $nfCoverT $nfCoverR 0 0 $rc $ro 0 360;      # Define the cover patch
        set theta [expr 360.0/$numBarsCol];                                 #   Determine   angle   increment
between bars
        layer circ $IDreinf $numBarsCol $barAreaCol 0 0 $rc $theta 360;     # Define reinforcing layer
  };    # end of fibersection definition

set ColTransfTag 1;                             # associate a tag to column transformation
geomTransf Linear $ColTransfTag  ;

# element connectivity:
set numIntgrPts 5;
element nonlinearBeamColumn 1 1 2 $numIntgrPts $ColSecTag $ColTransfTag;
```

```
# Define RECORDERS ----------------------------------------------------------------
recorder Node -file Moyervalidationcyclic/DFree.out -time -node 2 -dof 1 2 3 disp;
recorder Node -file Moyervalidationcyclic/RBase.out -time -node 1 -dof 1 2 3 reaction;


# define GRAVITY -----------------------------------------------------------------
pattern Plain 1 Linear {
  load 2 0 -$PCol 0
}

# Gravity-analysis parameters -- load-controlled static analysis
#
set Tol 1.0e-8;                         # convergence tolerance for test
constraints Plain;                      # how it handles boundary conditions
numberer Plain;                         # renumber dof's to minimize band-width (optimization)
system BandGeneral;                     # how to store and solve the system of equations in the analysis
test NormDispIncr $Tol 6 ;              # determine if convergence has been achieved at the end of an iteration step
algorithm Newton;                       # use Newton's solution algorithm: updates tangent stiffness at every
iteration
set NstepGravity 10;                    # apply gravity in 10 steps
set DGravity [expr 1./$NstepGravity];   # first load increment;
integrator LoadControl $DGravity;       # determine the next time step for an analysis
analysis Static;                        # define type of analysis static or transient
analyze $NstepGravity;                  # apply gravity
loadConst -time 0.0                     # maintain constant gravity loads and reset time to zero
puts "Model Built"
puts "Model Built"
set omega2 [eigen 1];
set omega1 [expr pow($omega2 ,0.5)];
set period1 [expr 2*3.1415/$omega1];
puts "  OpenSees Calculated Period of First mode= $period1"

# STATIC PUSHOVER ANALYSIS ---------------------------------------------------------------------------------------
-----
#
set IDctrlNode 2;                       # node where displacement is read for displacement control
set IDctrlDOF 1;                        # degree of freedom of displacement read for displacement control
#set Dmax [expr 0.1*$LCol];             # maximum displacement of pushover. push to 10% drift.
#set Dincr [expr 0.001*$LCol];          # displacement increment for pushover

# create load pattern for lateral pushover load
set Hload $Weight;
pattern Plain 200 Linear {;             # define load pattern -- generalized
        load 2 $Hload 0.0 0.0 ;         # define lateral load in static lateral analysis
}

#  set up analysis parameters


constraints Plain;
numberer Plain
system BandGeneral
set Tol 1.e-5;
set maxNumIter 10;
set printFlag 0;
set TestType EnergyIncr ;
test $TestType $Tol $maxNumIter $printFlag;

set algorithmType Newton
algorithm $algorithmType;
analysis Static

foreach Dincr { 4.064 -8.128 10.16 -12.192 14.224 -16.256 18.288 -20.32 22.352 -24.384 26.416 -28.448 14.224 }
{
        integrator DisplacementControl  $IDctrlNode   $IDctrlDOF $Dincr
        analyze 10
```

```
}


# perform Static Pushover Analysis
set Nsteps [expr int($Dmax/$Dincr)];        # number of pushover analysis steps
analyze $Nsteps

set ok [analyze $Nsteps];               # this will return zero if no convergence problems were encountered

#  in case of convergence problems
#if {$ok != 0} {
# change some analysis parameters to achieve convergence
# performance is slower inside this loop
        set ok 0;
        set controlDisp 0.0;            # start from zero
        set D0 0.0;                     # start from zero
        set Dstep [expr ($controlDisp-$D0)/($Dmax-$D0)]
        while {$Dstep < 1.0 && $ok == 0} {
                set controlDisp [nodeDisp $IDctrlNode $IDctrlDOF ]
                set Dstep [expr ($controlDisp-$D0)/($Dmax-$D0)]
                set ok [analyze 1 ]
                if {$ok != 0} {
                        puts "Trying Newton with Initial Tangent .."
                        test NormDispIncr   $Tol 2000  0
                        algorithm Newton -initial
                        set ok [analyze 1 ]
                        test $TestType $Tol $maxNumIter  0
                        algorithm $algorithmType
                }
                if {$ok != 0} {
                        puts "Trying Broyden .."
                        algorithm Broyden 8
                        set ok [analyze 1 ]
                        algorithm $algorithmType
                }
                if {$ok != 0} {
                        puts "Trying NewtonWithLineSearch .."
                        algorithm NewtonLineSearch .8
                        set ok [analyze 1 ]
                        algorithm $algorithmType
                }
        }
        };      # end if ok !0

puts "DonePushover"
```

ANNEX B

Tcl code for the OpenSees model of the Bijaypur Bridge. Other bridges can be modeled using their own geometric and sectional properties.

```
# Bridge pier of Bijaypur Bridge
#
#
# SET UP ---------------------------------------------------------------------
# units: kN, mm, sec
wipe;
file mkdir Data;
set Tanalysis 60;
model BasicBuilder -ndm 3 -ndf 6;

# define GEOMETRY
set LCol 7880 ;
set Weight 4424.310;
# define section geometry
set DCol 1950;
set pi [expr acos(-1)];

# calculated parameters
set PCol [expr $Weight];
set g 9810              ;
set Mass [expr $PCol/$g];
# calculated geometry parameters
set ACol [expr $pi*$DCol*$DCol/4.];
set IzCol [expr 1./64.*pow($DCol,4)];

# nodal coordinates:
node 1 0 0 0;
node 2 0 0 $LCol;

# Single point constraints
fix 1 1 1 1 1 1 1;

# nodal masses:
mass 2 $Mass $Mass $Mass 0.1 0.1 0.1;


# Define ELEMENTS & SECTIONS
set ColSecTag 1;
# define section geometry
set coverCol 75.;
set numBarsCol 38;
set barAreaCol [expr $pi*32*32/4] ;

# MATERIAL parameters
set IDconcCore 1;
set IDconcCover 2;
set IDreinf 3;
# nominal concrete compressive strength
set fc -.030;
set Ec [expr 5.000*sqrt(-$fc*1000)];
# confined concrete
set Kfc 1.3;
set fc1C [expr $Kfc*$fc];
set eps1C [expr 2.*$fc1C/$Ec];
set fc2C [expr 0.2*$fc1C];
set eps2C [expr 5*$eps1C];

# unconfined concrete
```

```
set fc1U                $fc;
set eps1U-0.003;
set fc2U   [expr 0.2*$fc1U];
set eps2U-0.01;
set lambda 0.1;
# tensile-strength properties
set ftU [expr -0.14*$fc1U];
set ftC [expr -0.14*$fc1C];
set Ets [expr $ftU/0.002];
# -----------
set Fy .500;
set Es 200.000;
set Bs 0.01;
set R0 18;
set cR1 0.925;
set cR2 0.15;
uniaxialMaterial Concrete02 $IDconcCore $fc1C $eps1C $fc2C $eps2C $lambda $ftC $Ets;
uniaxialMaterial Concrete02 $IDconcCover $fc1U $eps1U $fc2U $eps2U $lambda $ftU $Ets;
uniaxialMaterial Steel02 $IDreinf $Fy $Es $Bs $R0 $cR1 $cR2;


# FIBER SECTION properties -------------------------------------------------------------
# symmetric section
# column is circular
# RC section:
   set ri 0.0;
   set ro [expr $DCol/2.];
   set nfCoreR 8;
   set nfCoreT 8;
   set nfCoverR 4;
   set nfCoverT 8;



   section fiberSec $ColSecTag -GJ 1e14  {;
            set rc [expr $ro - $coverCol];
            patch circ $IDconcCore $nfCoreT $nfCoreR 0 0 $ri $rc 0 360;
            patch circ $IDconcCover $nfCoverT $nfCoverR 0 0 $rc $ro 0 360;
            set theta [expr 360.0/$numBarsCol];
            layer circ $IDreinf $numBarsCol $barAreaCol 0 0 $rc $theta 360;
   };

set ColTransfTag 1;
geomTransf LinearWithPDelta $ColTransfTag 1 0 0 ;

set numIntgrPts 5;
element nonlinearBeamColumn 1 1 2 $numIntgrPts $ColSecTag $ColTransfTag;

# Define RECORDERS ----------------------------------------------------------
recorder Node -file Data/DFree2_10.out -time -node 2 -dof 1 2 3 disp;
recorder Node -file Data/RBase1_10.out -time -node 1 -dof 1 2 3 reaction;

logFile logFileResults.txt

# define GRAVITY -------------------------------------------------------------
pattern Plain 1 Constant {
   load 2 0 0 [expr -$Weight]  0 0 0

}

puts "gravity loads assigned"

#Analysis


# Gravity-analysis parameters --
```

```
set Tol 1.0e-8;
constraints Plain;
numberer Plain;
system BandGeneral;
test NormDispIncr $Tol 15 ;
algorithm Newton;
set NstepGravity 1;
set DGravity [expr 1./$NstepGravity];
integrator LoadControl $DGravity;
analysis Static;
analyze 10;
loadConst -time 0.0

puts "Gravity Analysis is done!"

# Define Rayleigh damping (modes 1 and 3)
# D=$alphaM*M + $betaKcurr*Kcurrent + $betaKcomm*KlastCommit + $beatKinit*$Kinitial
set xDamp 0.02
set MpropSwitch 1; # where M/K proportionality lies.
set KcurrSwitch 0 ;
set KcommSwitch 1;
set KinitSwitch 0;
set nEigenI 1; # mode 1
set nEigenJ 3; # mode 3
set lambdaN [eigen [expr $nEigenJ]]; # eigenvalue analysis for nEigenJ modes
set lambdaI [lindex $lambdaN [expr $nEigenI-1]]; # eigenvalue mode i
set lambdaJ [lindex $lambdaN [expr $nEigenJ-1]]; # eigenvalue mode j
set omegaI [expr pow($lambdaI,0.5)];
set omegaJ [expr pow($lambdaJ,0.5)];
set alphaM [expr $MpropSwitch*$xDamp*(2*$omegaI*$omegaJ)/($omegaI+$omegaJ)];
set betaKcurr [expr $KcurrSwitch*2.*$xDamp/($omegaI+$omegaJ)];
set betaKcomm [expr $KcommSwitch*2.*$xDamp/($omegaI+$omegaJ)];
set betaKinit [expr $KinitSwitch*2.*$xDamp/($omegaI+$omegaJ)];
rayleigh $alphaM $betaKcurr $betaKinit $betaKcomm;
########################################################################
# Define earthquake (Displacements)
########################################################################
set dt 0.005
set tableISOlong "Path -filePath ISOlong.txt -dt $dt -factor -9810"
#set tableISOtran "Path -filePath ISOtran.txt -dt $dt -factor 2.0"
puts "earthquake loaded"

# Create Load Pattern
pattern UniformExcitation 200001 1 -accel $tableISOlong
########################################################################
test          NormUnbalance     1.0e-5     25
algorithm Newton
system UmfPack
constraints Penalty 1e14 1e14
#                  gamma beta
integrator Newmark   0.5  0.25
numberer RCM
analysis Transient
set ok 0
set maxNumIter 400;
set tol 1e-3;
set testtype NormDispIncr
set DtAnalysis 0.0005;
set tFinal $Tanalysis
set tCurrent 0.0

while {$tCurrent < $tFinal && $ok == 0} {
            # original algorithm and time step
            test $testtype $tol $maxNumIter 0;
            set ok [analyze 1 $DtAnalysis]
            # analysis did not converge, reduce time step
```

```
	if {$ok != 0} {
		puts "$ok != 0 repeat initial time step"
		test $testtype $tol $maxNumIter 2;
		set ok [analyze 1 [expr $DtAnalysis/1.0]];
	}
###modified by Gang Wang %%%%%%%%%%%%%%%%%%
	if {$ok != 0} {
		puts "$ok != 0 reduce to 1/2 time step"
		test $testtype $tol $maxNumIter 2;
		set ok [analyze 1 [expr $DtAnalysis/2.0]];
	}
	if {$ok != 0} {
		puts "$ok != 0 reduce to 1/5 time step"
		test $testtype $tol $maxNumIter 2;
		set ok [analyze 1 [expr $DtAnalysis/5.0]];
	}
	if {$ok != 0} {
		puts "$ok != 0 reduce to 1/10 time step"
		test $testtype $tol $maxNumIter 2;
		set ok [analyze 1 [expr $DtAnalysis/10.0]];
	}
#### modified by Gang Wang END %%%%%%%%%%%%%%%%%%
	if {$ok != 0} {

		puts "$ok != 0 reduce to 1/20 time step"
		test $testtype $tol $maxNumIter 2;
		set ok [analyze 1 [expr $DtAnalysis/20.0]];
	}
	# analysis did not converge ?reduce time step
	if {$ok != 0} {
		puts "$ok != 0, reduce to 1/100 time step"
		test $testtype $tol $maxNumIter 2;
		set ok [analyze 1 [expr $DtAnalysis/100.0]];
	}
	# analysis did not converge ?reduce time step
	if {$ok != 0} {
		puts "$ok != 0 reduce to 1/500 time step"
			test $testtype $tol $maxNumIter 2;
		set ok [analyze 1 [expr $DtAnalysis/500.0]];
	}
	# analysis did not converge ?reduce time step
	if {$ok != 0} {

		puts "$ok != 0 reduce to 1/2500 time step"
		test $testtype $tol $maxNumIter 2;
		set ok [analyze 1 [expr $DtAnalysis/2500.0]];
	}
	# analysis did not converge ?reduce time step
	if {$ok != 0} {

		puts "$ok != 0 reduce to 1/10000 time step"
		test $testtype $tol $maxNumIter 2;
		set ok [analyze 1 [expr $DtAnalysis/10000.0]];
	}
	# analysis did not converge ?reduce time step
	if {$ok != 0} {

		puts "$ok != 0 reduce to 1/50000 time step"
		test $testtype $tol $maxNumIter 2;
		set ok [analyze 1 [expr $DtAnalysis/50000.0]];
	}
	# analysis did not converge ?reduce time step
	if {$ok != 0} {

		puts "$ok != 0 reduce to 1/250000 time step"
		set ok [analyze 1 [expr $DtAnalysis/250000.0]];
```

```
		}
		# analysis did not converge ?reduce time step
		if {$ok != 0} {

			puts "$ok != 0 reduce to 1/1000000 time step"
			set ok [analyze 1 [expr $DtAnalysis/1000000.0]];
		}
		# analysis did not converge ?reduce time step
		if {$ok != 0} {
			puts "$ok != 0 reduce to 1/5000000 time step"
			set ok [analyze 1 [expr $DtAnalysis/5000000.0]];
		}
		# analysis did not converge ?reduce time step
		if {$ok != 0} {
			puts "$ok != 0 reduce to 1/25000000 time step"
			set ok [analyze 1 [expr $DtAnalysis/25000000.0]];
		}
		# analysis did not converge ?reduce time step and try Newton w/ initial tangent
		 if {$ok != 0} {
			puts "$ok != 0 reduce time step and try Newton w/ initial tangent"
			test $testtype $tol 1000 2;
			algorithm Newton -initial
			set ok [analyze 1 [expr $DtAnalysis/100000.0]]
			test $testtype $tol $maxNumIter 2;
		}
# analysis did not converge ?reduce time step and try Broyden
		if {$ok != 0} {
			puts "Trying Broyden .."
			algorithm Broyden 8
			set ok [analyze 1 [expr $DtAnalysis/100000.0]]}
# analysis did not converge ?reduce time step and try Newton w/ with line search
		if {$ok != 0} {
			puts "Trying NewtonWithLineSearch .."
			algorithm NewtonLineSearch .8
			set ok [analyze 1 [expr $DtAnalysis/100000.0]]
			algorithm Newton
		}
	    set tCurrent [getTime]
	puts $tCurrent
}
```

ANNEX C (LAMAHA NADI BRIDGE)

Time history, hysteresis and drift time-history plot for Lamaha Nadi Bridge.

Tabas Earthquake

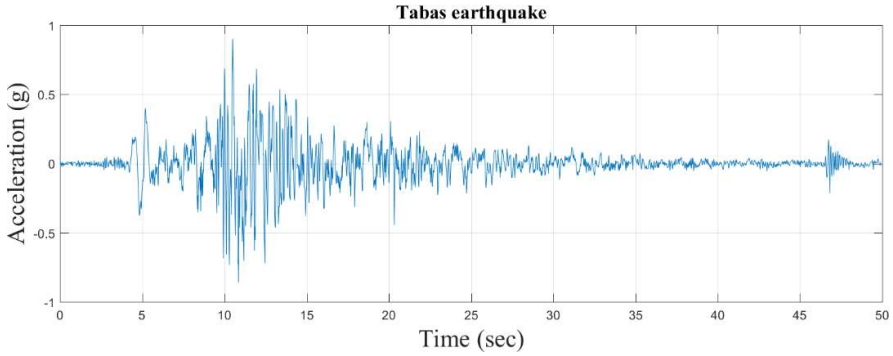

Figure 59: Time history of Tabas Earthquake.

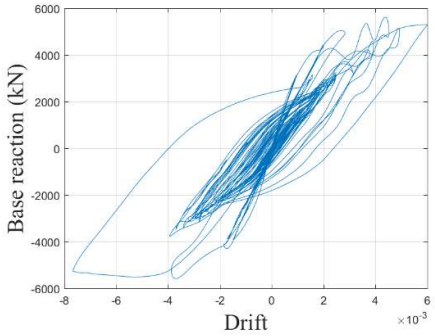

Figure 60: Hysteresis plot for Tabas Earthquake.

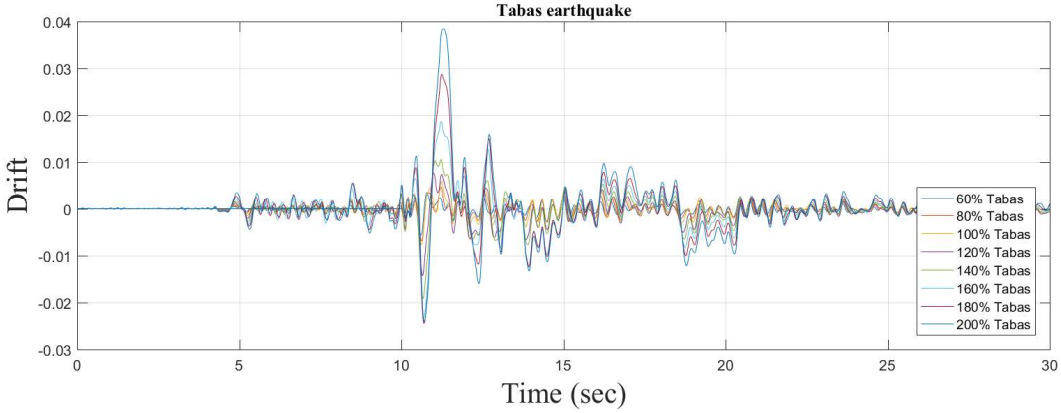

Figure 61: Drift time history for Tabas Earthquake.

LomaPrieta Losgatos Earthquake

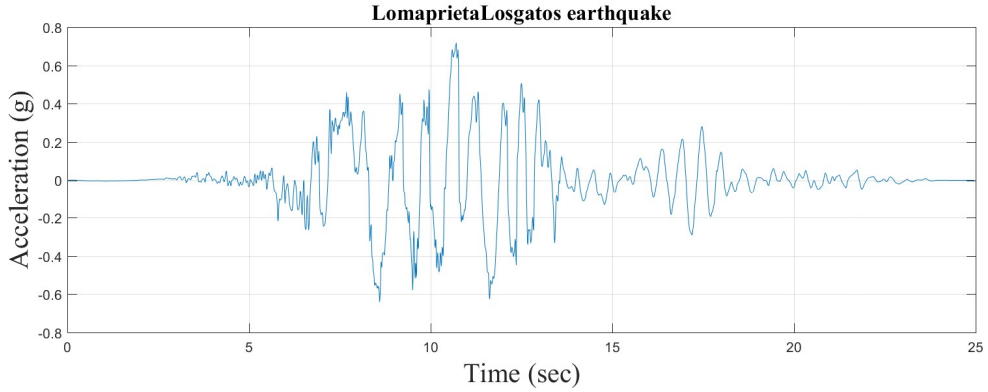

Figure 62: Time history of LomaPrieta Losgatos Earthquake.

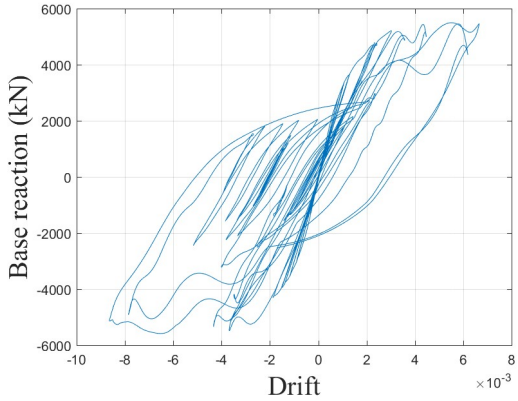

Figure 63: Hysteresis plot for LomaPrieta Losgatos Earthquake.

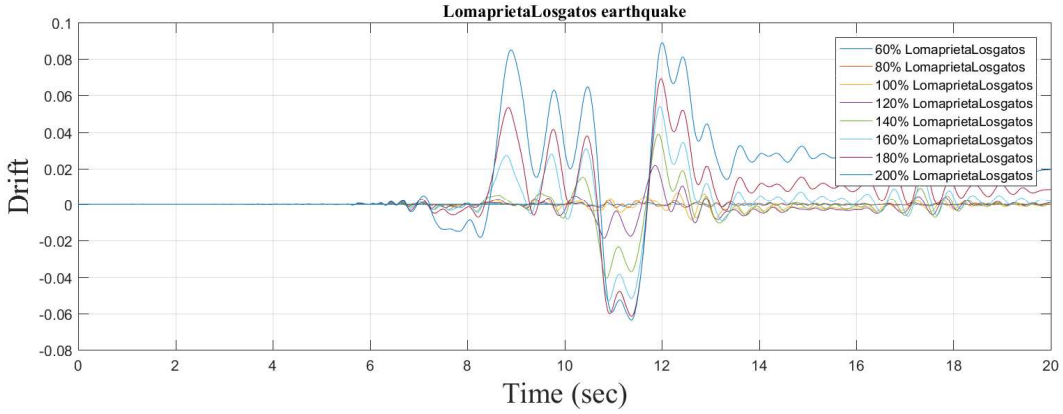

Figure 64: Drift time history for LomaPrieta Losgatos Earthquake.

LomaPrieta Lexington Dam Earthquake

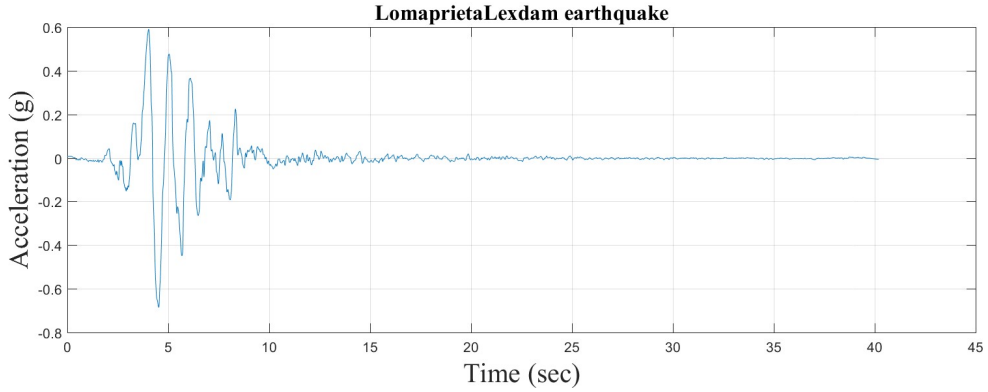

Figure 65: Time history of LomaPrieta Lexington Dam Earthquake.

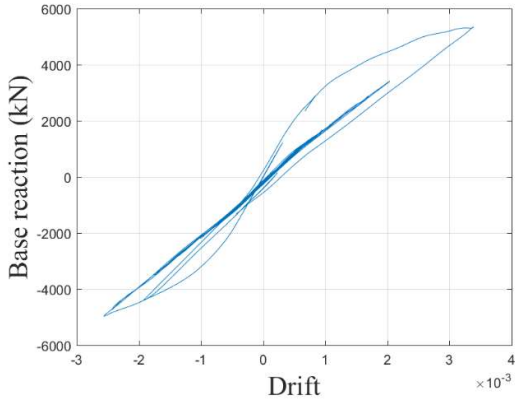

Figure 66: Hysteresis plot for LomaPrieta Lexington Dam Earthquake.

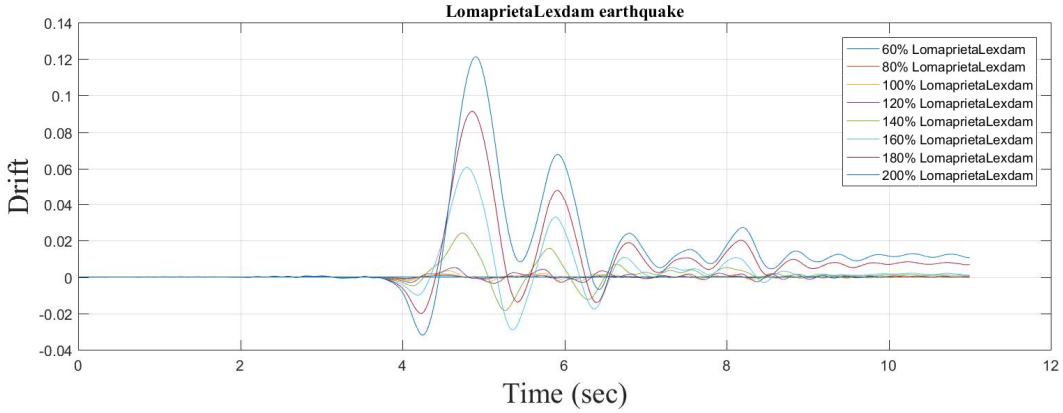

Figure 67: Drift time history for LomaPrieta Lexington Dam Earthquake.

Cape Mendecino Earthquake

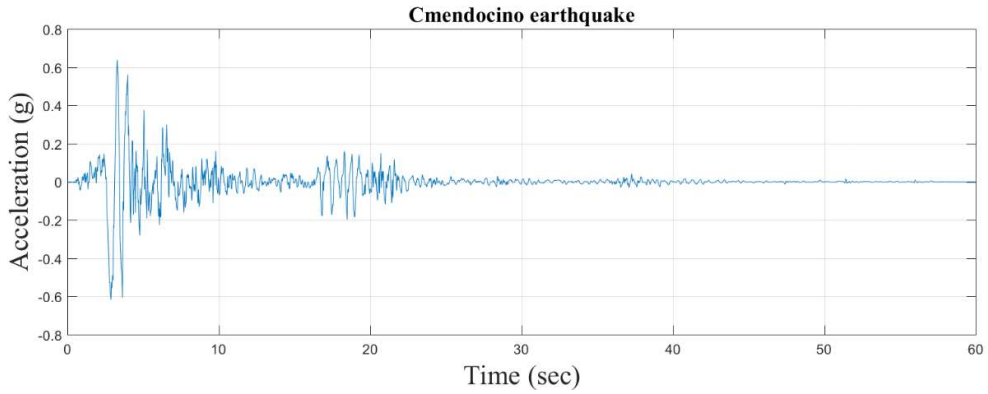

Figure 68: Time history of Cape Mendecino Earthquake.

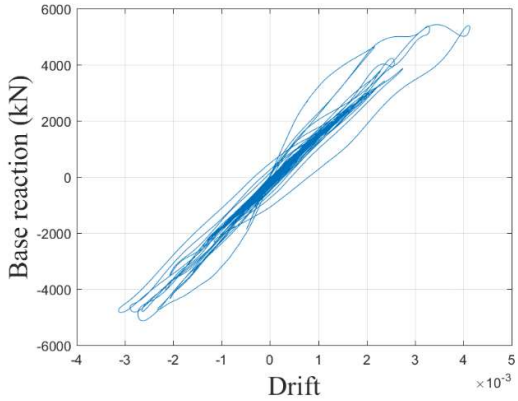

Figure 69: Hysteresis plot for Cape Mendecino Earthquake.

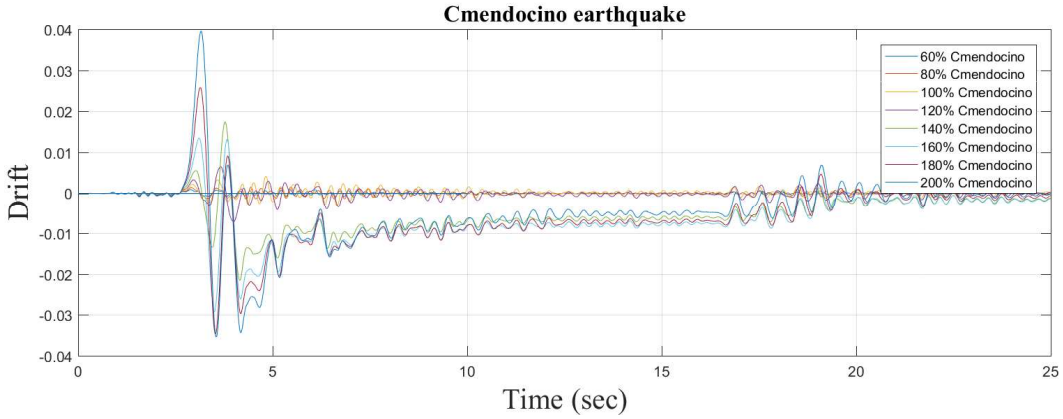

Figure 70: Drift time history for Cape Mendecino Earthquake.

Erzincan Earthquake

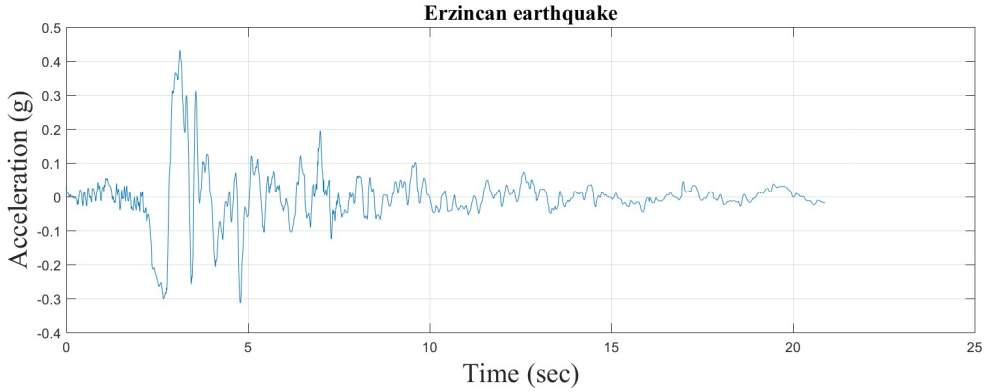

Figure 71: Time history of Erzincan Earthquake.

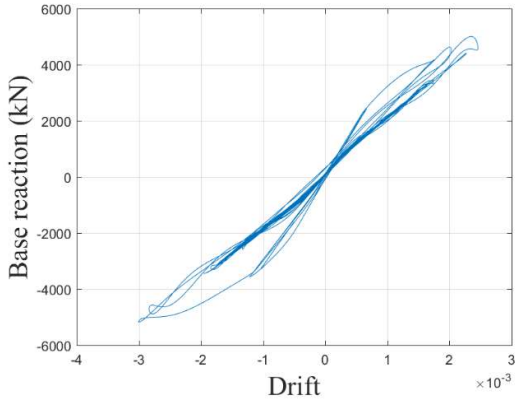

Figure 72: Hysteresis plot for Erzincan Earthquake.

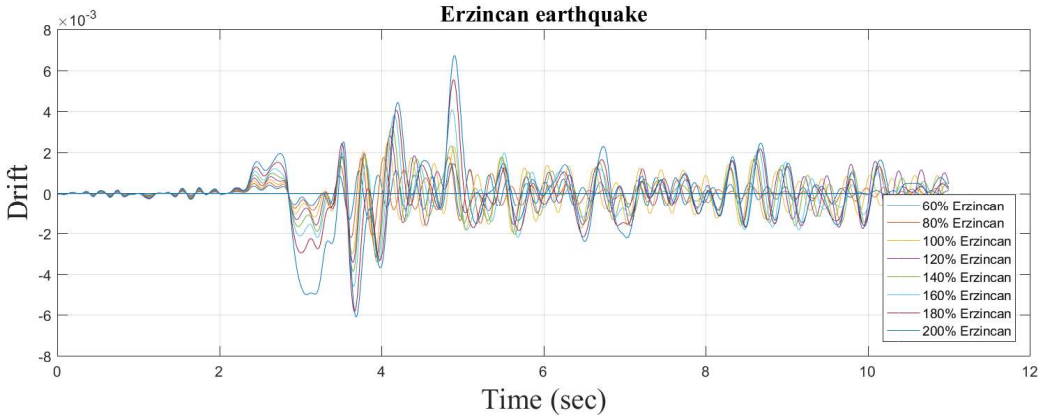

Figure 73: Drift time history for Erzincan Earthquake.

Landers Earthquake

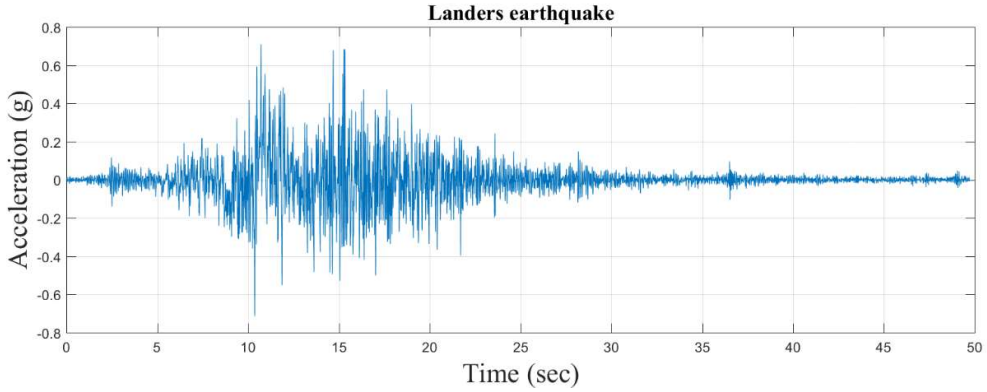

Figure 74: Time history of Landers Earthquake.

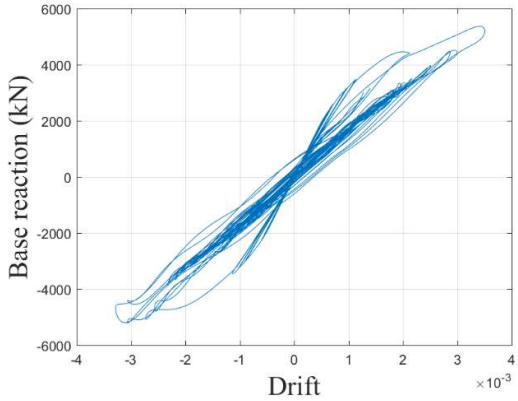

Figure 75: Hysteresis plot for Landers Earthquake.

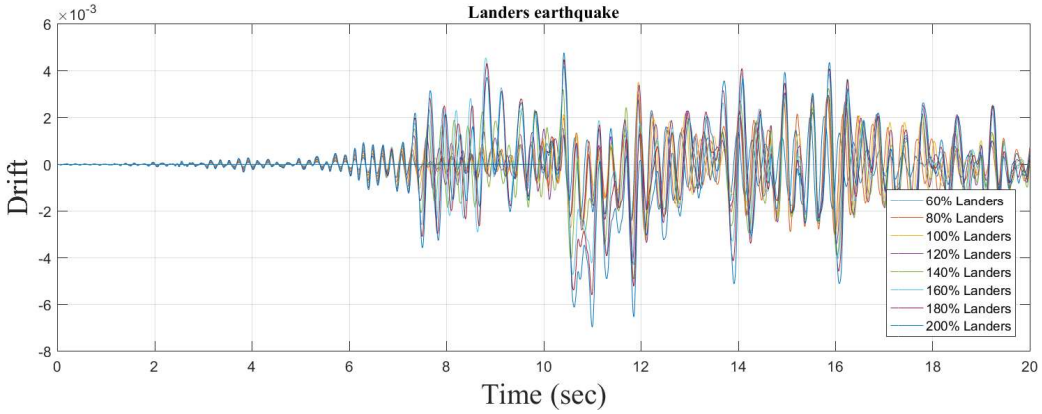

Figure 76: Drift time history for Landers Earthquake.

Northridge, Rinaldi Earthquake

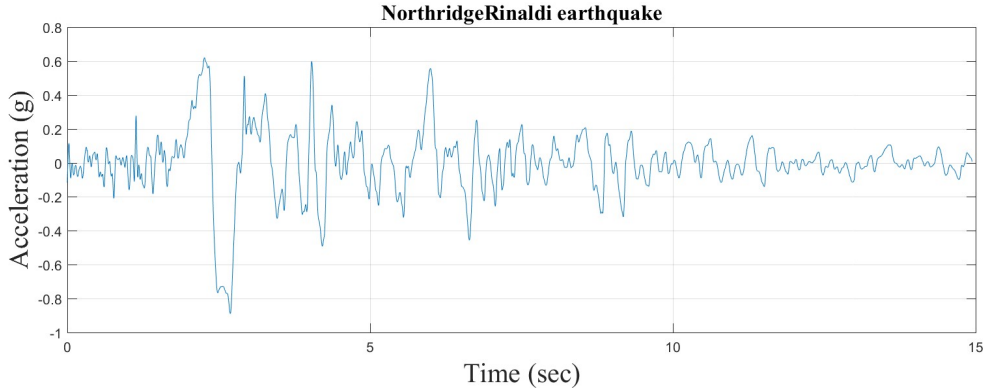

Figure 77: Time history of Northridge, Rinaldi Earthquake.

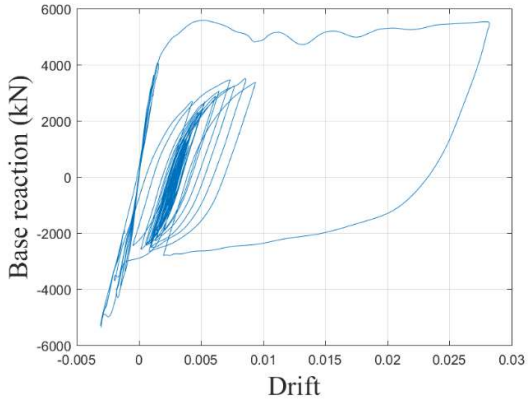

Figure 78: Hysteresis plot for Northridge, Rinaldi Earthquake.

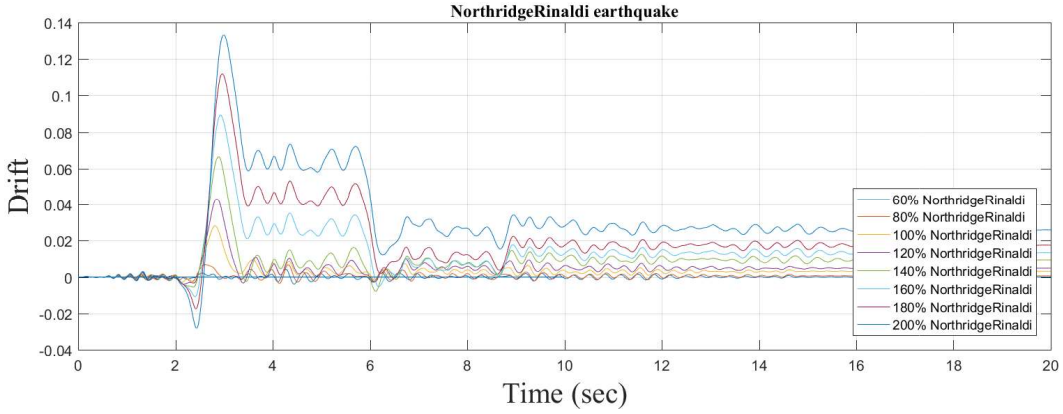

Figure 79: Drift time history for Northridge, Rinaldi Earthquake.

Northridge, Oliveview Earthquake

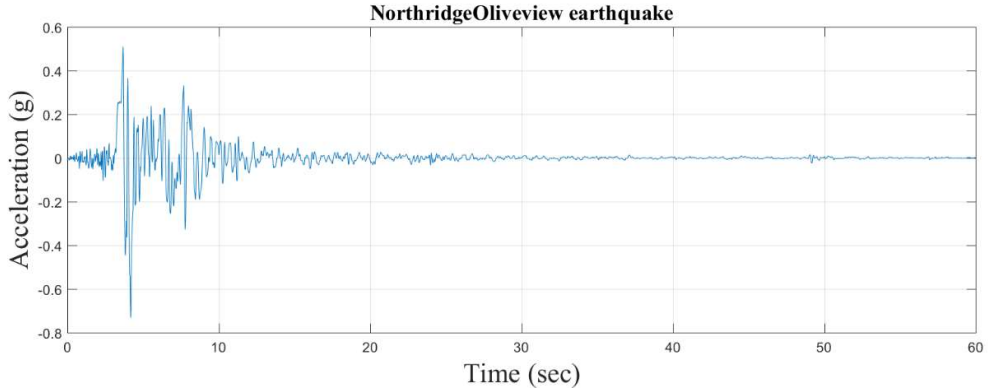

Figure 80: Time history of Northridge, Oliveview Earthquake.

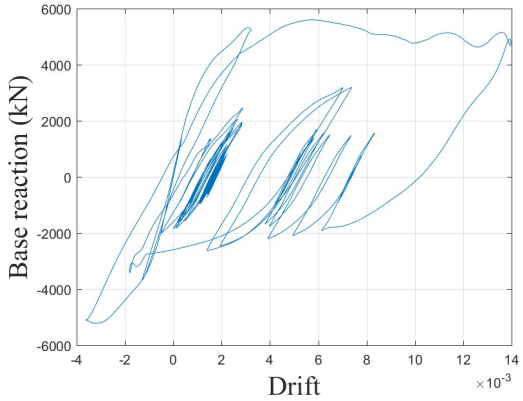

Figure 81: Hysteresis plot for Northridge, Oliveview Earthquake.

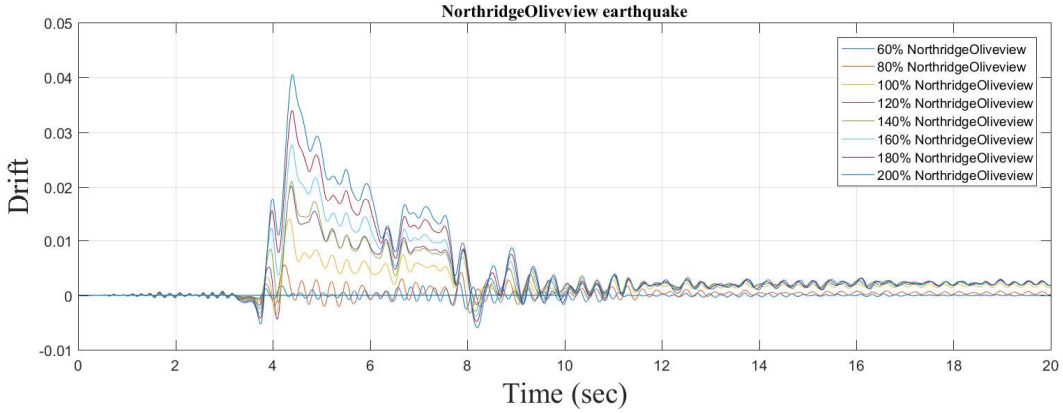

Figure 82: Drift time history for Northridge, Oliveview Earthquake.

Kobe Earthquake

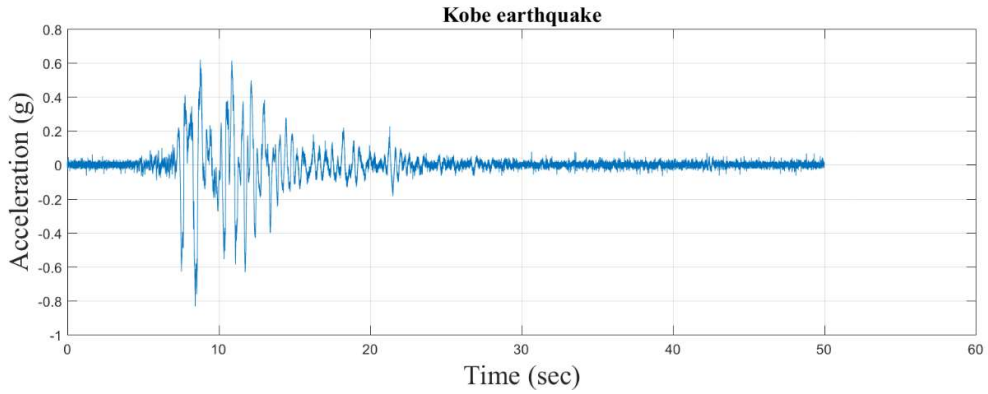

Figure 83: Time history of Kobe Earthquake.

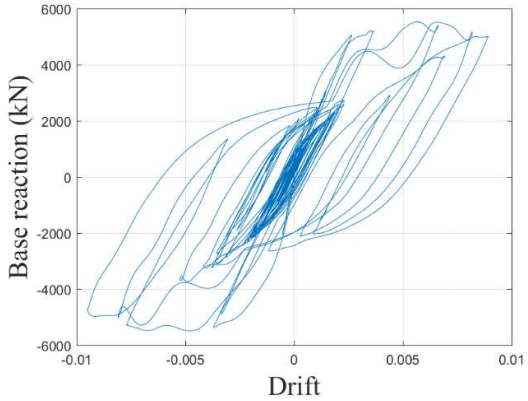

Figure 84: Hysteresis plot for Kobe Earthquake.

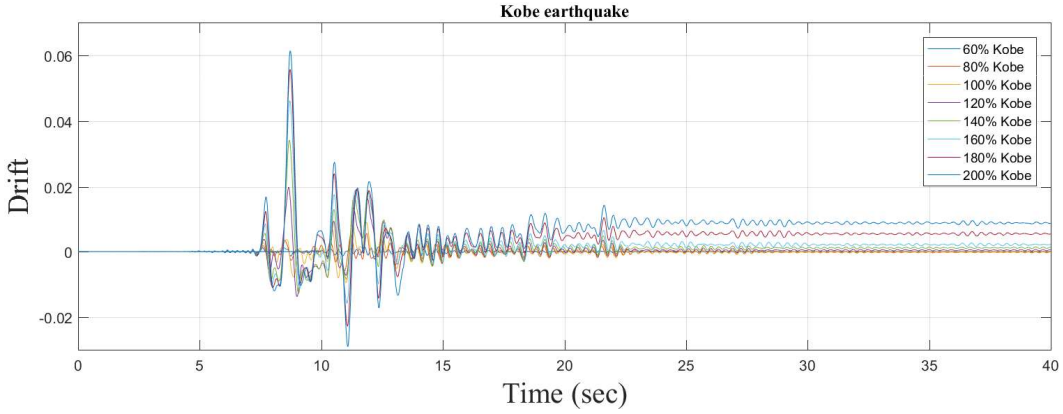

Figure 85: Drift time history for Kobe Earthquake.

Gorkha Earthquake

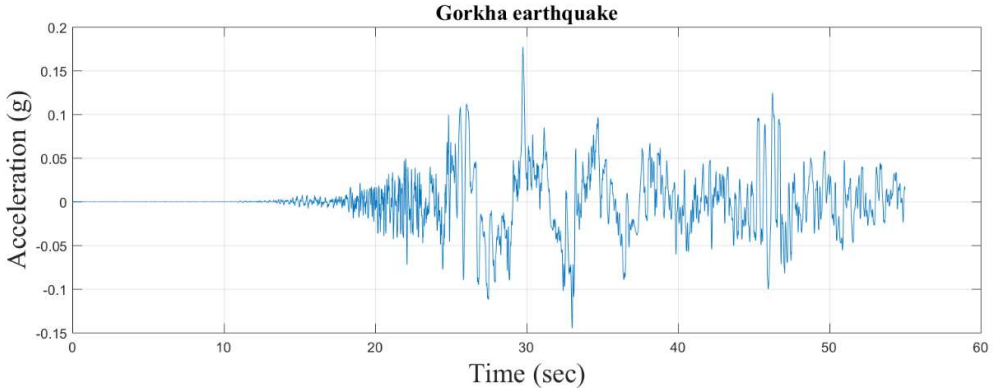

Figure 86: Time history of Gorkha Earthquake.

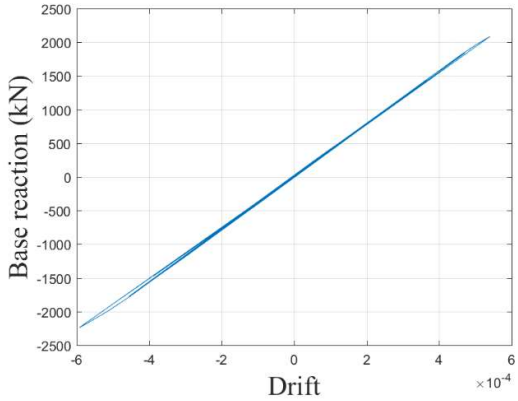

Figure 87: Hysteresis plot for Gorkha Earthquake.

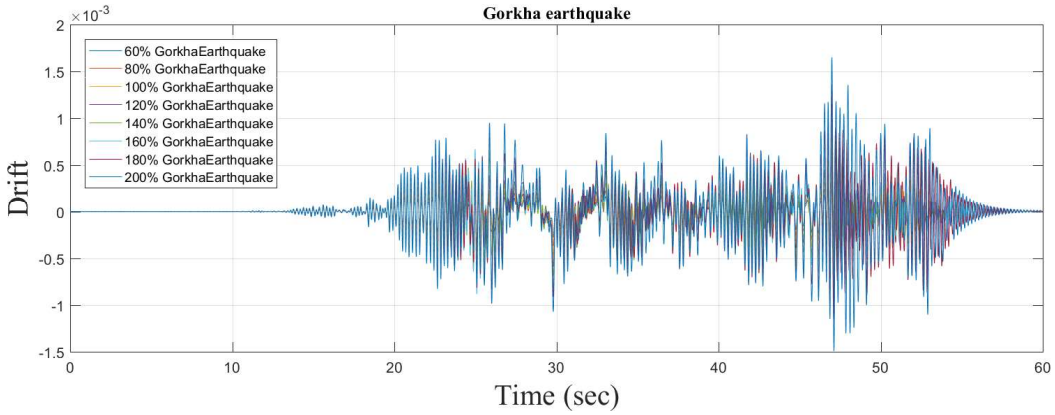

Figure 88: Drift time history for Gorkha Earthquake.

ANNEX D (SEWAR KHOLA BRIDGE)

Time history, hysteresis and drift time-history plot for Sewar Khola Bridge.

Tabas Earthquake

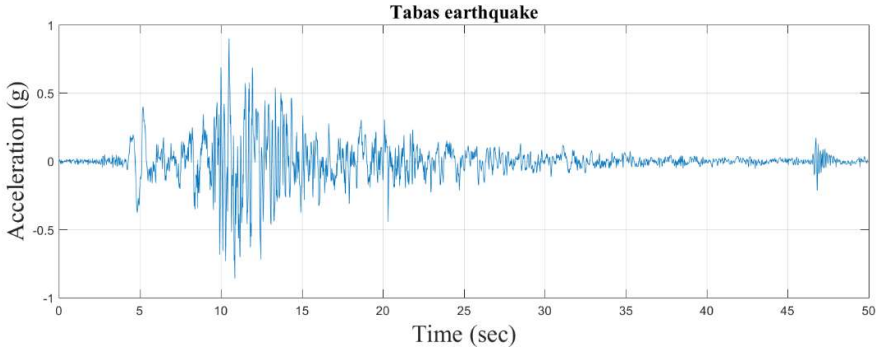

Figure 89: Time history of Tabas Earthquake.

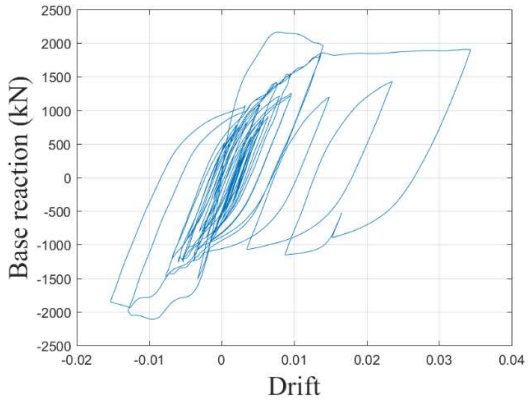

Figure 90: Hysteresis plot for Tabas Earthquake.

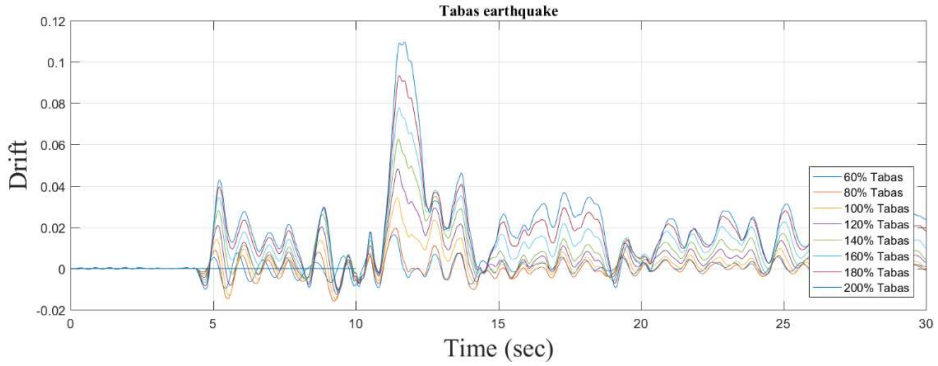

Figure 91: Drift time history for Tabas Earthquake.

LomaPrieta Losgatos Earthquake

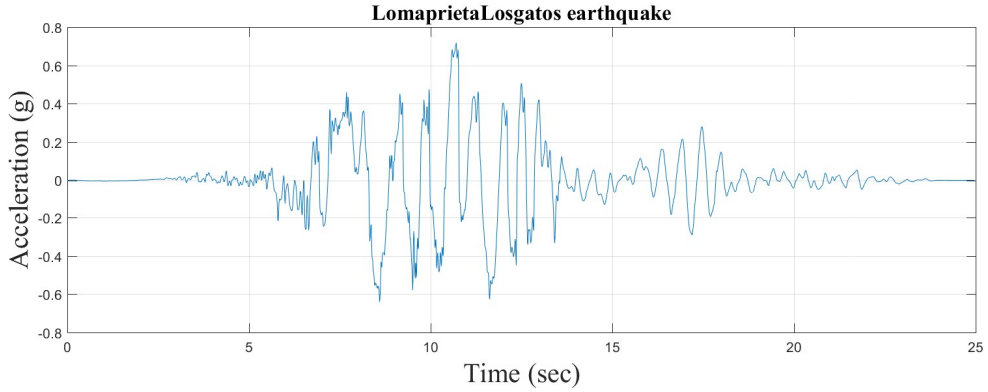

Figure 92: Time history of LomaPrieta Losgatos Earthquake.

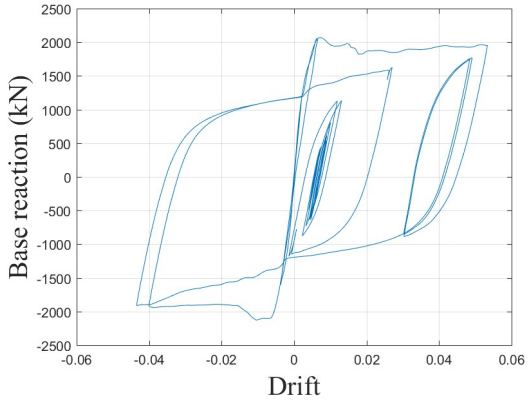

Figure 93: Hysteresis plot for LomaPrieta Losgatos Earthquake.

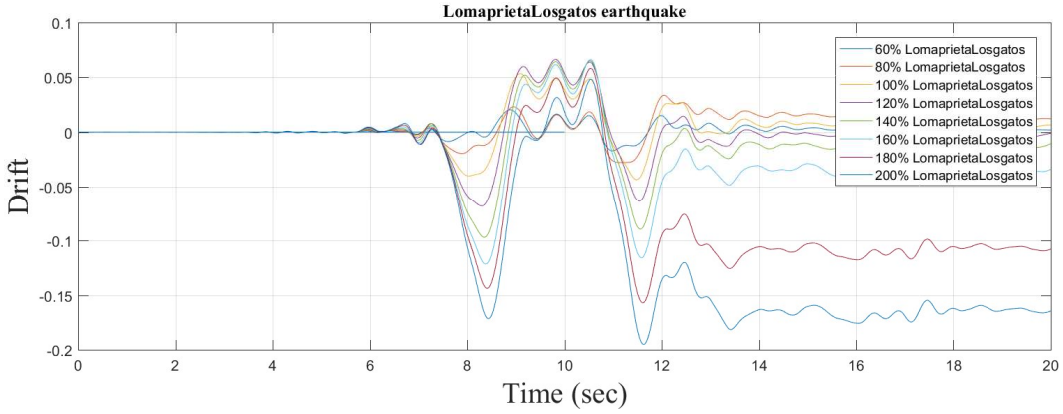

Figure 94: Drift time history for LomaPrieta Losgatos Earthquake.

LomaPrieta Lexington Dam Earthquake

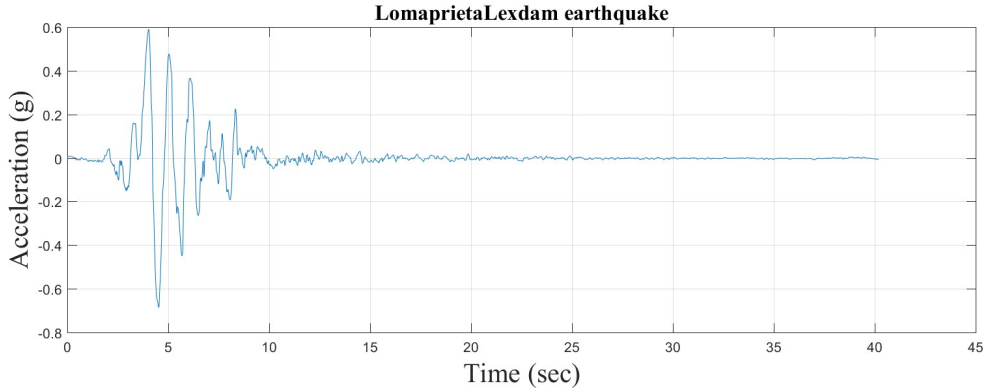

Figure 95: Time history of LomaPrieta Lexington Dam Earthquake.

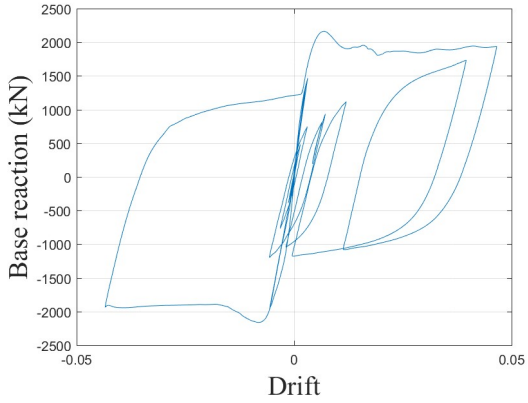

Figure 96: Hysteresis plot for LomaPrieta Lexington Dam Earthquake.

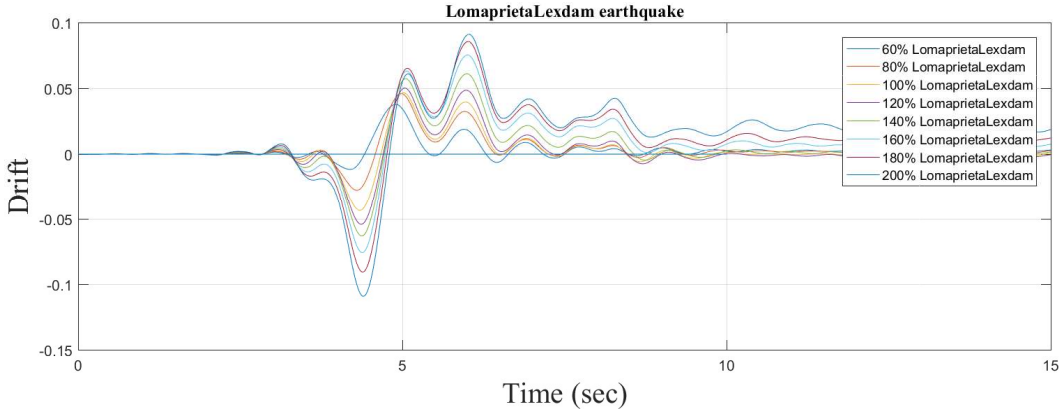

Figure 97: Drift time history for LomaPrieta Lexington Dam Earthquake.

Cape Mendecino Earthquake

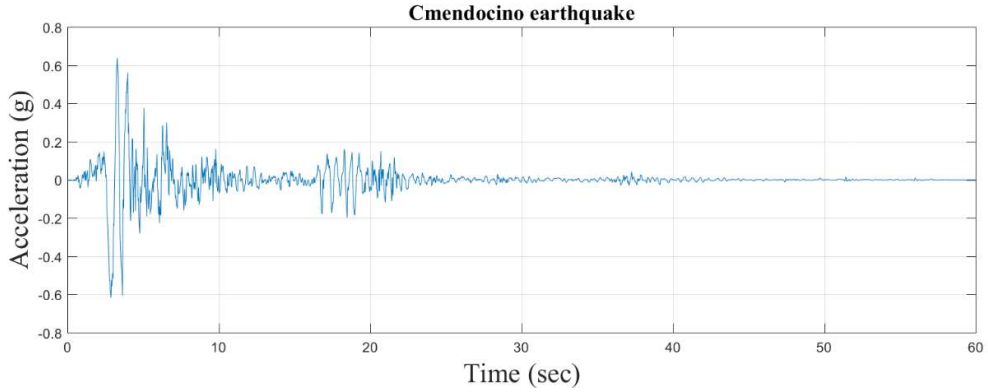

Figure 98: Time history of Cape Mendecino Earthquake.

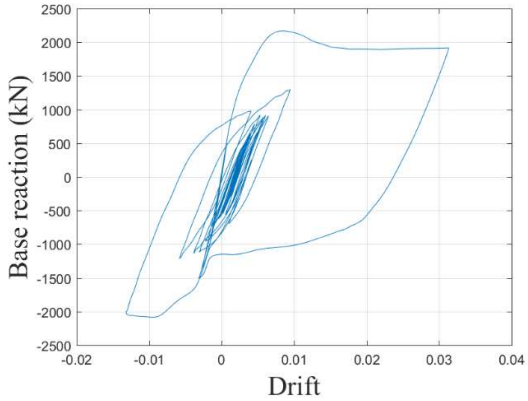

Figure 99: Hysteresis plot for Cape Mendecino Earthquake.

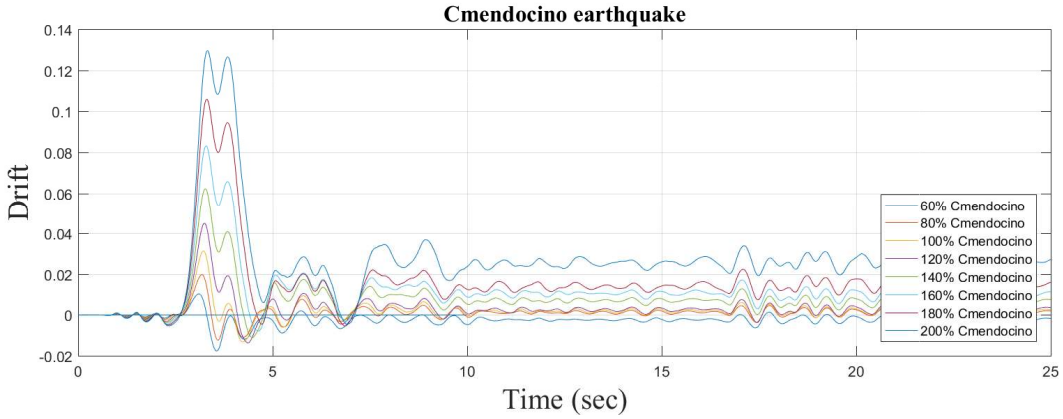

Figure 100: Drift time history for Cape Mendecino Earthquake.

Erzincan Earthquake

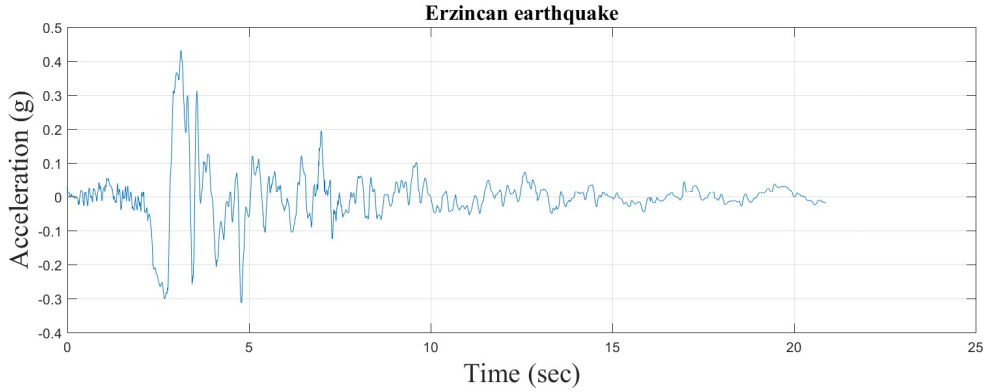

Figure 101: Time history of Erzincan Earthquake.

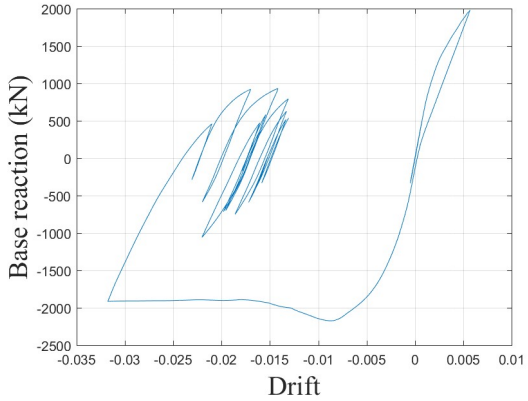

Figure 102: Hysteresis plot for Erzincan Earthquake.

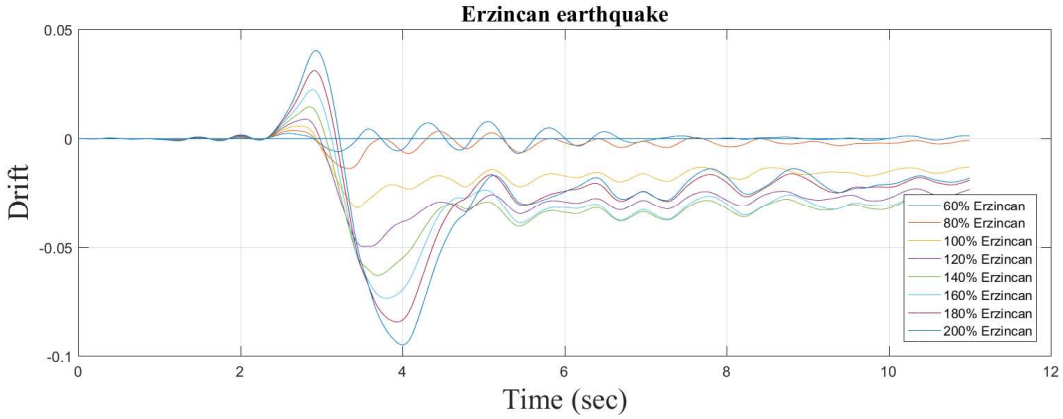

Figure 103: Drift time history for Erzincan Earthquake.

Landers Earthquake

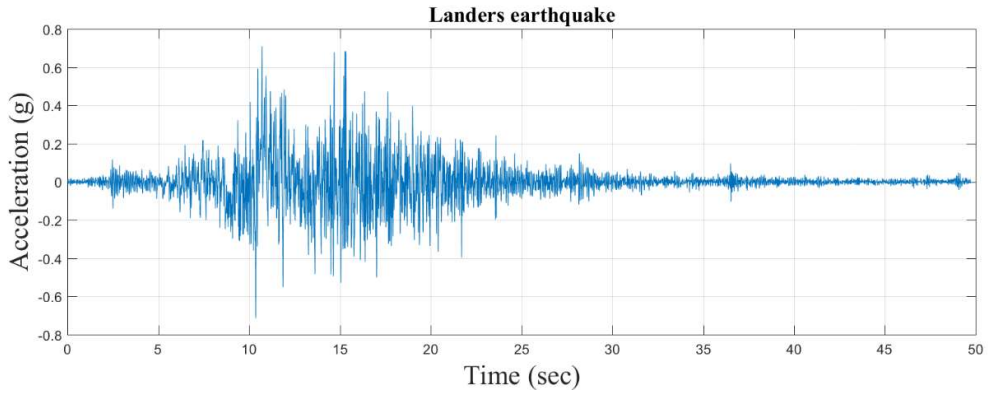

Figure 104: Time history of Landers Earthquake.

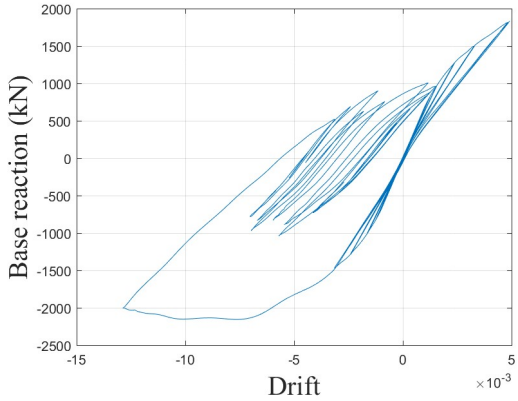

Figure 105: Hysteresis plot for Landers Earthquake.

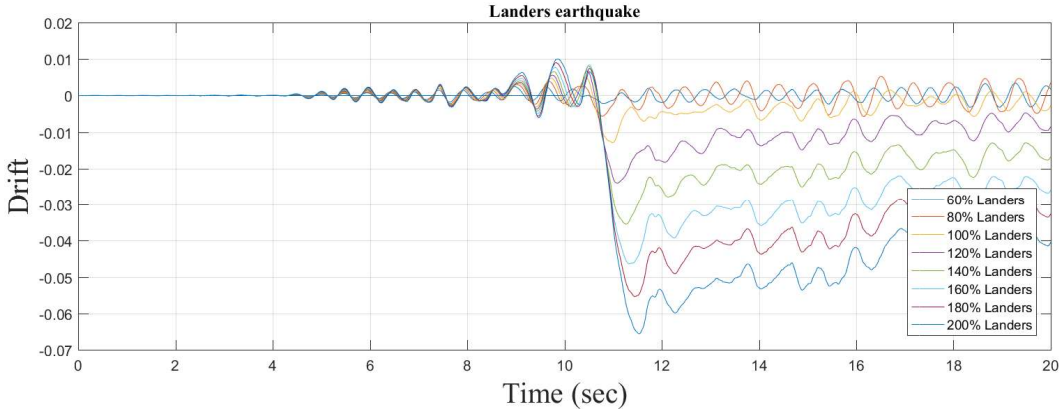

Figure 106: Drift time history for Landers Earthquake.

Northridge, Rinaldi Earthquake

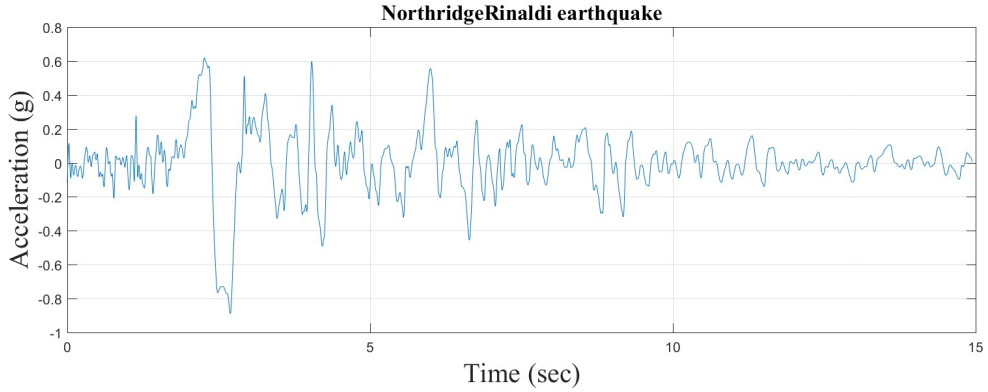

Figure 107: Time history of Northridge, Rinaldi Earthquake.

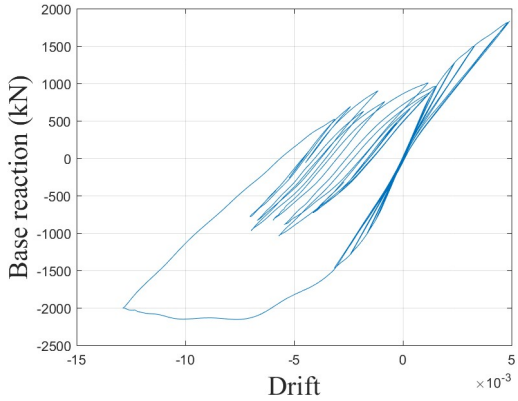

Figure 108: Hysteresis plot for Northridge, Rinaldi Earthquake.

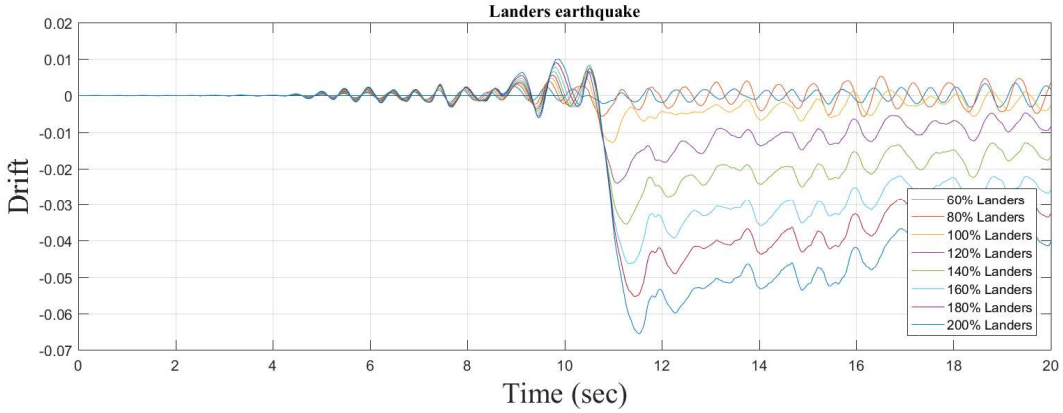

Figure 109: Drift time history for Northridge, Rinaldi Earthquake.

Northridge, Oliveview Earthquake

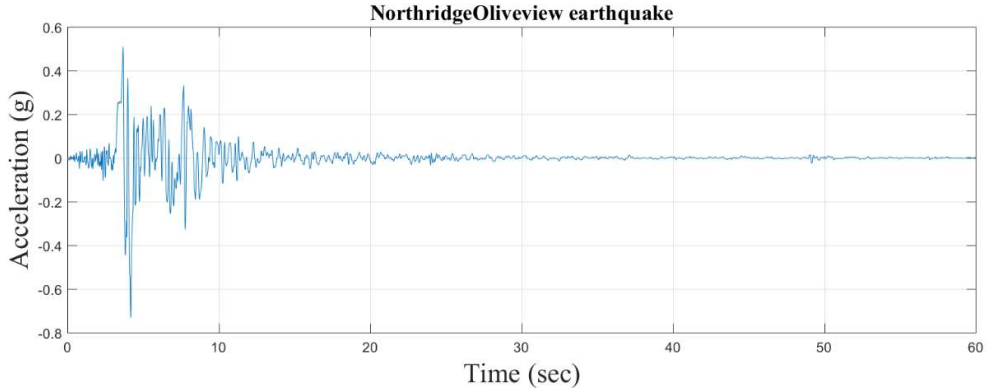

Figure 110: Time history of Northridge, Oliveview Earthquake.

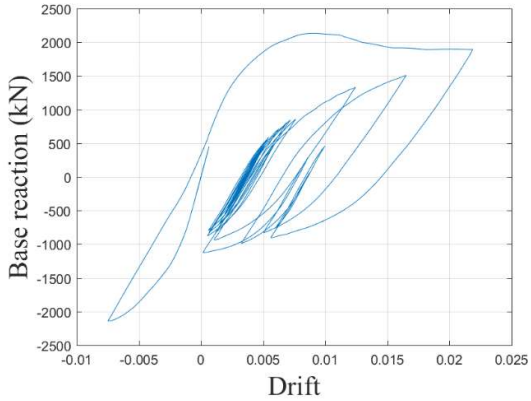

Figure 111: Hysteresis plot for Northridge, Oliveview Earthquake.

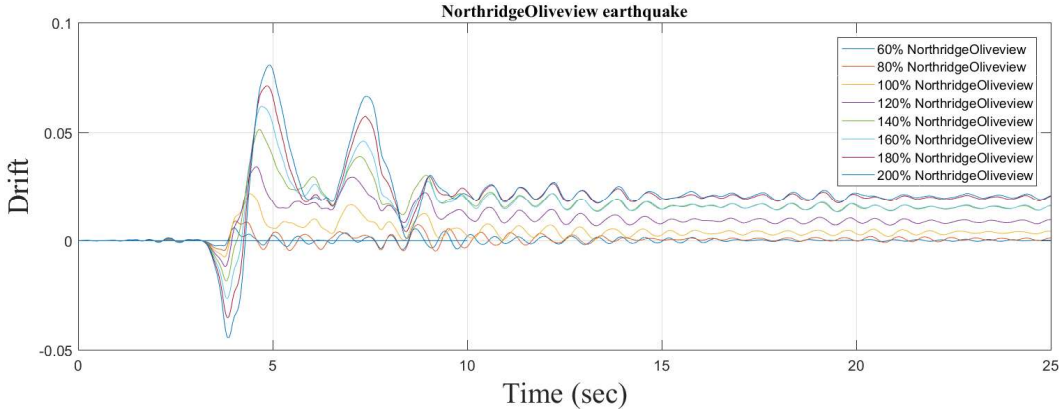

Figure 112: Drift time history for Northridge, Oliveview Earthquake.

Kobe Earthquake

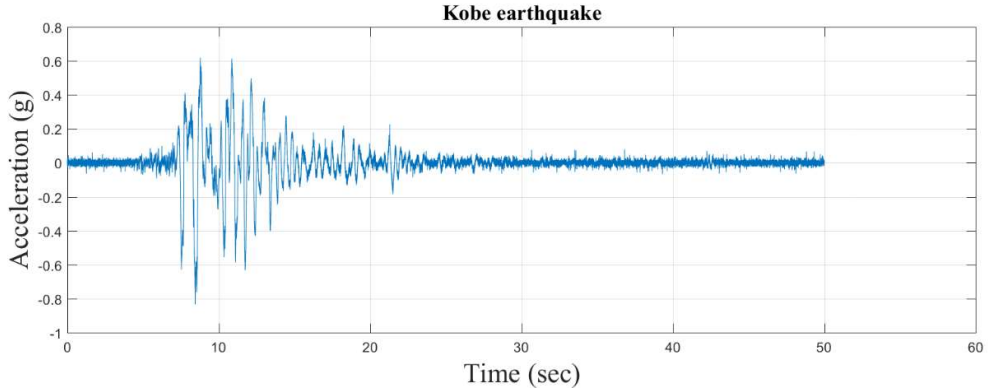

Figure 113: Time history of Kobe Earthquake.

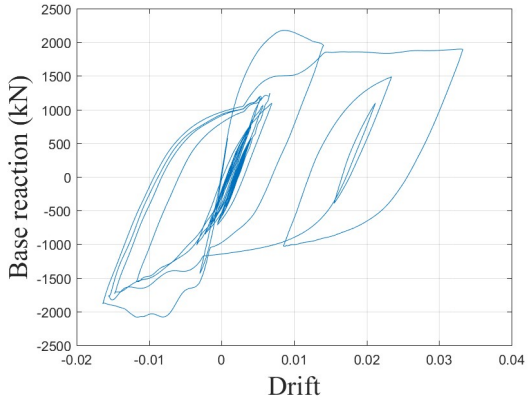

Figure 114: Hysteresis plot for Kobe Earthquake.

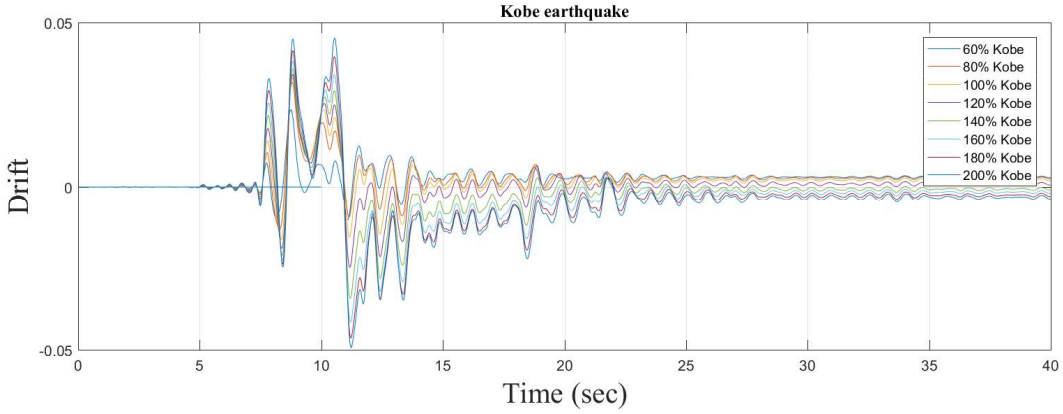

Figure 115: Drift time history for Kobe Earthquake.

Gorkha Earthquake

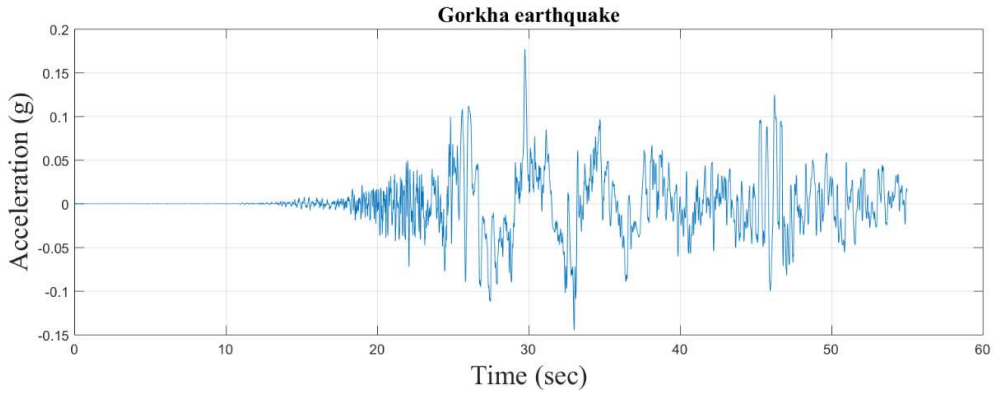

Figure 116: Time history of Gorkha Earthquake.

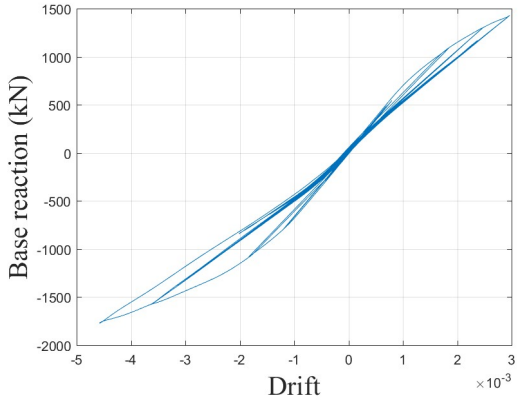

Figure 117: Hysteresis plot for Gorkha Earthquake.

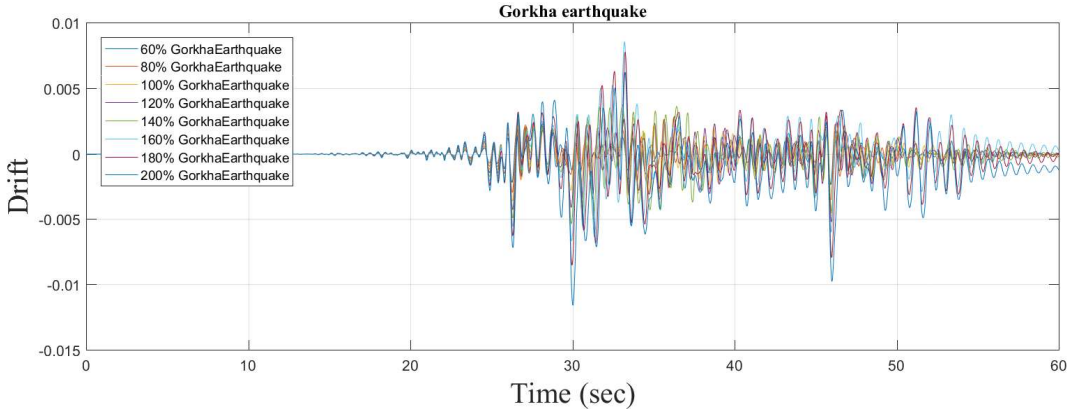

Figure 118: Drift time history for Gorkha Earthquake

ANNEX D (SUIKHET BRIDGE)

Time history, hysteresis and drift time-history plot for Suikhet Bridge.

Tabas Earthquake

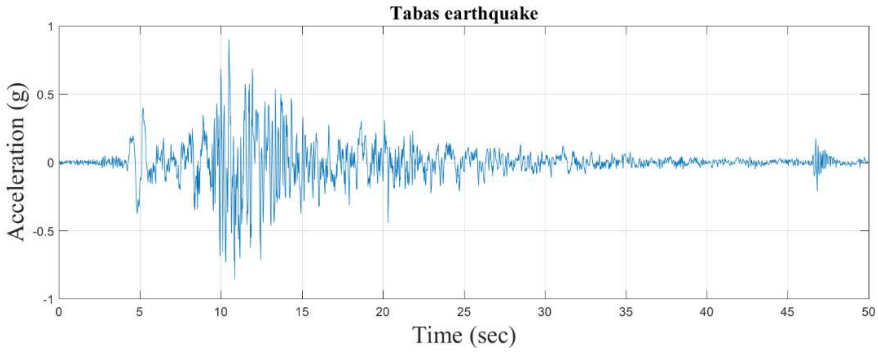

Figure 119: Time history of Tabas Earthquake.

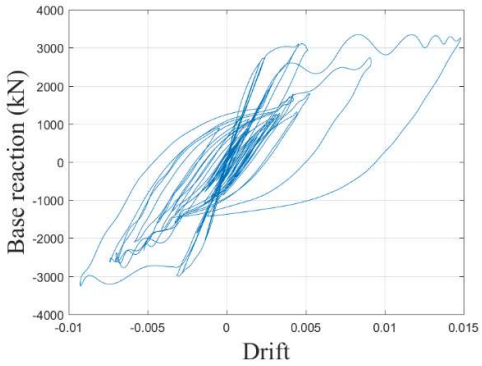

Figure 120: Hysteresis plot for Tabas Earthquake.

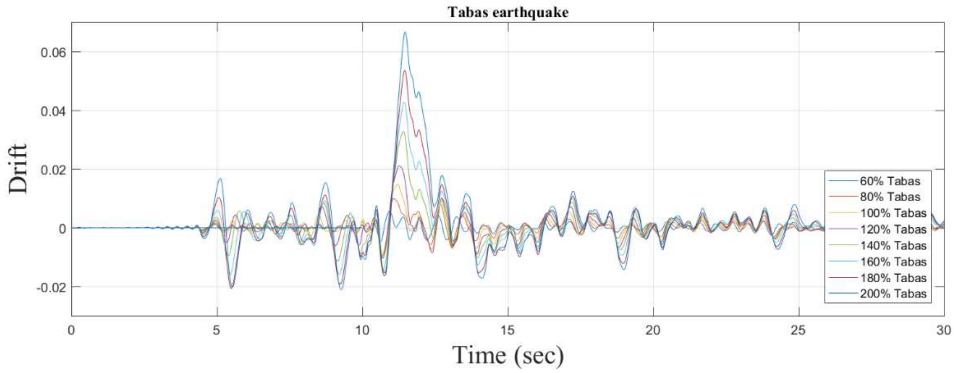

Figure 121: Drift time history for Tabas Earthquake.

LomaPrieta Losgatos Earthquake

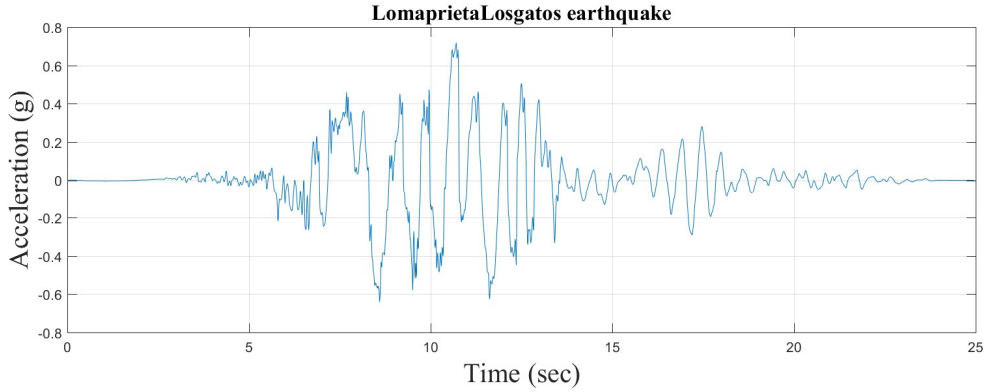

Figure 122: Time history of LomaPrieta Losgatos Earthquake.

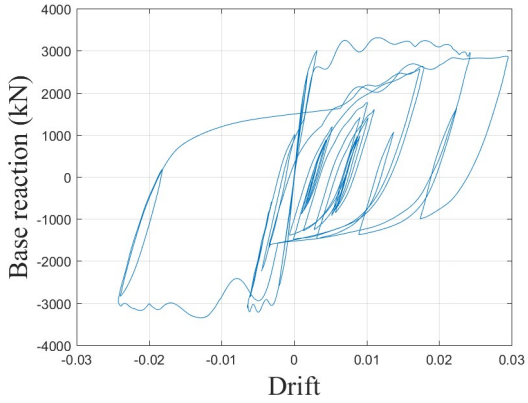

Figure 123: Hysteresis plot for LomaPrieta Losgatos Earthquake.

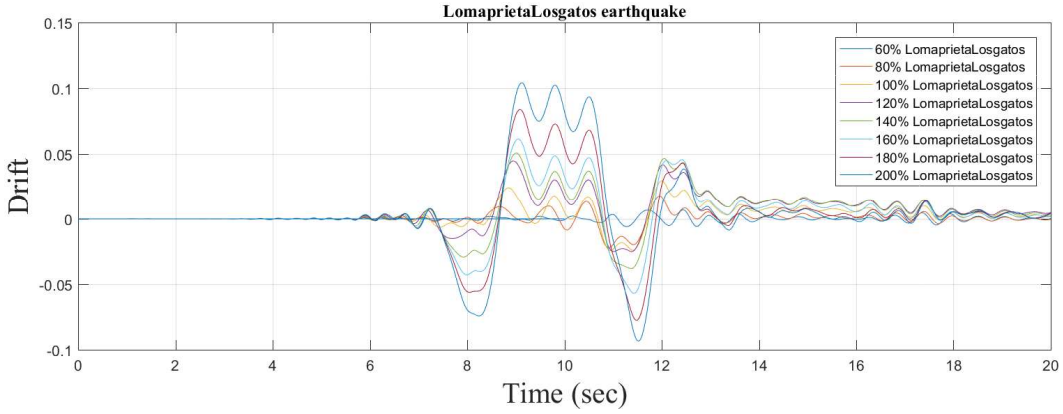

Figure 124: Drift time history for LomaPrieta Losgatos Earthquake.

LomaPrieta Lexington Dam Earthquake

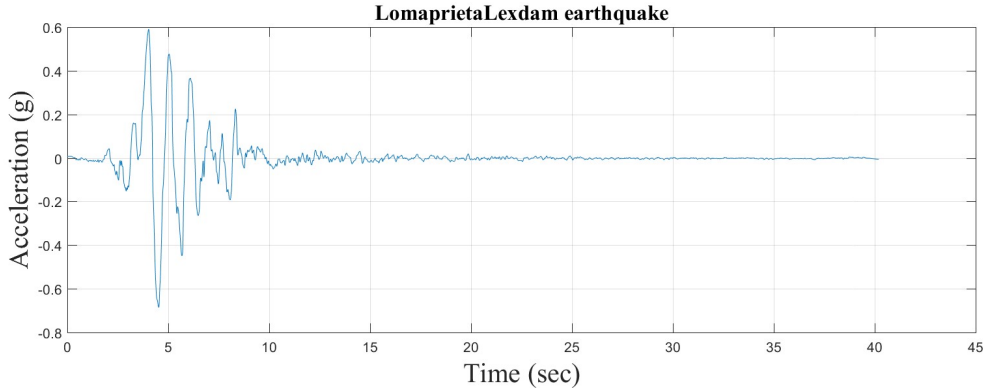

Figure 125: Time history of LomaPrieta Lexington Dam Earthquake.

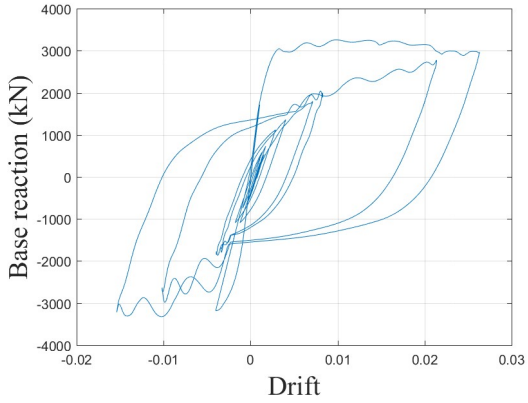

Figure 126: Hysteresis plot for LomaPrieta Lexington Dam Earthquake.

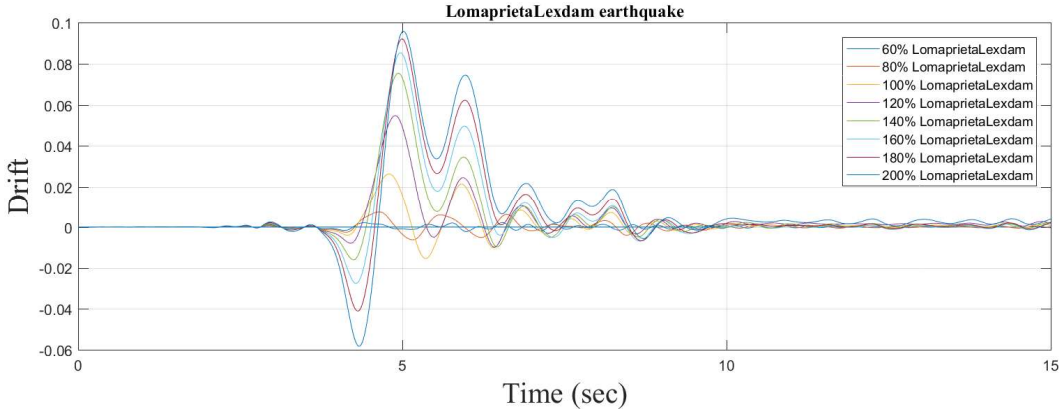

Figure 127: Drift time history for LomaPrieta Lexington Dam Earthquake.

Cape Mendecino Earthquake

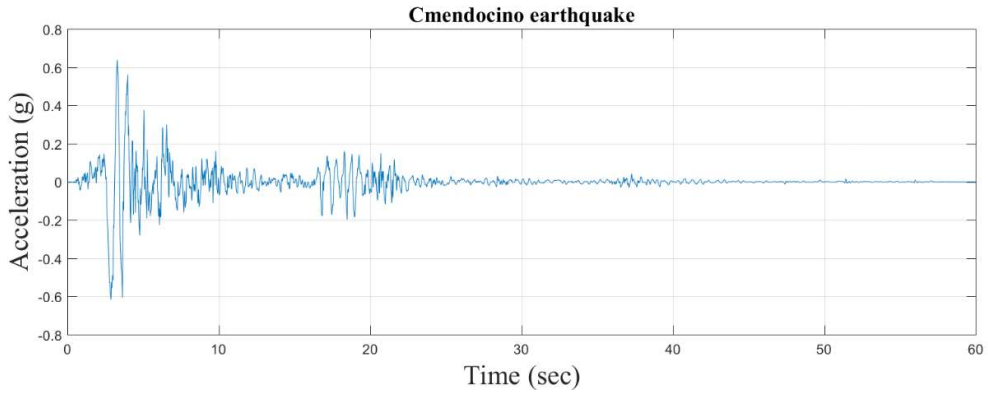

Figure 128: Time history of Cape Mendecino Earthquake.

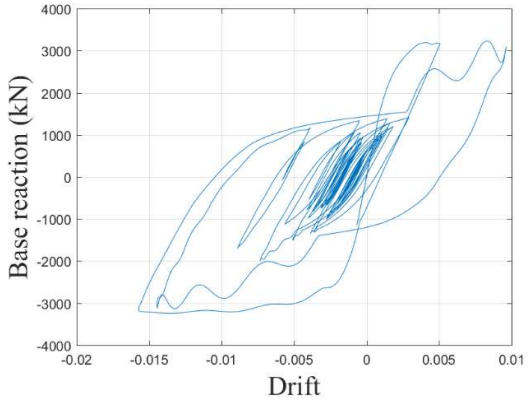

Figure 129: Hysteresis plot for Cape Mendecino Earthquake.

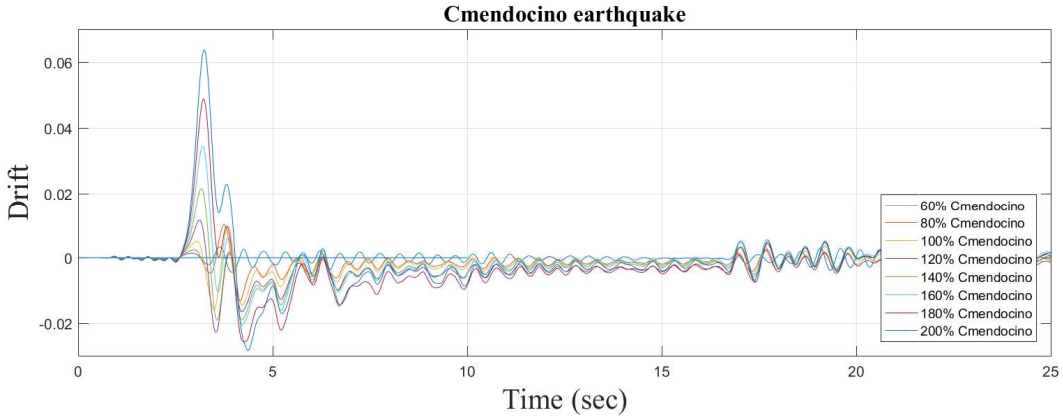

Figure 130: Drift time history for Cape Mendecino Earthquake.

Erzincan Earthquake

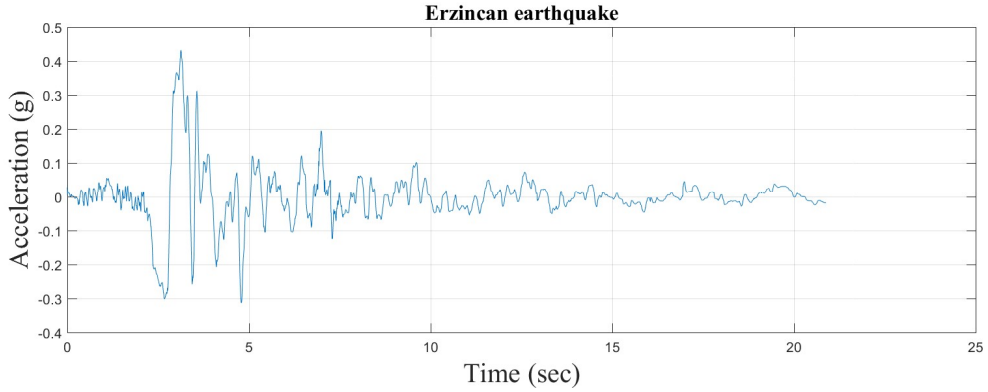

Figure 131: Time history of Erzincan Earthquake.

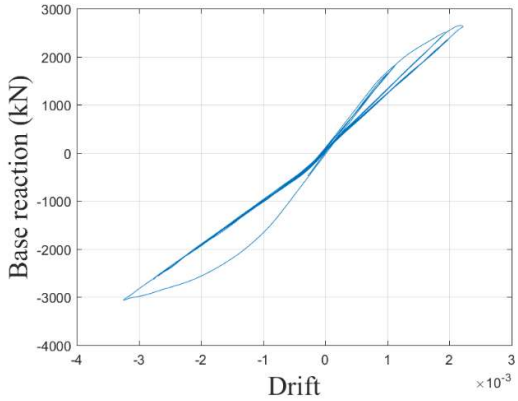

Figure 132: Hysteresis plot for Erzincan Earthquake.

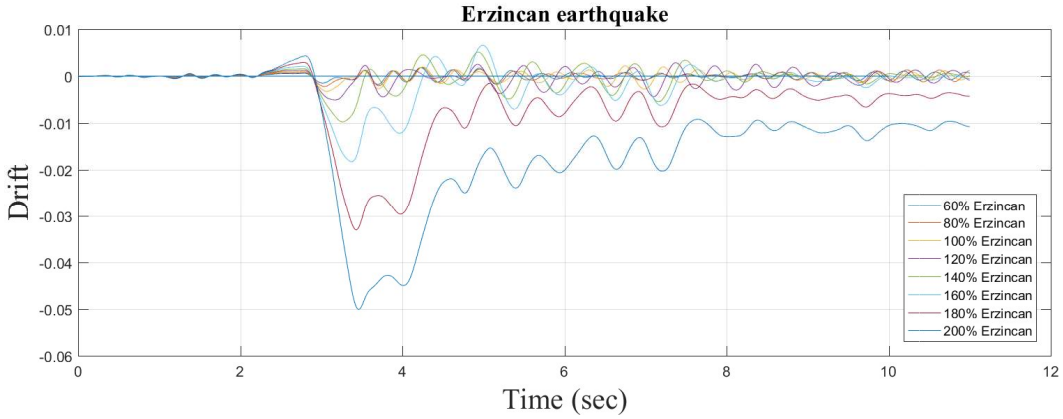

Figure 133: Drift time history for Erzincan Earthquake.

Landers Earthquake

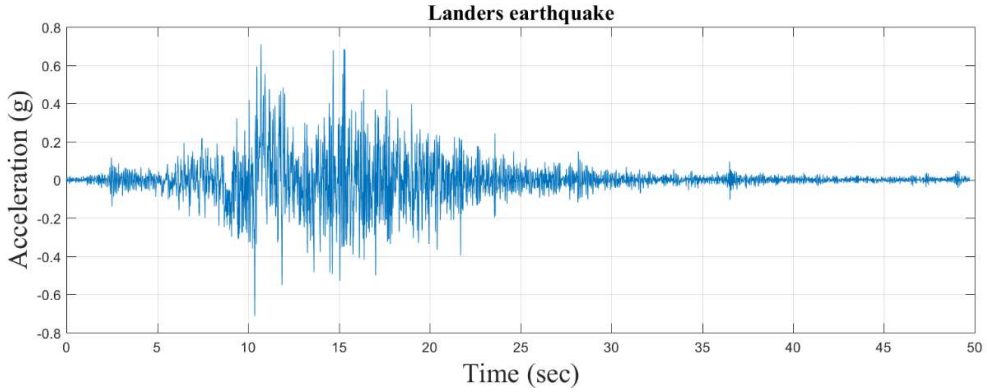

Figure 134: Time history of Landers Earthquake.

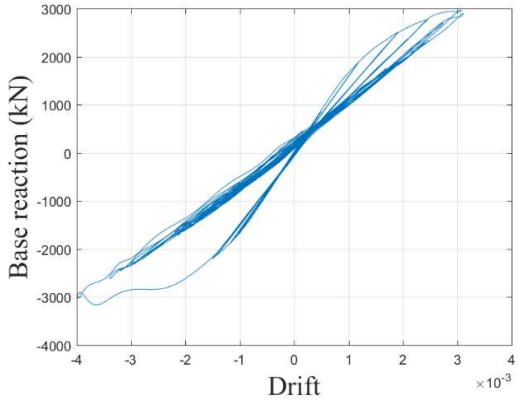

Figure 135: Hysteresis plot for Landers Earthquake.

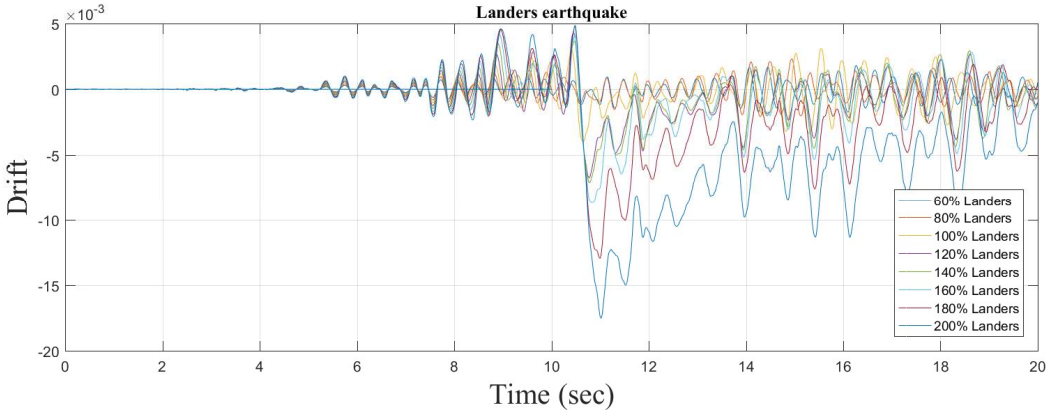

Figure 136: Drift time history for Landers Earthquake.

Northridge, Rinaldi Earthquake

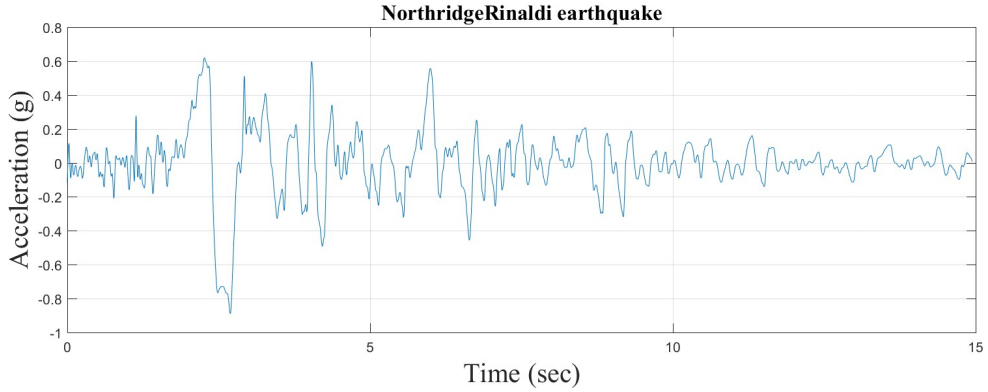

Figure 137: Time history of Northridge, Rinaldi Earthquake.

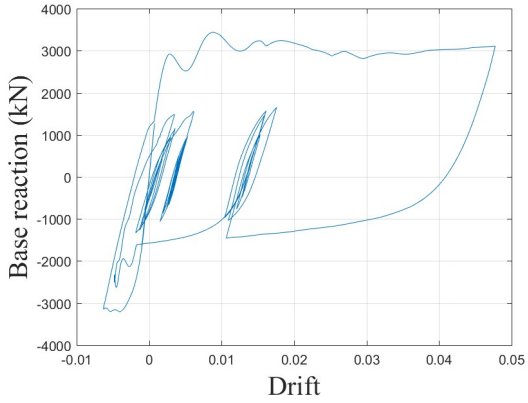

Figure 138: Hysteresis plot for Northridge, Rinaldi Earthquake.

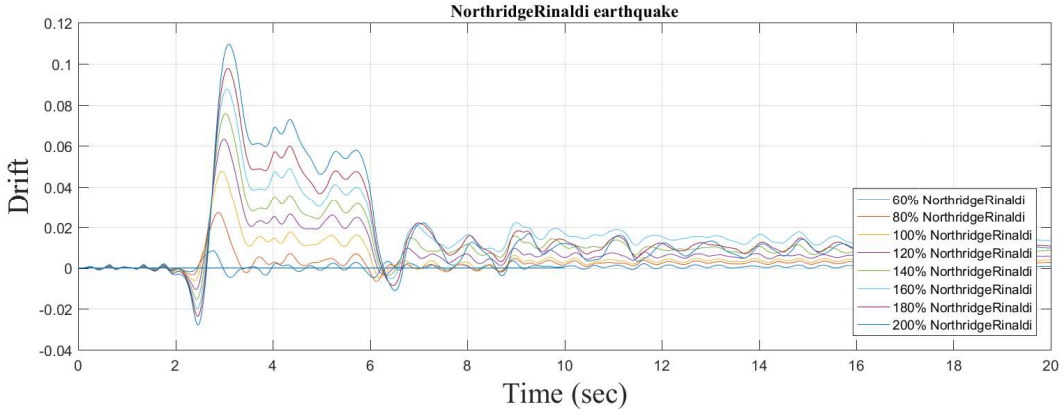

Figure 139: Drift time history for Northridge, Rinaldi Earthquake.

Northridge, Oliveview Earthquake

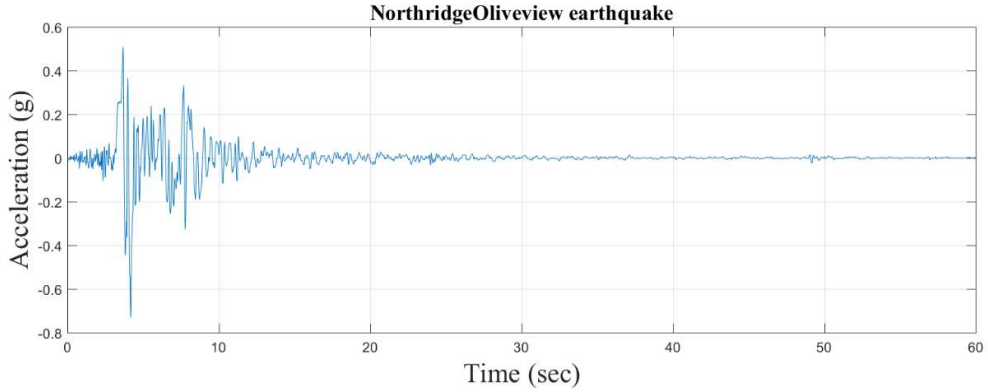

Figure 140: Time history of Northridge, Oliveview Earthquake.

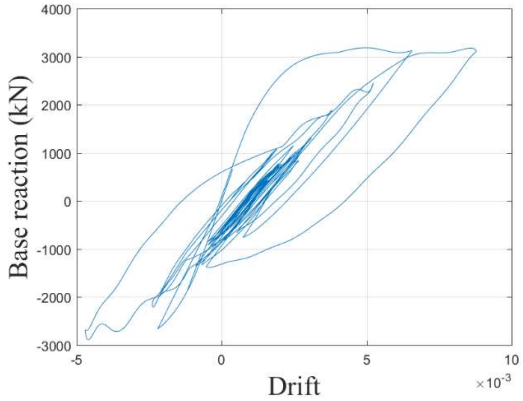

Figure 141: Hysteresis plot for Northridge, Oliveview Earthquake.

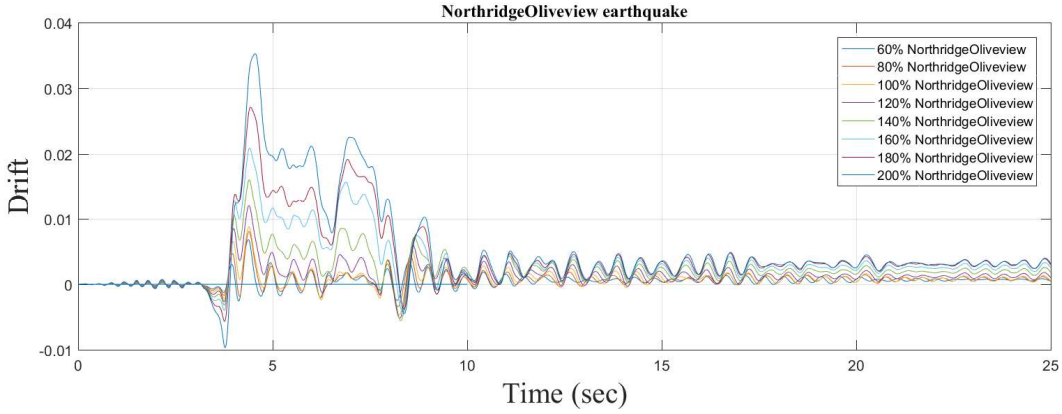

Figure 142: Drift time history for Northridge, Oliveview Earthquake.

Kobe Earthquake

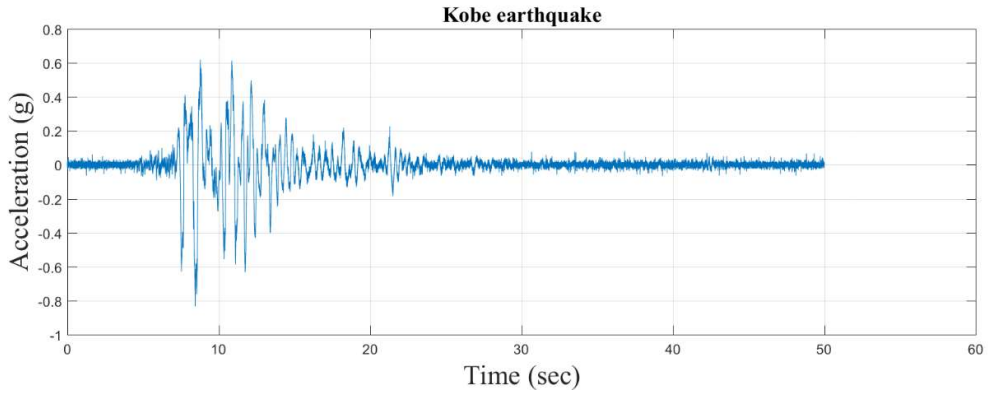

Figure 143: Time history of Kobe Earthquake.

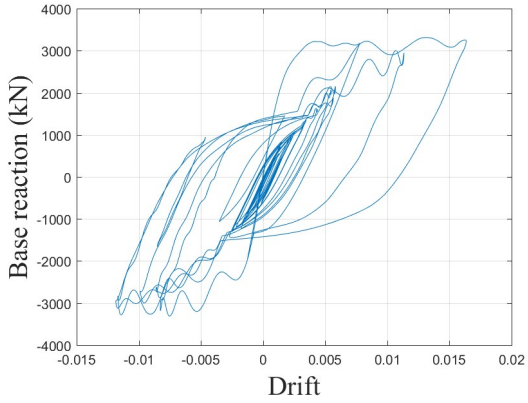

Figure 144: Hysteresis plot for Kobe Earthquake.

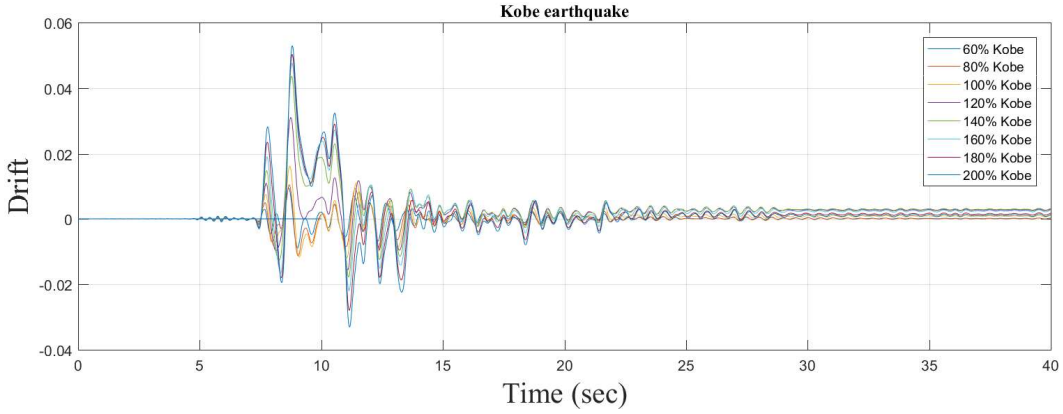

Figure 145: Drift time history for Kobe Earthquake.

Gorkha Earthquake

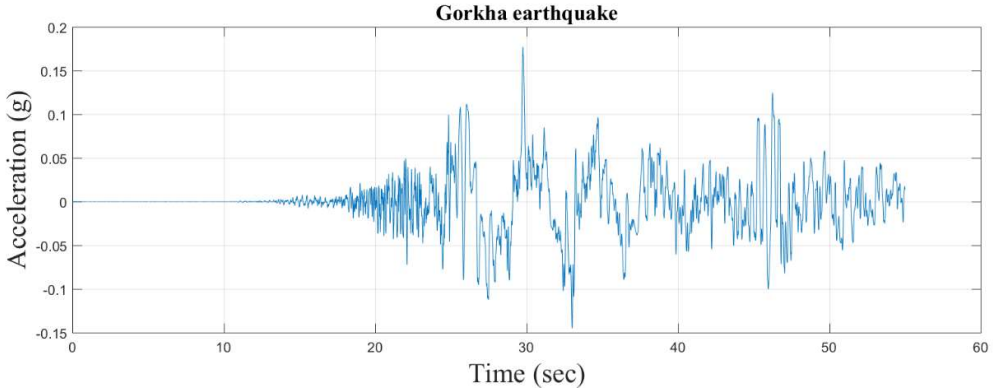

Figure 146: Time history of Gorkha Earthquake.

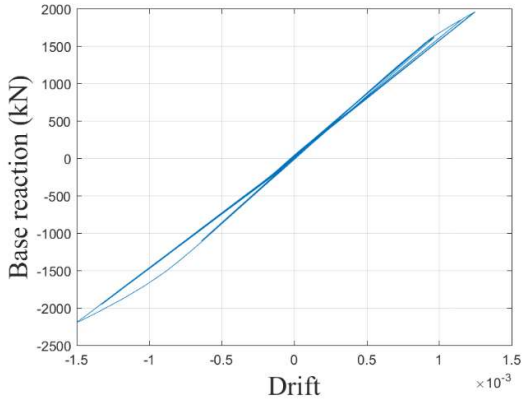

Figure 147: Hysteresis plot for Gorkha Earthquake.

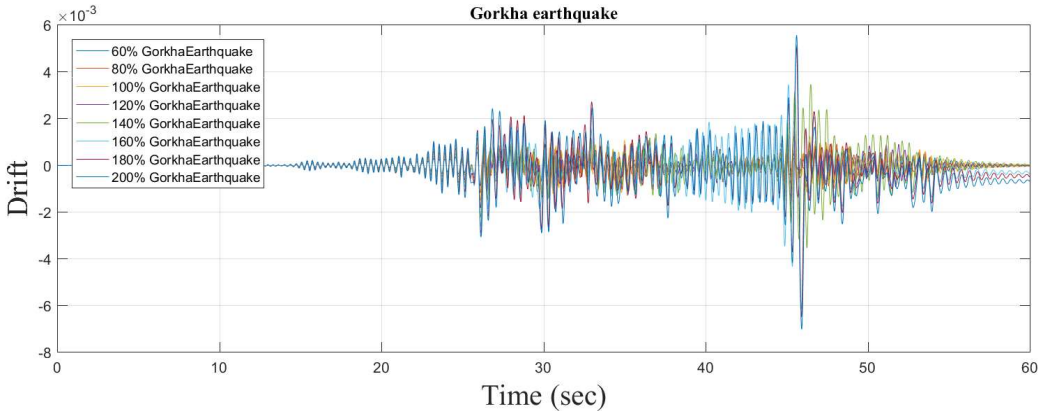

Figure 148: Drift time history for Gorkha Earthquake.